Alma Mater Studiorum · Università di Bologna

**Scuola di Scienze**
**Corso di Laurea Magistrale in Fisica**

# Geodesics Motion in Fuzzy Black Hole Space-Times

**Relatore:**
**Prof. Roberto Casadio**

**Correlatore:**
**Dott. Andrea Giusti**

**Presentata da:**
**Francesca Del Bonifro**

**Sessione II**
**Anno Accademico 2015/2016**

# Abstract

Classical General Relativity predicts the existence of space-times with non-trivial casual structures known as Black Holes. A classical black hole could form by the gravitational collapse of a compact object, which should end into a singularity covered by a (sharply defined) horizon, with a size equal to the gravitational radius of the matter source. In a quantum theory, the matter source is described by a quantum state, and one can correspondingly describe its gravitational radius by means of a Horizon Wave-Function. The resulting space-time is therefore expected to be "fuzzy", and so will be the geodesic motion of test particles. Orbits of massive particles as well as trajectories of light rays around such fuzzy gravitational sources are here analysed in details using both analytical approximations and numerical calculations. The uncertainty in the time of radial free fall and the effects on the out-going radiation emitted by the collapsing matter will also be presented.

# Sommario

La Relativitá Generale classica predice l'esistenza di spazio-tempi con strutture causali non banali conosciute come Buchi Neri. Un Buco Nero classico si potrebbe formare da un collasso gravitazionale di un oggetto compatto, il quale dovrebbe terminare in una singolaritá coperta da un (ben definito) orizzonte, di grandezza uguale al raggio gravitazionale della sorgente di materia. In una teoria quantistica, la sorgente di materia é descritta da uno stato quantistico, e corrispondentemente é possibile descrivere il suo raggio gravitazionale tramite la funzione d'onda dell'orizzonte. Lo spazio-tempo risultante che ci aspettiamo sará "sfumato" e cosí sará il moto geodetico per particelle di prova. In questa tesi vengono analizzate in dettaglio orbite di particelle massive cosí come le traiettorie dei raggi di luce attorno a queste sorgenti gravitazionali sfumate usando sia approssimazioni analitiche che calcoli numerici. Saranno discussi anche l'incertezza nel tempo di caduta radiale libera e gli effetti sulla radiazione uscente emessa da una sorgente che sta collassando.

# Contents

# Introduction

From General Relativity, we assist to the birth of various new scenarios. In fact, starting from Einstein field equations one can study different kind of space-time solutions related to some (physically reasonable) matter distribution. Moreover, we can faces with particular space-time structures known as Black Holes which arise as possible final states of important gravitational phenomena like gravitational collapses of matter sources. A Black Hole is, roughly speaking, an extremely compact object that consists in a portion of space-time delimited by means of a null-hypersurface called the event horizon, which is causally disconnected from the exterior region. In fact, from this region both massive and massless particles cannot escape and reach the future infinity. There are various kinds of Black Holes because of the different kind of the initial collapsing sources, in the following chapters we restrict ourselves in the case of spherically symmetric sources which, from Einstein equations, generate Schwarzschild space-times and, consequently, Schwarzschild Black Holes.

Thanks to their intense gravitational fields and their particular behavior, Black Holes are very useful objects for the studies of relativistic and gravitational phenomena. Although it is very difficult to detect Black Holes (because they are disconnected from the exterior region), it is possible to observe them studying the motion of particles and astrophysical objects in their gravitational fields. So, when particles are in the vicinity of a Black Hole, we can study their behavior and from their trajectories one can obtain information on the field source. In fact, as in the case of our Galaxy, we can state that at its center there would be a Supermassive Black Hole because of the observed motion of nearby stars.

For a generic Black Hole, the important quantities that characterize the Black Hole is its total energy-mass $m$, charge $Q$ and angular momentum $J$. In the simplest case of spherically symmetric source, in which there are no electric charge and no rotational motion, the only important quantity for the Black Hole is its mass $m$ that define the gravitational radius $r_H = 2m\frac{l_P}{m_P} = 2M$. For these reasons when we will consider some quantum aspects, Black Holes are objects of huge importance. For example, when one considers a source whose quantum nature cannot be neglected one has a wave function that codifies the states of a quantum source and from here a new concept of horizon and gravitational radius arise. In fact, starting from the source's quantum wave function, one would be able to define its Horizon Wave Function (HWF), a function that encodes the probability that the source has a certain gravitational radius and consequently, the probability to find an horizon at some value of $r$. From here we have an instrument that calculates the probability that the source is a Black Hole or an ordinary particle. In this view, also the gravitational radius changes its nature and become an operator. From here we have a distribution of values in $r_H$ and consequently in $M$. At this point, we can suppose that $M$ is represented by a certain probability distribution of values instead of a single precise value, in doing so, a corresponding fuzzy space-time arises. Consequently, this fact will

affect the particle motion and in this thesis, we are going to study precisely this situation.

Starting from a classic space-time with fixed gravitational radius we will extend the results to a fuzzy space-time with some reference to the gravitational collapse phenomena. Moreover, when we will talk about horizon wave function, we will see an example supposing that the source wave function is a Gaussian because any other localized wave function can be expressed in terms of Gaussian wave functions. As we will see, this example won't apply to the case of astrophysical objects because of the behavior of the $r_H$ fluctuations. In these cases will be useful an extended state wave function to describe the source instead of a localized one.

# Part I

# Classical Black Hole Space-Times

# Chapter 1

# Geometric properties of Black Hole Space-times

The study of General Relativity implies a strong background in Differential Geometry, for this reason here we will show some concepts related to the study of a generic manifold together with some theorems and properties which will be useful when we consider space-times manifold and the Black Hole physics.

## 1.1 Useful Geometrical concepts

We will start defining important types of vector, curves and hypersurfaces. In fact, when we have a manifold $(\mathcal{M}, g)$, vectors defined on it can be timelike,spacelike or lightlike (null). So we state that a vector is a **causal vector** if it is timelike or null. Consequently, a curve is a **causal curve** if its tangent vector is a causal one everywhere.

When a manifold admits a causal vector field it is called a **time-orientable** manifold. When one faces with this type of manifold, it is possible to define a future-orientation and a past-orientation: if one sets $T^a$ as the causal vector that defines the future-direction, all the other causal vectors will be future-directed if they lie in the same light cone of $T^a$ and are past-directed if they lie in the opposite light cone[1]. From here, a curve is **future(past)-directed** if its tangent vector is future(past)-directed everywhere. Moreover, such a curve is **future(past) inextendible** if it have not a future(past) endpoint[2]. Finally we have to state another important property that a manifold can have: extendibility. In fact, a manifold $(\mathcal{M}, g)$ is **extendible** if it is isometric to a proper subset of another space-time $(\mathcal{M}', g')$ which is called the **extension** of $\mathcal{M}$. If this were not happen $\mathcal{M}$ is an **inextendible** manifold.

## 1.2 Singularity theorem

In this section, we introduce the Singularity theorem which explains the fact that singularity is a general result for a complete gravitational collapse on the contrary of the Newtonian theory

[1] A time-orientable manifold admits two unequal time orientation, in the present example the other orientation occurs when one sets $T^a$ as the causal vector which define the past orientation.

[2] A point $p$ of a future(past)-directed curve $\gamma$ on a manifold $(M, g)$ is called a **future(past) endpoint** if for any neighborhood $O$ of $p$ there is $t_0$ such that $\gamma(t) \in O$ if $t > t_0$.

in which singularity occur only as a consequence of spherical symmetry of the collapse process. In fact, breaking the spherical symmetry one cannot avoid the singularity formation. To do that, we have to talk about trapped surfaces and other particular surfaces of the space-time manifold.

**Definition 1.** On a space-time, an hypersurface is defined to be a **null hypersurface** if its normal $n_a$ is null everywhere. For these surfaces, rising the index one obtains a vector $n^a$ whose integral curves lie on the surface and these are null geodesics called **generetors** of the null hypersurface.

Now, considering spacelike surfaces, one can state that every spacelike surface $S$ has two future-directed null vectors orthogonal to the surface in each point $p \in S$. If $S$ is orientable we can define these two vectors continuously, in this way these null geodesics form two null hypersurfaces (outgoing and ingoing null rays starting from $p$). All these considerations bring us to define another important kind of surface, the trapped surface, which will be important in the definition of apparent horizons and in the Singularity Theorem.

**Definition 2.** A **trapped surface** is a compact, orientable, spacelike 2-surface in which the two families of null geodesic have negative expansion[3] $\theta$.

The positivity or negativity of $\theta$ depends on the regions of space-time which one takes into account. A particular case is that of **marginally trapped surface** which satisfies the same conditions of a trapping surface but with $\theta = 0$.

Other kind of surface which we have to introduce to explain the singularity theorem are the Cauchy surfaces that are defined as follow:

**Definition 3.** An hypersurface on a manifold $(\mathcal{M}, g)$ with no two points connected by a causal curve in $\mathcal{M}$ is a **partial Cauchy surface**.[4]

Let $\Sigma$ be a partial Cauchy surface, we will call the **future(past) domain of dependence of** $\Sigma$: $D^+(\Sigma)(D^-(\Sigma))$. This is the set of points $p$ of $\mathcal{M}$ such that every past(future) inextendible causal curve through $p$ intersect $\Sigma$. One can make the union of future and past domain of dependence defining a region of space-time $D(\Sigma)$ in which, roughly speaking, one knows what happen from the knowledge of the data in $\Sigma$.

**Definition 4.** In a space-time $(\mathcal{M}, g)$, a **Cauchy surface** is a partial Cauchy surface $\Sigma$ such that $\mathcal{M} = D(\Sigma)$. A space-time which admits a Cauchy surface is **globally hyperbolic**.

If we consider a time-orientable manifold $(\mathcal{M}, g)$, from the definition of causal curves we can define the concept of **causal future (past)** of $U$ (where $U \subset \mathcal{M}$) $\mathcal{J}^+(U)$ $(\mathcal{J}^-(U))$. This is the union of $U$ and the point of the manifold which one can reach following a future (past)-directed causal curve starting from the points in $U$. Instead, if we consider points of the manifold which one can reach following a future (past)-directed timelike geodesic starting from the points in $U$ one can define the **chronological future (past)** of $U$: $I^+(U)$ $(I^-(U))$. Chronological future and past are open sets. From here we have:

**Definition 5.** Let $\Sigma$ be a Cauchy surface, the **future(past) Cauchy horizon** $H^+(\Sigma)$ $(H^-(\Sigma))$ is a surface such that $H^+(\Sigma) = D^+(\Sigma) \backslash I^-(D^+(\Sigma))$ $(H^-(\Sigma) = D^-(\Sigma) \backslash I^+(D^-(\Sigma)))$.

[3] If one considers a congruence of null geodesic on the space-time $(\mathcal{M}, g)$ and let $U^a$ be a tangent vector for this congruence, the **expansion** is represented by $\theta = \Delta_a U^a$.

[4] If we consider timelike curves instead of causal ones, we obtain the definition for **achronal surfaces**.

Now we present a fundamental theorem whose importance is due to the fact that this represents a lemma in the proof of the singularity theorem.

**Theorem 1** (Raychaudhuri's equation)**.** *Along a geodesic $\gamma(\lambda)$ (with tangent vector $U^a$) of a null geodesic congruence, the previously defined expansion $\theta$ satisfies:*

$$\frac{d\theta}{d\lambda} = -\frac{1}{2}\theta^2 - \widehat{\sigma}^{ab}\widehat{\sigma}_{ab} + \widehat{\omega}^{ab}\widehat{\omega}_{ab} - R_{ab}U^aU^b \tag{1.1}$$

*where $R_{ab}$ is the Ricci tensor, $\widehat{\sigma}^{ab}$ and $\widehat{\omega}^{ab}$ are the **shear** and **rotation** tensors for null geodesics.*

From Einstein equations, Ricci tensor is related to matter distribution in terms of its energy-momentum tensor $T^{ab}$, the requirement of the use of physically reasonable kind of matter reflects on the Ricci tensor too. From here one could require some conditions for the energy-momentum tensor:

- The **dominant energy condition** states that for any future-directed timelike vector $V^a$ one has that the vector $-T^a_bV^a$ is a future-directed causal vector. If in some region $S$ of a spacelike hypersurface $T^{ab}$ were null then this will be null in $D^+(S)$ too;
- The **weak energy condition** states that for any causal vector $V^a$ one has $T_{ab}V^aV^b \geqslant 0$ (this condition is also a consequence of the dominant energy condition);
- The **null energy condition** states that for any null vector $V^a$ one has $T_{ab}V^aV^b \geqslant 0$ (this condition is also a consequence of the weak energy condition);
- A less important condition is the **strongly energy condition** which states that for any causal vector $V^a$ the energy-momentum tensor satisfies $(T_{ab} - \frac{1}{2}g_{ab}T^c_c)V^aV^b \geqslant 0$. This means that gravity is attractive[5].

Now we have all the tools to enunciate the Penrose singularity theorem:

**Theorem 2.** *Let $\Sigma$ be a non compact Cauchy surface in a globally hyperbolic space-time $(\mathcal{M}, g)$ which follow Einstein equation and null energy condition for some $T^{ab}$. If we consider a trapped surface $T$ and set $\theta_0 < 0$ as the maximum value that the expansion of both the orthogonal null geodesic congruence can have, then at least one of these geodesics is future-inextendible (with affine length$\leqslant \frac{2}{|\theta_0|}$).*

We can adapt this theorem to space-time without the requirement to be globally hyperbolic. In this situation, we have to require the strong energy condition instead of the null one. From these new conditions we have that the space-time is geodesically incomplete[6], so a general gravitational collapse produces a singularity. This second form is known as the **Penrose-Hawking Singularity Theorem**.

Another observation can be done considering the **Cauchy stability** property of the Einstein equations, e.g. the solution in a compact region is depend continuously on the initial data set. As a consequence, if we consider a compact region with a trapped surface in a spherically symmetric gravitational collapse and perform a slightly deviation from the initial symmetry, trapped surface occurs again (also the trapped surface formation is general in gravitational collapses).

[5]Such a condition won't be satisfy for example where one consider a positive cosmological constant $\Lambda$ while the dominant energy condition is satisfied.

[6]A space-time is **geodesically complete** if all the inextendible causal geodesics are **complete**, i.e. if their affine parameter ranges from $-\infty$ to $\infty$

## 1.3 Asymptotically flat space-times

As we will see, a fundamental concept to represent the space-time due to isolated sources is the **asymptotic flatness** of a manifold. In this section we will formally define this property and talking about it. We have to start introducing a particular kind of transformations.

**Definition 6.** Let $(\mathcal{M}, g)$ be a *physical* space-time manifold, one can define a new *unphysical* metric as

$$\bar{g}_{\mu\nu}(x) = \Omega(x)^2 g_{\mu\nu}(x) \tag{1.2}$$

where $x \in \mathcal{M}$ and $\Omega(x)$ is a smooth, positive function on $\mathcal{M}$. Transformations of this kind are called **conformal transformations**.

With these transformations, one can have that the manifold $(\mathcal{M}, \bar{g})$ can be extended to a larger unphysical manifold $\left(\bar{\mathcal{M}}, \bar{g}\right)$ that contains the physical one. By definition, a conformal transformation preserves the causal structure of the physical space-time, i.e. the null, spacelike, timelike nature of vectors remains the same, so that one can study the causal structure of $(\mathcal{M}, g)$ by means of $\left(\bar{\mathcal{M}}, \bar{g}\right)$. These transformations are useful when one wants to study a manifold boundary behavior $\partial\mathcal{M}$ (which corresponds to the space-time infinity), in fact if we perform a conformal transformation on a manifold such that $\Omega(x)|_{\partial\mathcal{M}} = 0$ points at infinity can be seen at a "finite distance" By means of this transformation we can study points at infinity on an unphysical manifold without altering the causal structure, this is called the **conformal compactification**.

Intuitively, an asymptotically flat space-time has a conformal infinity like the Minkowski's one (see appendix A), but we'll define it precisely.

**Definition 7.** Let $(\mathcal{M}, g)$ a time-orientable space-time, this is called an **asymptotically flat space-time** (at null infinity) if there is another space-time $\left(\bar{\mathcal{M}}, \bar{g}\right)$ such that:

1. On $\mathcal{M}$ there is a function $\Omega$ from which one can define $\bar{g} = \Omega^2 g$ and $\left(\bar{\mathcal{M}}, \bar{g}\right)$ represents an extension of the other space-time;

2. $\mathcal{M} \cup \partial\mathcal{M}$ in $\bar{\mathcal{M}}$ represents a manifold with boundary;

3. We can extend $\Omega$ to a function on $\bar{\mathcal{M}}$ to obtain $\Omega|_{\partial\mathcal{M}} = 0$ and $d\Omega|_{\partial\mathcal{M}} \neq = 0$;

4. $\partial\mathcal{M}$ is formed by two disjoint part $\mathcal{I}^- \cap \mathcal{I}^+$;

5. Any future (past) causal curve does not intersect $\mathcal{I}^-(\mathcal{I}^+)$;

6. $\mathcal{I}^{\pm}$ are complete[7] null hypersurfaces.

With the first three requirements we are demanding the existence of a conformal compactification, the other three require that the manifold null conformal infinity shares the form of the Minkowski's one.

[7] If the affine parameter of the generators of the null hypersurfaces ranges in $(-\infty, \infty)$ the surface is **complete**.

## 1.4 Black Holes

Here we come with the precise definition for Black Holes which are important causal structures on the space-time which are predicted to exist by General Relativity. Formal definition of these objects are expressed by means of past and future surfaces that we have described in previous sections.

**Definition 8.** If we have an asymptotically flat (at null infinity) space-time $(\mathcal{M}, g)$ the **Black (White) Hole** region is defined as $\mathcal{B} = \mathcal{M} \backslash (\mathcal{M} \cap \mathcal{J}^- (\mathcal{I}^+))$ $(\mathcal{W} = \mathcal{M} \backslash (\mathcal{M} \cap \mathcal{J}^+ (\mathcal{I}^-)))$. And the **future(past) event horizon** is the boundary of this region $\mathcal{H}^+ = \partial\mathcal{B}$ $(\mathcal{H}^- = \partial\mathcal{W})$[8] and is a null hypersurface whose generators have no future (past) endpoints.

Another important definition strongly related to the Black Holes physics is the concept of predictability.

**Definition 9.** Let $(\mathcal{M}, g)$ be an asymptotically flat space-time, if we have an open region $\bar{V} \subset \bar{\mathcal{M}}$ so that $\mathcal{M} \cap \bar{\mathcal{J}}^- (\mathcal{I}^+) \subset \bar{V}$ and $\left(\bar{V}, \bar{g}\right)$ is globally hyperbolic, the space-time $(\mathcal{M}, g)$ is called **strongly asymptotic predictable**.

As a consequence we have that also $\left(\mathcal{M} \cap \bar{V}, g\right)$ (which is the the portion of space-time without the region of the Black Hole) is globally hyperbolic. So we can state that the physics is predictable on and outside $\mathcal{H}^+$. If an asymptotically flat space-time which is not strongly asymptotic predictable contains a naked singularity, i.e. a singularity which is not covered by means of the event horizon.

## 1.5 Apparent horizons

In this section we introduce another kind of horizon, the apparent horizon. Conversely to the definitions of future and past event horizons these are defined locally. Let's start with a theorem on the trapped surfaces that we have defined in the previous sections.

**Definition 10.** If we have a globally hyperbolic space-time $(\mathcal{M}, g)$ we can choose $\Sigma_t$ as a Cauchy surface in $\mathcal{M}$. The set of point $p \in \Sigma_t$ for which there is a trapped surface $S$ such that $p \in S \subset \Sigma_t$ is called the **trapped region** of $\Sigma_t$: $\mathcal{T}_t$. The boundary of this region is called the **apparent horizon** $\mathcal{A}_t = \partial\mathcal{T}_t$

**Theorem 3.** *In a strongly asymptotic predictable space-time, a trapped surface $T$ which satisfies the null energy condition, also satisfies $T \subset \mathcal{B}$.*

[8] This definitions are non-local.

# Chapter 2

# Spherically Symmetric Sources

## 2.1 Mass in General Relativity

From General Relativity, we obtain the following Einstein field equations:

$$G_{\mu\nu} = R_{\mu\nu} - \frac{1}{2}Rg_{\mu\nu} = 8\pi T_{\mu\nu} \tag{2.1}$$

in which $G_{\mu\nu}$ is the Einstein tensor, $R_{\mu\nu}$ is the curvature tensor (Ricci tensor), $R$ is the scalar curvature, $g_{\mu\nu}$ is the metric of the space-time and $T_{\mu\nu}$ is the energy-momentum tensor of a given region that describes matter distributions in terms of their energy and momentum (density and flux). From the structure of $R_{\mu\nu}$[1], Einstein equations are second order non-linear partial differential in $g_{\mu\nu}$ and define the space-time manifold due to the presence of a certain energy-momentum distribution and, in this view, $T_{\mu\nu}$ represents the source of the gravitational field.

The energy-momentum tensor does not consider the energy due to the gravitational field, in fact this latter is included in the right hand side of the equation (2.1) and there is no way to put these two pieces together in a tensor in such a way that we have a mathematical object that describes all the energy sources for a generic observer, in fact considering the equivalence principle one has the non-locality of the gravitational energy and one has to extend $T_{\mu\nu}$ to the energy-momentum pseudotensor (which is a frame dependent object) to include gravitational potential energy e.g.the Landau-Lifshits energy pseudotensor.

From the non-locality of the gravitational energy, it is convenient to define the total mass of a system in an asymptotic way measuring this quantity at infinity on the asymptotic metric. We can simplify the problem of the total mass definition in some special space-time such as those which have the property of asymptotic flatness, these space-times are due to the presence of isolated sources. Although physically there are no completely isolated systems one can use these models to describe some massive objects ignoring the action of other distant mass' sources, in this way one obtains space-time metrics that become flat far from the sources. At this point, one has to be able to define this asymptotic flatness in a coordinate independent way and the definition has to be such that the evaluation of any relevant physical quantity at large distance is not ambiguous. To overcome these difficulties, one defines the asymptotic flatness when it is possible to represent points at infinity as a space-time boundary, e.g. with conformal compactification (see Chapter 1 Section 1.3). However once one defines the asymptotic flatness,

[1]Ricci tensor is defined in terms of Christoffel symbols $R_{\mu\nu} = \partial_\alpha \Gamma^\alpha_{\nu\mu} - \partial_\nu \Gamma^\alpha_{\alpha\mu} + \Gamma^\alpha_{\alpha\lambda}\Gamma^\lambda_{\nu\mu} - \Gamma^\alpha_{\nu\lambda}\Gamma^\lambda_{\alpha\mu}$.

a quantity which represents the total energy in these special space-times could be the ADM (Arnowitt-Deser-Misner) mass:

$$m(t) = \lim_{r\to\infty} m\left(t,r\right) = \lim_{r\to\infty} 4\pi \int_0^r d\tilde{r}\tilde{r}^2 \rho\left(t,\tilde{r}\right) \tag{2.2}$$

where $\rho\left(t,r\right)$ is the classical energy density. The quantity $m\left(t,r\right)$ represents the Misner-Sharp (MS) mass and in a spherically symmetric system it represents the active gravitational mass (mass energy and gravitational potential energy) inside the sphere of an area $4\pi r^2$. There are also other kinds of definitions of mass but we use the AMD and MS definitions in the following chapters.

## 2.2 Spherically symmetric sources

If we consider the particular case of spherically symmetric, non rotating sources with null electric charge and surrounded by vacuum, we have a static (time- independent and with the discrete time-reversal isometry) metric which reads:

$$ds^2 = g_{tt}(x^j)dt^2 - 2g_{ti}(x^j)dtdx^i - g_{ik}(x^j)dx^i dx^k \tag{2.3}$$

where $i$, $j$, $k$= 1,2,3 and the spherical symmetry implies that the most general line element is:

$$ds^2 = e^{2\Phi(r)}dt^2 - e^{2\Psi(r)}dr^2 - r^2\left(d\theta^2 + \sin^2\theta d\phi^2\right) \tag{2.4}$$

In the exterior region, we have $T_{\mu\nu} = 0$, $R = 0$, $R_{\mu\nu} = 0$ and, from the definition of these quantities, one obtains the asymptotically flat, static solution:

$$ds^2 = \left(1 - \frac{2M}{r}\right)dt^2 - \left(1 - \frac{2M}{r}\right)^{-1} dr^2 - r^2 d\theta^2 - r^2\sin\theta^2 d\phi^2 \tag{2.5}$$

which is known as the Schwarzschild solution. Here $r$ represents the area-radius,defined as $r(p) = \sqrt{\frac{A(p)}{4\pi}}$ and $A(p)$ is the area of the $S^2$ 2-sphere which represent the $SO(3)$ orbit of $p$, so $r$ does not correspond to the proper distance from the center of the sphere which reads $r_* = \int_0^r \sqrt{g_{r'r'}}dr'$. The coordinate $t$ is defined as the time measured by an asymptotic observer. In (2.5), the parameter $M = \frac{Gm}{c^2}$ represents the total mass of the Schwarzschild field (we will use $c = 1$ so we obtain $G = \frac{l_P}{m_P}$ with $l_P$, $m_P$ Planck length and mass respectively) and from the field equations (2.1) is defined by the relation:

$$M = 4\pi\frac{l_P}{m_P}\int_0^R \rho(r)r^2 dr \tag{2.6}$$

where $R$ is the radius of the source and since $\rho(r) = 0$ for $r > R$ equation (2.6) corresponds to the ADM mass definition. This equation is the same of the total mass in classical Newton theory but the identification of these two quantities is formal only. In fact if we want to integrate density over a certain volume, from the line element we have:

$$M' = 4\pi\int_0^R dr\frac{\rho(r)r^2}{\sqrt{1-\frac{2M}{r}}} \tag{2.7}$$

which does not correspond to the (2.6) definition.

The line element (2.5) is singular for $r = 0$ and $r = 2M$. The first one is a physical singularity (curvature diverges here), the second one depends only on the coordinates system (curvature remains finite) and defines the Schwarzshild radius $R_H$. At this radius $R_H$, the coordinates change their meaning. In fact, in the region $r < R_H$, $t$ becomes a space coordinate ($g_{tt} < 0$) while $r$ becomes a time coordinate ($g_{rr} > 0$) and we observe that particles moving through this hypersurface show particular behaviors. In fact, if the radius of the source $R$ verifies the condition $R < R_H$, we have a Black Hole and once a particle (even a photon) reaches this value for $r$ it cannot escape. If a radially outgoing photon were emitted at this radius, it remains there and will not be able to reach null infinity, so this surface represents a null hypersurface and it is called the event horizon because the region inside it is causally disconnected from the rest of the space-time.

In previous chapters we have introduced the apparent horizon, which represents the boundary of the trapping surfaces (surfaces from which both ingoing and outgoing radially photon trajectories converge), so the apparent horizon occurs when the expansion parameter of the radial null out-going geodesics is null. This means that the divergence of these null geodesics is null on the apparent horizon and this condition is[2]:

$$|\nabla r|^2 = g^{ij}\nabla_i r \nabla_j r = 0 \tag{2.8}$$

which reads:

$$g^{rr} = \frac{2M}{r} - 1 = 0 \tag{2.9}$$

Generally this surface does not coincide with the event horizon and their location depends on the observer. In doing so, we define the gravitational radius (as a function of $r$):

$$r_H(r) = 2m\,(r)\,\frac{l_P}{m_P} \tag{2.10}$$

This quantity will become useful later, for the moment we limit ourselves to say that an horizon appears when:

$$r_H\,(r) = r \tag{2.11}$$

## 2.3 Gullstrand-Painlevé coordinates

Starting from the Schwarzschild solution (2.5), we make a change of coordinates system to obtain a regular line element. As we will see, in the Schwarzschild coordinate system a particle reaches the event horizon in an infinite amount of time $t$. Instead, if one studies the trajectories in terms of the proper falling time, the particle can reach the horizon in a finite proper time. So to avoid singularity at this value for the area radius, we could use the proper time of a free falling observer $t_P$ as time coordinate instead of Schwarzschild time coordinate $t$. In doing so, we should obtain a metric which is not singular for $r = 2M$ but still describes the space-time of the vacuum around the spherically symmetric source. This new metric is known as the Gullstrand-Painlevé metric and it is useful in the study of the motion of radially infalling

[2]Here $\nabla_i r$ is perpendicular to the surface with $r = const$.

particles. To obtain this metric we have to relate $t_P$ and $t$. To do so, we note that for the symmetries of the system $t_P = t_P(t, r)$, so we can write:

$$dt_P = \frac{\partial t_P}{\partial t}|_r dt + \frac{\partial t_P}{\partial r}|_t dr \tag{2.12}$$

Consider the case $r = const$, two clocks '1' and '2' falling from $r_0$ which start their motion at $t_1$ and $t_2$ respectively, when they cross a fixed $r$ they measure $t_1' = t_1 + \Delta t$ and $t_2' = t_2 + \Delta t$. So the time difference at $r$:

$$dt|_r = t_2 + \Delta t - t_1 - \Delta t = t_2 - t_1 \tag{2.13}$$

Now, both clocks follow the same trajectory, so one has $t_{P1} = t_1 + \Delta\tau$ and $t_{P2} = t_2 + \Delta\tau$:

$$dt_P|_r = t_2 - t_1 = dt|_r \tag{2.14}$$

$$\frac{\partial t_P}{\partial t}|_r = 1 \tag{2.15}$$

The second step is to consider the case $t = const$. As we will see later, the equations of motion for a free falling particle (radial motion) which starts from $r = \infty$ with $\dot{r} = 0$ are:

$$\dot{r} = -\sqrt{\frac{2M}{r}} \tag{2.16}$$

$$\dot{t} = E\left(1 - \frac{2M}{r}\right)^{-1} \tag{2.17}$$

$$\frac{dr}{dt} = -\left(1 - \frac{2M}{r}\right)\sqrt{\frac{2M}{r}} \tag{2.18}$$

dots represent derivative w.r.t. proper time $\tau$. The quantity in (2.18) is important in the synchronization of the clocks and represents the time difference of two events with spacial separation $dr$:

$$dt = -\left(1 - \frac{2M}{r}\right)^{-1}\sqrt{\frac{r}{2M}}dr \tag{2.19}$$

Then we have to consider also the proper time difference due to the different motion (from (2.16)) which reads:

$$d\tau = \sqrt{\frac{r}{2M}}dr \tag{2.20}$$

minus sign is dropped because we need $\tau_2 - \tau_1$ instead of $\tau_1 - \tau_2$. In the G-P coordinates, we have to keep into account both contributes and one obtains:

$$dt_P = \frac{\sqrt{\frac{2M}{r}}}{1 - \frac{2M}{r}}dr \tag{2.21}$$

Now, from (2.12), (2.15) and (2.21), we finally have:

$$dt = dt_P - \frac{\sqrt{\frac{2M}{r}}}{1 - \frac{2M}{r}}dr \tag{2.22}$$

Inserting these results in the line element (2.5) we obtain

$$\begin{aligned} ds^2 &= \left(1-\frac{2M}{r}\right)\left(dt_P^2+\frac{\frac{2M}{r}}{\left(1-\frac{2M}{r}\right)^2}dr^2-2\frac{\sqrt{\frac{2M}{r}}}{1-\frac{2M}{r}}drdt_P\right)-\left(1-\frac{2M}{r}\right)^{-1}dr^2-r^2d\Omega^2 \\ &= \left(1-\frac{2M}{r}\right)dt_P^2-2\sqrt{\frac{2M}{r}}dt_Pdr-dr^2-r^2d\theta^2-r^2\sin\theta^2d\phi^2 \end{aligned} \tag{2.23}$$

which is not singular in $r = 2M$ and represents the **Gullstrand-Painlevé metric**, i.e. the metric of the space-time around the spherically symmetric source described by a free falling observer which starts its motion at rest at infinity.

These results can be obtained in another way by studying the geodesics motion of the free falling observer on the space-time manifold. Actually, radially infalling particles subject only to the gravitational force follow geodesics which four-velocity has the form $u^\mu = \frac{dx^\mu}{d\tau}$ and represents the trajectory's tangent vector ($x^\mu(\tau)$ are the coordinates $\tau$ which parametrizes these curves and in the massive observer case represents the proper time). Starting from (2.5) in the case of a radial motion ($d\theta = 0$, $d\phi = 0$) and from the property:

$$g_{\mu\nu}u^\mu u^\nu = \left(1-\frac{2M}{r}\right)\dot{t}^2-\left(1-\frac{2M}{r}\right)^{-1}\dot{r}^2 = 1 \tag{2.24}$$

we obtain:

$$u^\mu = \left(\dot{t},-\sqrt{\left(1-\frac{2M}{r}\right)^2\dot{t}^2-\left(1-\frac{2M}{r}\right)},0,0\right) = \left(\dot{t},-v\left(r\right),0,0\right) \tag{2.25}$$

$u^\mu$ is orthogonal to the surface $\tau = const$ and from the definition of the GP time coordinate $t_P = \tau$ so:

$$u_\mu = \frac{\partial t_P}{\partial x_s^\mu} \tag{2.26}$$

so $t_P$ depends on the Schwarzschild coordinates and its variation is:

$$\begin{aligned} dt_P &= \frac{\partial t_P}{\partial x_s^\mu}dx_s^\mu = u_\mu ds_s^\mu = u^\nu dx_s^\mu g_{\nu\mu} = \frac{\partial t_P}{\partial t}dt+\frac{\partial t_P}{\partial r}dr \\ &= \dot{t}\left(1-\frac{2M}{r}\right)dt+\frac{v(r)}{1-\frac{2M}{r}}dr \end{aligned} \tag{2.27}$$

as we will see in the next section, the quantity $\left(1-\frac{2M}{r}\right)\dot{t}$ is conserved during the particle motion and in the Schwarzschild coordinates represents the particle energy $E$. So the Schwarzschild time coordinate variation takes the form

$$dt = \frac{dt_P}{E}-\frac{v(r)}{E\left(1-\frac{2M}{r}\right)}dr \tag{2.28}$$

and considering the definition of $v(r)$, the new line element reads:

$$\begin{aligned} ds^2 &= \left(1-\frac{2M}{r}\right)\left(\frac{dt_P^2}{E^2}+\frac{v(r)^2}{E^2\left(1-\frac{2M}{r}\right)^2}dr^2-2\frac{v(r)}{E^2\left(1-\frac{2M}{r}\right)}drdt_P\right)-\frac{dr^2}{1-\frac{2M}{r}}-r^2d\Omega^2 \\ &= \frac{1-\frac{2M}{r}}{E^2}dt_P^2-2\frac{v(r)}{E^2}dt_Pdr-\frac{dr^2}{E^2}-r^2d\Omega^2 \end{aligned} \tag{2.29}$$

This is the most general G-P line element and the time coordinate represents the proper time of a radially falling observer. This observer can start its motion at any value of the $r$ coordinate with a given value of $\dot{r}$. These conditions fix the values of $E = \sqrt{1 - \frac{2M}{r(0)}}$ and, consequently, $v(r) = \sqrt{\frac{2M}{r} - \frac{2M}{r(0)}}$, in fact, if we consider as in the previous case an observer which starts its motion at $r(0) = \infty$ with $\dot{r}(0) = 0$ one has $0 = \dot{r}(0)^2 = E^2 - 1 + \frac{2M}{r(0)} = E^2 - 1$, so one obtain the constant value $E = 1$ and the expression $v(r) = \sqrt{\frac{2M}{r}}$. With such conditions, as expected, the line element corresponds to (2.23).

If we use general G-P line element in such a way that $\dot{r}(0)$ and $r(0)$ of the particle are the same of the observer ones the following properties are satisfied:

$$\begin{cases} \dot{r} = -v(r) \\ t_P = \tau \end{cases} \tag{2.30}$$

In the following sections we study particle motion using the particle proper time.

# Chapter 3

# Geodesic Motion in Black Hole Space-Times

Now we are ready to study the trajectories followed by test particles (massive or massless) which are only subject to a gravitational filed. From General Relativity and differential geometry, we know that these particles follow particular curves, the so-called geodesics of the manifold which is generated by the source. We will obtain the equations of these curves in two different ways, from a Lagrangian method and by means of the Christoffel symbols. Finally we check that one obtains the same results.

## 3.1 Conserved quantities

As a starting point, we investigate if in the present case there are some particular quantities which remains constant during the motion.

We know that from a given metric tensor $g_{\mu\nu}$, one can write the corresponding Lagrangian:

$$\mathcal{L} = g_{\mu\nu}\dot{x}^\mu \dot{x}^\nu \tag{3.1}$$

in the case of G-P metric (2.23), the corresponding Lagrangian (restricting us in a planar motion $\theta = \theta_0 = \frac{\pi}{2}$, $\dot{\theta} = 0$) is:

$$\mathcal{L} = \frac{\left(1 - \frac{2M}{r}\right)}{E^2}\dot{t}^2 - \frac{2}{E^2}\sqrt{\frac{2M}{r} - \frac{2M}{r_0}}\dot{t}\dot{r} - \frac{\dot{r}^2}{E^2} - r^2\dot{\phi}^2 \tag{3.2}$$

Particles in this manifold are governed by the Euler-Lagrange equations that are of the form:

$$\frac{d}{d\tau}\frac{\partial \mathcal{L}}{\partial \dot{x}^\mu} - \frac{\partial \mathcal{L}}{\partial x^\mu} = 0 \tag{3.3}$$

with $\dot{x}^\mu = \frac{dx^\mu}{d\tau}$. So in the present case, one can obtain two conservation equations:

$$\frac{d}{d\tau}\left(\left(1 - \frac{2M}{r}\right)\dot{t} - \sqrt{\frac{2M}{r} - \frac{2M}{r_0}}\dot{r}\right) = 0 \tag{3.4}$$

$$\frac{d}{d\tau}\left(r^2\dot{\phi}\right) = 0 \tag{3.5}$$

Obtaining the corresponding quantities:

$$E = \left(1 - \frac{2M}{r}\right)\dot{t} - v(r)\dot{r} \tag{3.6}$$

$$L = r^2\dot{\phi} \tag{3.7}$$

which are conserved during the motion and represent energy and angular momentum of the particle respectively.

The same results could be reached considering that the metric (2.23) is independent from $t$ and $\phi$, so we have two Killing vectors on this manifold:

$$\xi^\mu = (1, 0, 0, 0) \tag{3.8}$$

$$\zeta^\mu = (0, 0, 0, 1) \tag{3.9}$$

Along a geodesic (with $u^\mu = \frac{dx^\mu}{d\tau}$ tangent vector), the following quantities are conserved:

$$E = \xi^\mu u_\mu = \xi^0 u^0 g_{00} + \xi^0 u^1 g_{01} = \frac{dt}{d\tau}\left(1 - \frac{2M}{r}\right) - \sqrt{\frac{2M}{r}}\frac{dr}{d\tau} \tag{3.10}$$

$$L = \zeta^\mu u_\mu = \zeta^3 u^3 g_{33} = \left(\frac{d\phi}{d\tau}\right) r^2 \sin^2\left(\frac{\pi}{2}\right) = \dot{\phi} r^2 \tag{3.11}$$

which have the same form of the quantities obtained in (3.6) and (3.7) from the Euler-Lagrange equations. If one considers the Schwarzschild coordinate system, the conserved quantities are:

$$L = \zeta^3 u^3 g_{33} = \left(\frac{d\phi}{d\tau}\right) r^2 \sin^2\left(\frac{\pi}{2}\right) = \dot{\phi} r^2 \tag{3.12}$$

$$E = \xi^0 u^0 g_{00} = \frac{dt}{d\tau}\left(1 - \frac{2M}{r}\right) = \left(1 - \frac{2M}{r}\right)\dot{t} \tag{3.13}$$

in which $E$ has a different form because of the different definition of the time coordinate. In fact if we insert (2.22) in (3.13) we recover the result in (3.6).

## 3.2 Geodesics for test particles

Let us describe the equations of these geodesics followed by the particles in a gravitational field. They are defined by the geodesics equation:

$$\frac{d^2x^\gamma}{d\tau^2} + \Gamma^\gamma_{\mu\nu}\frac{dx^\mu}{d\tau}\frac{dx^\nu}{d\tau} = 0 \tag{3.14}$$

where $\Gamma^\gamma_{\mu\nu}$ represents the Christoffel symbols for a certain coordinates system (in this case for the Schwarzschild coordinates) and, in the case of an holonomic basis, they are given by:

$$\Gamma^\gamma_{\mu\nu} = \frac{1}{2}g^{\gamma\sigma}\left(g_{\sigma\nu,\mu} + g_{\sigma\mu,\nu} - g_{\mu\nu,\sigma}\right) \tag{3.15}$$

Let's start calculating these quantities:

$$\Gamma^t_{tr} = \Gamma^t_{rt} = \frac{M}{r^2(1 - \frac{2M}{r})} \tag{3.16}$$

$$\Gamma^r_{tt} = \frac{M}{r^2}\left(1 - \frac{2M}{r}\right) \tag{3.17}$$

$$\Gamma^r_{rr} = -\frac{M}{r^2\left(1 - \frac{2M}{r}\right)} \tag{3.18}$$

$$\Gamma^\theta_{r\theta} = \Gamma^\theta_{\theta r} = \frac{1}{r} \tag{3.19}$$

$$\Gamma^r_{\theta\theta} = -r\left(1 - \frac{2M}{r}\right) \tag{3.20}$$

$$\Gamma^\phi_{\phi r} = \Gamma^\phi_{r\phi} = \frac{1}{r} \tag{3.21}$$

$$\Gamma^r_{\phi\phi} = -r\left(1 - \frac{2M}{r}\right)\sin^2\theta \tag{3.22}$$

$$\Gamma^\theta_{\phi\phi} = -\sin\theta\cos\theta \tag{3.23}$$

$$\Gamma^\phi_{\theta\phi} = \Gamma^\phi_{\phi\theta} = \frac{\cos\theta}{\sin\theta} \tag{3.24}$$

So we have four equations:

$$0 = \frac{d^2t}{d\tau^2} + \frac{2M}{r^2\left(1 - \frac{2M}{r}\right)}\frac{dr}{d\tau}\frac{dt}{d\tau} \tag{3.25}$$

$$\begin{aligned} 0 &= \frac{d^2r}{d\tau^2} + \frac{M}{r^2}\left(1 - \frac{2M}{r}\right)\left(\frac{dt}{d\tau}\right)^2 - \frac{M}{r^2\left(1 - \frac{2M}{r}\right)}\left(\frac{dr}{d\tau}\right)^2 - r\left(1 - \frac{2M}{r}\right)\left(\frac{d\theta}{d\tau}\right)^2 \\ &- r\left(1 - \frac{2M}{r}\right)\sin^2\theta\left(\frac{d\phi}{d\tau}\right)^2 \end{aligned} \tag{3.26}$$

$$0 = \frac{d^2\theta}{d\tau^2} + \frac{2}{r}\frac{dr}{d\tau}\frac{d\theta}{d\tau} - \sin\theta\cos\theta\left(\frac{d\phi}{d\tau}\right)^2 \tag{3.27}$$

$$0 = \frac{d^2\phi}{d\tau^2} + \frac{2}{r}\frac{dr}{d\tau}\frac{d\phi}{d\tau} + 2\frac{\cos\theta}{\sin\theta}\frac{d\phi}{d\tau}\frac{d\theta}{d\tau} \tag{3.28}$$

Restricting in a planar motion $\theta = \frac{\pi}{2}$ and $\frac{d\theta}{d\tau} = 0$, the equation (3.27) becomes an identity $0 = 0$. (3.28) is equivalent to the angular momentum conservation equation:

$$0 = \frac{d}{d\tau}\left(r^2\dot{\phi}\right) \tag{3.29}$$

$$L = r^2\dot{\phi} \tag{3.30}$$

(3.25) represents the energy conservation equation:

$$0 = \left(1 - \frac{2M}{r}\right)\frac{d^2t}{d\tau^2} + \frac{2M}{r^2}\frac{dt}{d\tau}\frac{dr}{d\tau} = \frac{d}{d\tau}\left(\left(1 - \frac{2M}{r}\right)\dot{t}\right) \tag{3.31}$$

$$E = \left(1 - \frac{2M}{r}\right)\dot{t} \tag{3.32}$$

Finally the (3.26) equation:

$$\ddot{r} + \frac{ME^2}{r^2\left(1-\frac{2M}{r}\right)} - \frac{M}{r^2\left(1-\frac{2M}{r}\right)}\dot{r}^2 - \left(1-\frac{2M}{r}\right)\frac{L^2}{r^3} = 0 \tag{3.33}$$

is equivalent to the condition:

$$\left(1-\frac{2M}{r}\right)\dot{t}^2 - \frac{\dot{r}^2}{\left(1-\frac{2M}{r}\right)} - r^2\dot{\phi}^2 = \kappa \tag{3.34}$$

where we set $\kappa = 1$ for massive particles, $\kappa = 0$ for massless particles. From here, the equations of motion are given by:

$$\dot{r}^2 = E^2 - \frac{L^2}{r^2}\left(1-\frac{2M}{r}\right) - \left(1-\frac{2M}{r}\right) \tag{3.35}$$

for massive particles, and

$$\dot{r}^2 = E^2 - \frac{L^2}{r^2}\left(1-\frac{2M}{r}\right) \tag{3.36}$$

for massless particles.

We can reach the same results from the Lagrangian method, in fact, from the Schwarzschild Lagrangian and the Euler-Lagrange equation for $r$ coordinate one has:

$$\frac{d}{d\tau}\left(-\frac{2\dot{r}}{1-\frac{2M}{r}}\right) - \frac{2M}{r^2}\dot{t}^2 - \frac{2M}{r^2\left(1-\frac{2M}{r}\right)}\dot{r}^2 + 2r\dot{\phi}^2 = 0 \tag{3.37}$$

the Euler-Lagrange equations for $t$ and $\phi$ coordinates give the same conservation equations in (3.13) and (3.12). Substituting $E$ and $L$ in (3.37) we obtain again (3.33), (3.35) and (3.36).

The form of these equations of motion suggests that the gravitational potential in massive case could be written as:

$$V_{eff} = \left(1-\frac{2M}{r}\right)\left(1+\frac{L^2}{r^2}\right) \tag{3.38}$$

in which we have a correction of $o\left(\frac{1}{r^3}\right)$ order at the Newtonian potential:

$$V_N = 1 + \frac{L^2}{r^2} - \frac{2M}{r} \tag{3.39}$$

The corrections due to General Relativity are important only for relatively small $r$ as we can see in Fig. 3.1. For massless particles we have (Fig. 3.2):

$$V_{eff} = -\frac{2ML^2}{r^3} + \frac{L^2}{r^2} \tag{3.40}$$

From these equations of $V_{eff}$ the shape of the potential is defined by the value of $L$ as we can see in Fig. 3.3, 3.4, 3.5.

If we want to use the G-P coordinates (for example in case $\dot{r} = 0$ at $r = \infty$) we obtain different $\Gamma^{\gamma}_{\mu\nu}$ and different Euler-Lagrange equations because of the different form of the line element. However, the final equation shares the same form of equations (3.35) and (3.36), because dots represent derivation w.t.r. to $\tau$ which is the proper time and correspond to $t_P$.

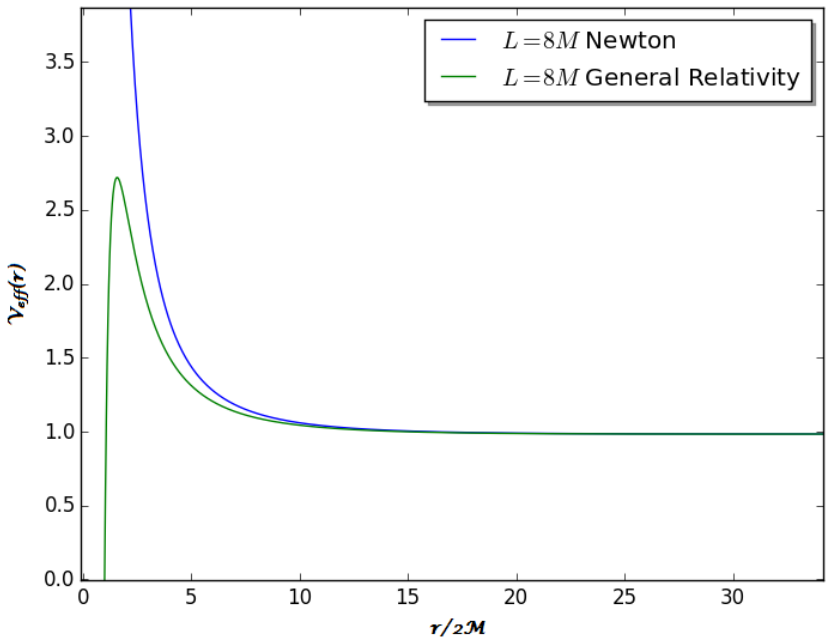


Figure 3.1: For small values of $r$, $V_{eff}$ has a minimum and a maximum and is different from the Newton potential. For big values of $r$, the potentials share the same behavior.

If we differentiate (3.35) w.r.t. $\tau$:

$$\ddot{r} = -\kappa \frac{M}{r^2} \tag{3.41}$$

which shares the same form of the equation of motion in a Newtonian gravitational field but it is not the same equation because, in this case, the coordinate $r$ is not the flat radius coordinate (proper distance from the center in a flat space), but it represents the area-radius (as we have already seen). In these equations dots represent derivative with respect to proper time which parametrizes the geodesics, while if we had used the Schwarzschild time coordinate $t_S$ from (3.13) and (3.36):

$$t_{Sf} - t_{Si} = \int_{t_{Si}}^{t_{Sf}} dt_S = w \int_{r_i}^{r_f} dr \frac{E}{\left(1 - \frac{2M}{r}\right)\sqrt{E^2 - \kappa\left(1 - \frac{2M}{r}\right)}} \tag{3.42}$$

Here we see that in (3.42) the integrand becomes divergent at $r = 2M$ and the Schwarzschild time needed to reach this radius become infinite. This reflects the singular behavior of the Schwarzschild coordinate system at this radius.

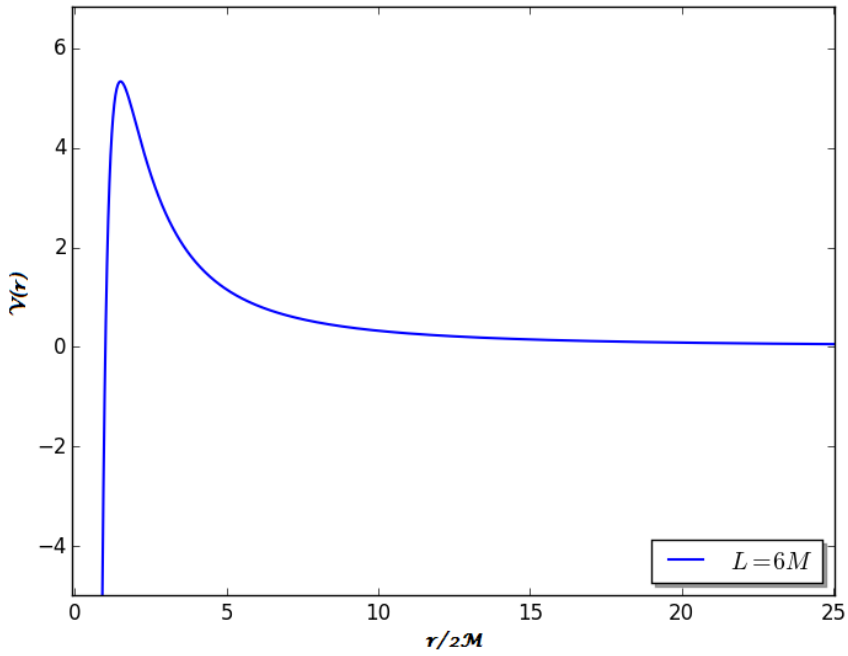


Figure 3.2: $V_{eff}$ for massless particle. Radius for the circular orbit does not depend on $L$.

## 3.3 Radially infalling particle

Taking into account the equations of motion in terms of the proper time $\tau$, now we consider the radial motion of a massive particle, in this case we have $L = 0$ and $\kappa = 1$, so from (3.35):

$$\dot{r} = -\sqrt{E^2 - 1 + \frac{2M}{r}} \tag{3.43}$$

and, as shown in Fig. 3.6 the potential becomes:

$$V(r) = 1 - \frac{2M}{r} \tag{3.44}$$

Integrate equation (3.43):

$$\int_{r(\tau_0)=r_0}^{r(\tau)=r} \frac{dr'}{\sqrt{E^2 - 1 + \frac{2M}{r'}}} = -\int_{\tau_0}^{\tau} d\tau' \tag{3.45}$$

The constant $E$ is fixed by initial conditions, for example, the simple case in which a particle is at rest ($\dot{r} = 0$) at $r = \infty$, we have the corresponding conserved energy $E = 1$ and (3.45) becomes:

$$\tau - \tau_0 = \frac{2}{3\sqrt{2M}} \left( \sqrt{r_0^3} - \sqrt{r^3} \right) \tag{3.46}$$

In this case, if we have two spherically symmetric sources with different masses $M_1$ and $M_2$, a radially infalling particle which satisfies $r(\tau_0) = r_0$, has a free fall time $\tau_1$ and $\tau_2$ respectively

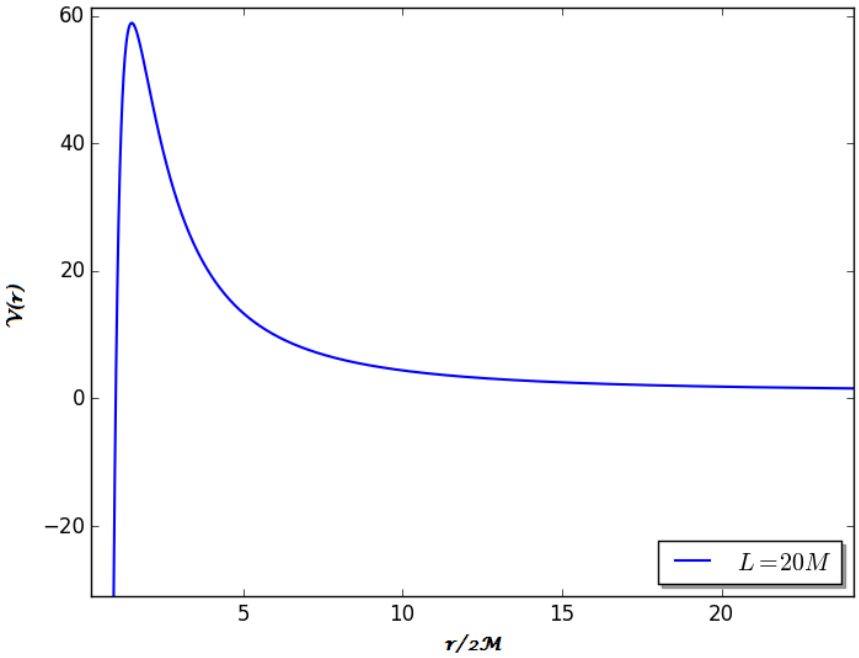


Figure 3.3: $V_{eff}$ for high values of $L$.

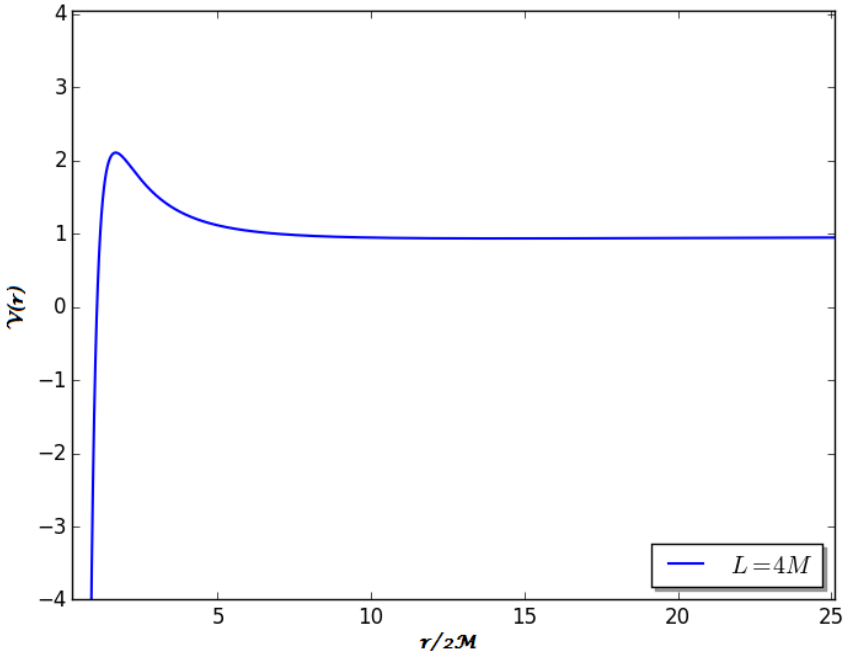


Figure 3.4: $V_{eff}$ for intermediate values of $L$.

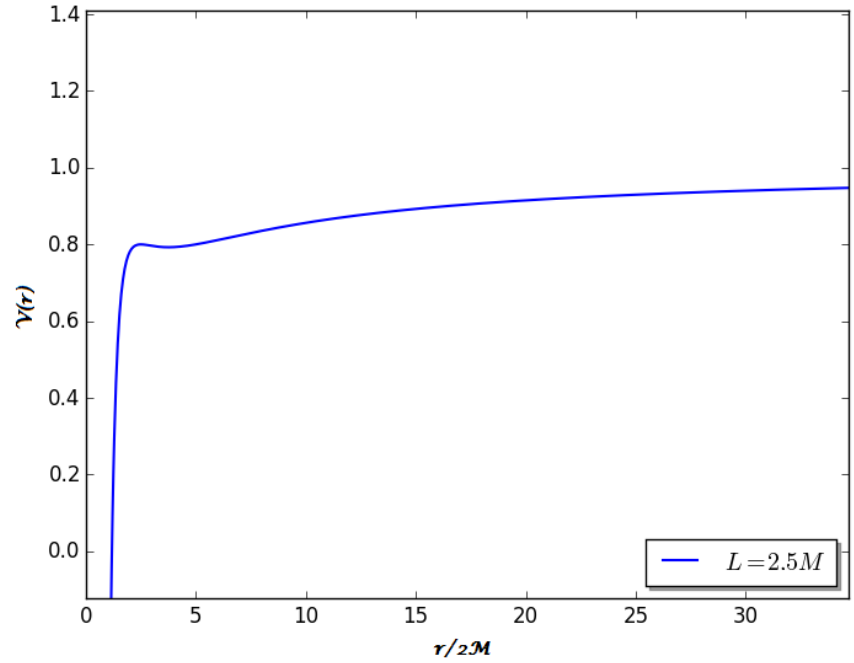


Figure 3.5: $V_{eff}$ for low values of $L$.

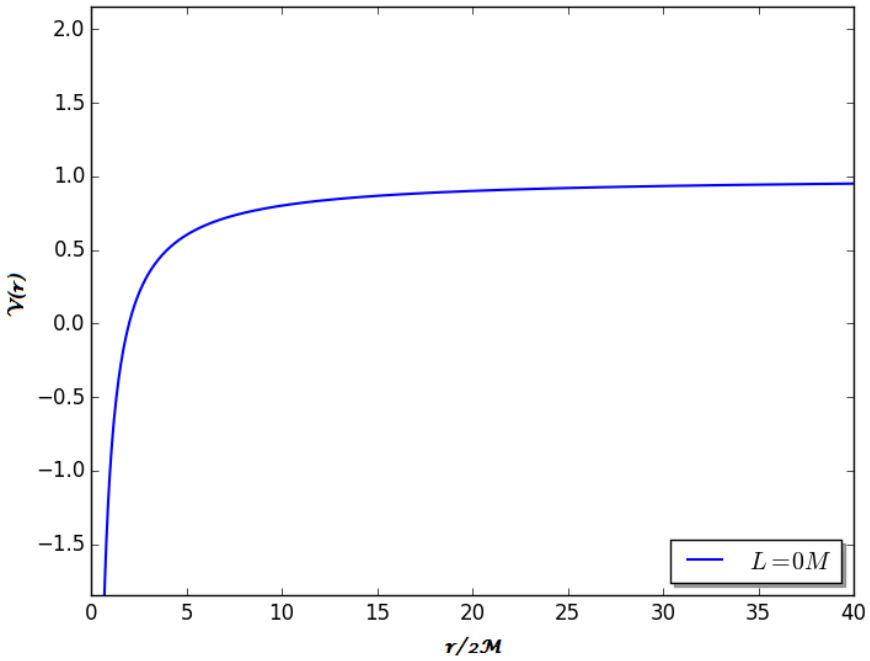


Figure 3.6: $V$ for $L = 0$ which represent the potential for a free radially infalling particle.

to reach the singularity in $r = 0$.

$$\Delta\tau = \tau_2 - \tau_1 = \frac{2\sqrt{r_0^3}}{3}\left(\frac{1}{\sqrt{2M_1}} - \frac{1}{\sqrt{2M_2}}\right) \tag{3.47}$$

Returning to the general case (if the particle starts from $r = r_0 \neq \infty$ with $\dot{r} = 0$ we have $E < 1$) we obtain:

$$\tau - \tau_0 = \left[ -\frac{r'}{\sqrt{1-E^2}}\sqrt{\frac{2M}{r'\left(1-E^2\right)} - 1} - \frac{2M}{2\sqrt{\left(1-E^2\right)^3}} \arctan\left(\frac{\frac{2M}{1-E^2} - 2r'}{2r'\sqrt{\frac{2M}{r'(1-E^2)} - 1}}\right)\right]_r^{r_0} \tag{3.48}$$

Now if we consider $\dot{r}(\tau_0) = 0$ and $r(\tau_0) = r_0$ we know that $1 - E^2 = \frac{2M}{r_0}$ and the proper time needed to reach $r$ is:

$$\tau - \tau_0 = \frac{M\pi}{2\sqrt{\left(\frac{2M}{r_0}\right)^3}} + \frac{r}{\sqrt{\frac{2M}{r_0}}}\sqrt{\frac{r_0}{r} - 1} + \frac{M}{\sqrt{\left(\frac{2M}{r_0}\right)^3}} \arctan\left(\frac{r_0 - 2r}{2r\sqrt{\frac{r_0}{r} - 1}}\right) \tag{3.49}$$

For example, if we are looking for a falling particle that reaches $r = 0$:

$$\begin{aligned} \tau - \tau_0 &= \frac{M\pi}{2\sqrt{\left(1-E^2\right)^3}} - \frac{r_0}{\sqrt{1-E^2}}\sqrt{\frac{2M}{r_0\left(1-E^2\right)} - 1} \\ &- \frac{2M}{2\sqrt{\left(1-E^2\right)^3}} \arctan\left(\frac{\frac{2M}{1-E^2} - 2r_0}{2r_0\sqrt{\frac{2M}{r_o(1-E^2)} - 1}}\right) \end{aligned} \tag{3.50}$$

And if $\dot{r} = 0$ when $r = r_0$ as in (3.49) we have the simpler result:

$$\tau - \tau_0 = \frac{\pi r_0}{2}\sqrt{\frac{r_0}{2M}} \tag{3.51}$$

Now like in (3.47) if we have two sources with masses $M_1$ and $M_2$ (with $R_{H1} = 2M_1$ e $R_{H1} = 2M_1$) and the particle's motion satisfies $r(\tau_0) = r_0$ and $\dot{r}(\tau_0) = 0$ in both cases, the energies are $E_1 = \sqrt{1 - \frac{2M_1}{r_0}}$ and $E_1 = \sqrt{1 - \frac{2M_1}{r_0}}$ respectively, so from (3.49) the proper time difference (to reach certain value for $r$) is:

$$\begin{aligned} \Delta\tau &= \tau_1 - \tau_2 = \frac{M_1\pi}{2\sqrt{\left(\frac{2M_1}{r_0}\right)^3}} + \frac{r}{\sqrt{\frac{2M_1}{r_0}}}\sqrt{\frac{r_0}{r} - 1} + \frac{M_1}{\sqrt{\left(\frac{2M_1}{r_0}\right)^3}} \arctan\left(\frac{r_0 - 2r}{2r\sqrt{\frac{r_0}{r} - 1}}\right) \\ &- \frac{M_2\pi}{2\sqrt{\left(\frac{2M_2}{r_0}\right)^3}} - \frac{r}{\sqrt{\frac{2M_2}{r_0}}}\sqrt{\frac{r_0}{r} - 1} - \frac{M_2}{\sqrt{\left(\frac{2M_2}{r_0}\right)^3}} \arctan\left(\frac{r_0 - 2r}{2r\sqrt{\frac{r_0}{r} - 1}}\right) \end{aligned} \tag{3.52}$$

and for $r = 0$:

$$\tau_1 - \tau_2 = \frac{\pi r_0}{2}\sqrt{\frac{r_0}{2}}\left(\frac{1}{\sqrt{M_1}} - \frac{1}{\sqrt{M_2}}\right) \tag{3.53}$$

these formulae will become useful later.

## 3.4 Orbits around a Black Hole

If we want to obtain the equations of the trajectories in the plane of motion $\theta = \frac{\pi}{2}$, we have to write the equation for $r$ in function of the angle $\phi$. To do this, we begin with:

$$\dot{r} = \frac{L}{r^2}\frac{dr}{d\phi} \tag{3.54}$$

then from (3.35) we have:

$$\ddot{r} = -\frac{L^2}{r^2}\frac{d^2}{d\phi^2}\left(\frac{1}{r}\right) = \frac{1}{2}\left(-\frac{2M}{r^2} + \frac{2L^2}{r^3} - \frac{6L^2M}{r^4}\right) = -\frac{d}{dr}V_{eff} \tag{3.55}$$

for the massive particles and from (3.36):

$$\ddot{r} = \frac{L^2}{r^3} - \frac{3ML^2}{r^4} \tag{3.56}$$

for the massless case.

Now we set $\frac{1}{r} = u$, in doing so we obtain for $\kappa = 1$:

$$\frac{d^2u}{d\phi^2} = \frac{M}{L^2} + 3Mu^2 - u \tag{3.57}$$

which is a non-linear non-homogeneous second-order differential equation, and for $\kappa = 0$:

$$\frac{d^2u}{d\phi^2} = -u + 3Mu^2 \tag{3.58}$$

which does not depend on $L$. In Newtonian mechanics, the orbit equation for a massive particle has the form:

$$\frac{d^2u}{d\phi^2} = \frac{M}{L^2} - u \tag{3.59}$$

so in (3.57) we have a correction term of $u^2$ order to the Newtonian case, this means that for high values of $r$, the Newtonian solutions approximate in a good way the solutions of the General Relativity. However, from the form of $V_{eff}(r)$, we note that there are different kind of orbits, in fact for a massive particle:

- for $E = V_{eff}(r_{0+})$ where $r_{0+} = \frac{L^2+L\sqrt{L^2-12M^2}}{2M}$, $V_{eff}(r)$ has a minimum which corresponds to the stable circular orbit;
- for $E = V_{eff}(r_{0+})$ where $r_{0-} = \frac{L^2-L\sqrt{L^2-12M^2}}{2M}$, $V_{eff}(r)$ has a maximum which corresponds to the unstable circular orbit;
- bound orbits;
- scattered orbits;
- capture orbits.

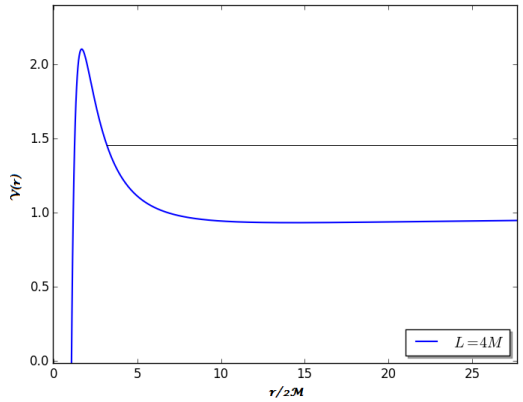


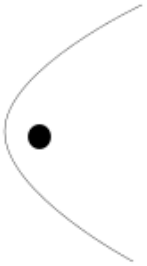

Figure 3.7: Energy level corresponding to a scattering orbit.

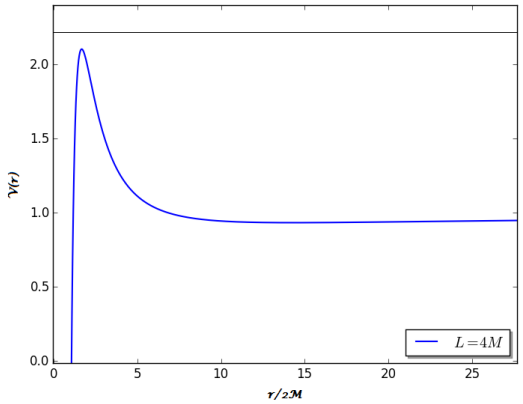


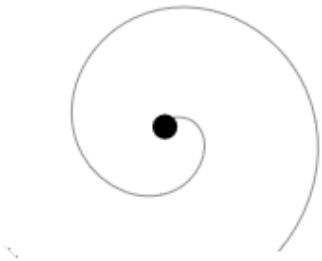

Figure 3.8: Energy level corresponding to a particle capture orbit.

As $L$ decreases, the maximum decreases and when $L < \sqrt{12}M$ there are no maxima or minima; in fact fixing the values of the constants $L$ and $E$ we define the shape of the function $V_{eff}(r)$ and the energy level. Some situations that one can face with are shown in Fig. 3.7, 3.8 and 3.9.

It is possible to solve exactly the orbit equation by using the elliptical functions obtaining:

$$u = u_1 + (u_2 - u_1)\, sn^2 \left( \frac{\phi}{2} \sqrt{2M\,(u_3 - u_1)} + \delta \right) \tag{3.60}$$

in which $sn$ is one of the Jacobi elliptical functions where $\delta$ is an integration constant dependent on the initial conditions and $u_1$, $u_2$, $u_3$ are the solutions for the equation:

$$E^2 - 1 + 2Mu - L^2u^2 + 2L^2Mu^3 = 0 \tag{3.61}$$

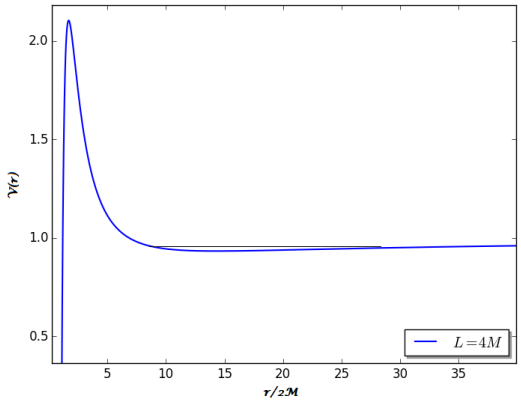


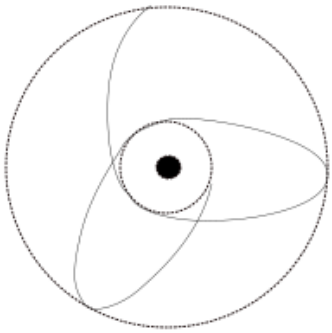

Figure 3.9: Energy level corresponding to a bound precessing orbit.

which corresponds to:

$$\frac{du}{d\phi} = 0 \tag{3.62}$$

They satisfy the equation:

$$u_1 + u_2 + u_3 = \frac{1}{2M} \tag{3.63}$$

We are now going to study a particular particle orbit: the unstable circular one. Circular orbits occur when the first derivative of the potential is null, i.e. when the following equation holds:

$$\frac{d^2u}{d\phi^2} = \frac{M}{L^2} + 3Mu^2 - u = 0 \tag{3.64}$$

which is satisfied for these two values for $u$:

$$u_{0\pm} = \frac{1 \pm \sqrt{1 - 12\frac{M^2}{L^2}}}{6M} \tag{3.65}$$

here $u_{0+}$ is the unstable one while $u_{0-}$ is the stable one. From these results we can see that we have maxima and minima only if $L \geqslant \sqrt{12}M$.

If we start with the initial conditions for the unstable circular orbit:

$$\begin{cases} u(0) = u_{0+} \\ \dot{u}(0) = 0 \end{cases} \tag{3.66}$$

a particle remains at this value for $r$ (or $u$) if the system is not perturbed. Even a small perturbation causes a completely different result, we are going to study precisely these situations. We could have little deviations from the unstable circular orbit initial conditions or in the mass measure, both bring to an orbit different from the circular one but they affect the motion in different ways. Let's start from fixed initial conditions given in (3.66), if we modify the mass source with a small correction $M \to M + \Delta M$ for some $\Delta M$, the orbit equation becomes:

$$\frac{d^2u}{d\phi^2} = 3Mu^2 + 3\Delta Mu^2 - u + \frac{M}{L^2} + \frac{\Delta M}{L^2} \tag{3.67}$$

Now we solve this new equation by means of perturbation method, in fact if we consider small deviation from $M$ we can set $\epsilon = 3\delta M = 3\frac{\Delta M}{M}$ and the new solution will be of the form:

$$u = u_{0+} + \epsilon u_1 + o\left(\epsilon^2\right) \tag{3.68}$$

(small deviations imply $|\epsilon| << 1$). So at zero order in $\epsilon$ we have the equation for $u$ corresponding to (3.64) which bring to the circular unstable orbit, while at first order we find:

$$\frac{d^2u_1}{d\phi^2} = 6Mu_{0+}u_1 + Mu_{0+}^2 - u_1 + \frac{M}{3L^2} \tag{3.69}$$

From (3.65) we have to resolve the equation for $u_1$:

$$\frac{d^2u_1}{d\phi^2} = \sqrt{1 - 12\frac{M^2}{L^2}}u_1 + Mu_{0+}^2 + \frac{M}{3L^2} \tag{3.70}$$

and the solution is of the form:

$$u_1 = A\cosh\left(\sqrt[4]{1 - 12\frac{M^2}{L^2}}\phi\right) + B\sinh\left(\sqrt[4]{1 - 12\frac{M^2}{L^2}}\phi\right) - M\frac{u_{0+}^2 + \frac{1}{3L^2}}{\sqrt{1 - 12\frac{M^2}{L^2}}} \tag{3.71}$$

We fix the constant $A$ and $B$ from the initial conditions (3.66) which read:

$$\begin{cases} u_1(0) = 0 \\ \dot{u}_1(0) = 0 \end{cases} \tag{3.72}$$

and finally one has:

$$A = M\frac{u_{0+}^2 + \frac{1}{3L^2}}{\sqrt{1 - 12\frac{M^2}{L^2}}} \tag{3.73}$$

$$B = 0 \tag{3.74}$$

So the perturbed solution at first order is:

$$u(\phi) = u_{0+} + 3\Delta M\left(\frac{u_{0+}^2 + \frac{1}{3L^2}}{\sqrt{1 - 12\frac{M^2}{L^2}}}\cosh\left(\sqrt[4]{1 - 12\frac{M^2}{L^2}}\phi\right) - \frac{u_{0+}^2 + \frac{1}{3L^2}}{\sqrt{1 - 12\frac{M^2}{L^2}}}\right) \tag{3.75}$$

so the particle falls through the singularity of the source forming a spiral when we have positive corrections $\Delta M > 0$ while particle become more and more distant from the circular orbit if we have negative corrections $\Delta M < 0$ instead of remaining at a fixed radius as shown in Fig. 3.10. In fact, if we started with $E$ and $L$ such that we have the unstable circular orbit, a correction to $M$ modifies the position of the maximum of $V_{eff}$ and so we have a motion different from the circular one.

The solution found with these perturbation method can be compared with the numerical solution obtained from a calculator as we can see in Fig. 3.11. As expected for small value of $u$ the solution obtained with the two methods are practically the same and begin to be different from each other as $u$ increases, in fact the perturbation solution is accurate enough in the range of small $\frac{\Delta R_H}{r}$ and $|\epsilon| << 1$, if these conditions are not satisfied one has to consider also higher

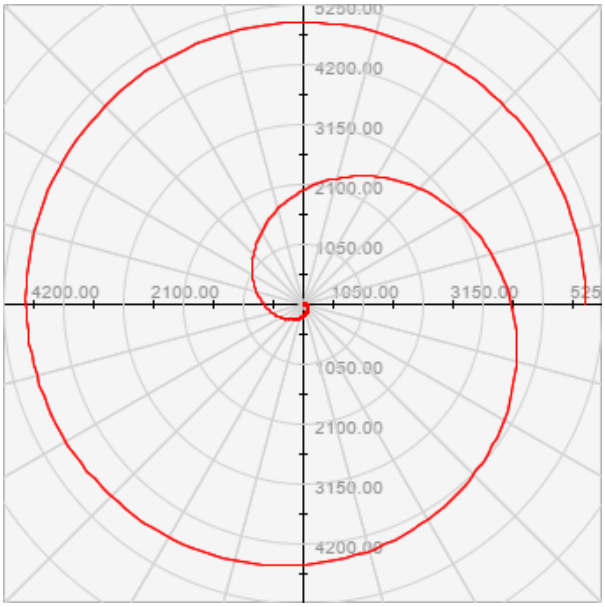


Figure 3.10: Modified orbit with $M \longrightarrow M + \Delta M$ in the case $R_H = 3000m$, $\Delta M = 0.001M$ if we have a massive particle.

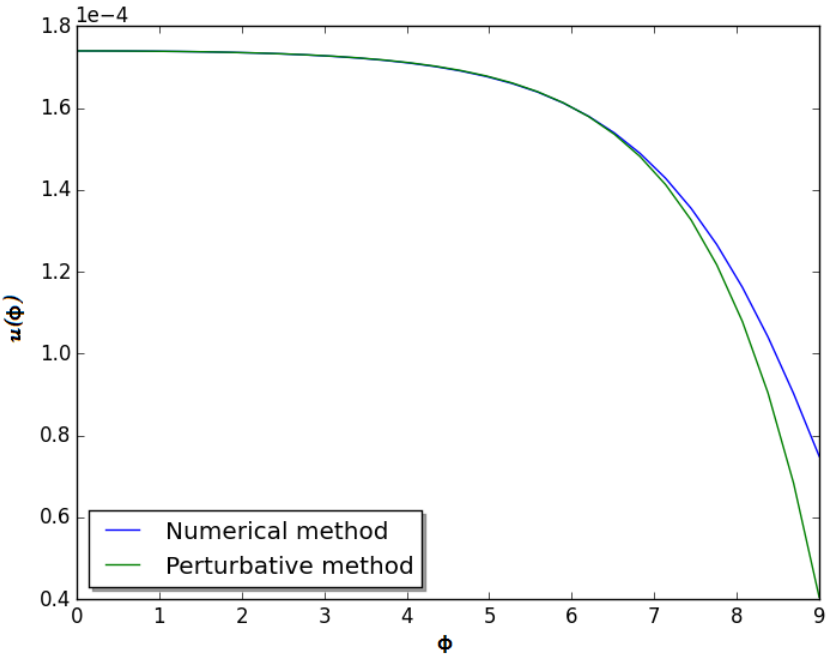


Figure 3.11: The corrected orbits $u(\phi)$ generate from $\Delta M = -1.5m$ obtained with numerical and perturbation method. (For $M = 1500m$ and $L = 6300m$)

order corrections (in a semilogarithmic scale this can be seen in a better way as shown in Fig. 3.12).

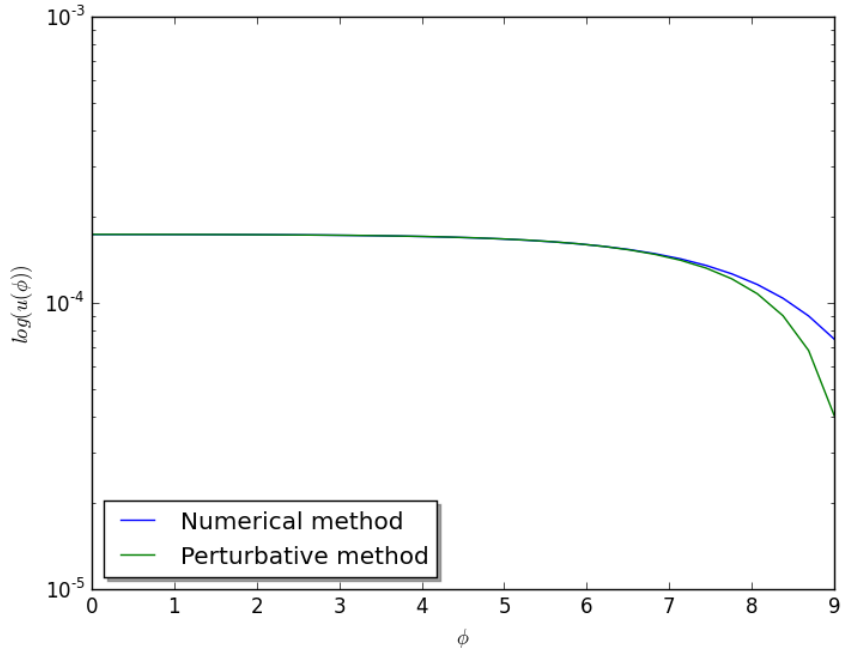


Figure 3.12: The corrected orbits $u(\phi)$ generate from $\Delta M = -1.5m$ obtained with numerical and perturbation method in semilogarithmic scale. (For $M = 1500m$ and $L = 6300m$)

We can find a lower limit on the correction $\Delta M$, in fact if we want an appreciable effect, we have to be able to see an effective diminution of the radius in a reasonable amount of time or number of turn around the source. Inverting the equation (3.75) we obtain the number of turns needed to reach some value $r$ starting from $u_{0+}$ as a function of $\Delta M$:

$$\phi_r(\Delta M) = \frac{\cosh^{-1}\left(1 + \frac{\sqrt{1-12\frac{M^2}{L^2}}\left(\frac{1}{r}-u_{0+}\right)}{3\Delta M\left(u_{0+}^2+\frac{1}{3L^2}\right)}\right)}{\left(1-12\frac{M^2}{L^2}\right)^{1/4}} \tag{3.76}$$

we see that the argument in $\cosh^{-1}$ is in the interval $[1,\infty)$, in fact if one has $\Delta M = \infty$ there will be the corresponding $\cosh^{-1}(1) = 0$ which means $\phi_r = 0$ but this situation is out of our condition $\frac{\Delta M}{M} << 1$, the other extreme of the domain gives us the situation $\Delta M = 0$ which reads $\cosh^{-1}(\infty) = \infty = \phi_r$ so we can never reach $r$ starting from $r_0 = \frac{1}{u_{0+}}$ with $\Delta M = 0$ (without perturbations particle remains at that radius). Fixing an upper limit to $\phi$ (the maximum number of turns in which one has to be able to reach $r$) we impose a lower one to $\Delta M$.

Now if we consider the massless case we can have a different function for $V_{eff}(r)$ and as we see in Fig. 3.13 and 3.14 we can have:

- capture trajectories;
- scattering trajectories;

- unstable circular orbit for $r = r_0 = 3M$.

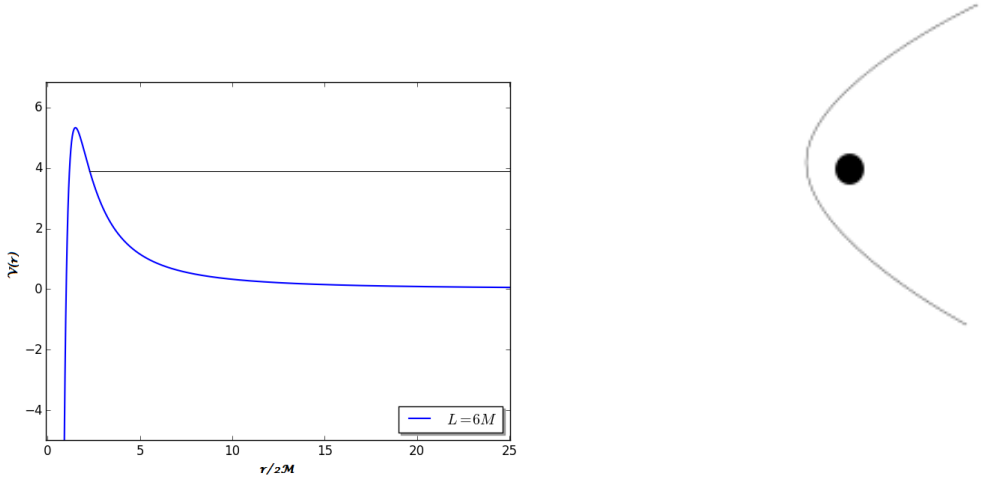


Figure 3.13: Energy level corresponding to a (massless) particle scattering orbit.

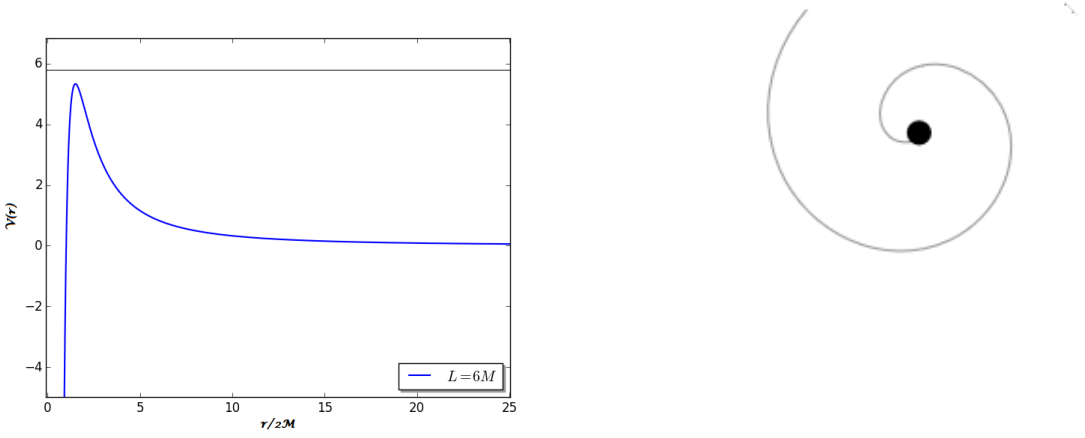


Figure 3.14: Energy level corresponding to (massless) particle capture.

From here we proceed as in the massive case and we can study the perturbed unstable circular orbit. If we add a correction $\Delta M$ to $M$ such that $\left|\frac{\Delta M}{M}\right| << 1$ we obtain the perturbed orbit

equation:

$$\frac{d^2u(\phi)}{d\phi^2} = 3Mu^2 + 3\Delta M u^2 - u \tag{3.77}$$

and, if we set $\epsilon = 3\frac{\Delta M}{M}$, the perturbed solution can be expressed in the form:

$$u(\phi) = u_0 + \epsilon u_1(\phi) \tag{3.78}$$

in which $u_0 = \frac{1}{3M} = u(0)$ with $\dot{u}(0) = 0$.

At the first order we obtain the equation for $u_1$ which reads:

$$\frac{d^2u_1(\phi)}{d\phi^2} = u_1(\phi) + \frac{1}{9M} \tag{3.79}$$

knowing the initial conditions our result is:

$$u(\phi) = \frac{1}{3M} + \epsilon\left(\frac{\cosh(\phi)}{9M} - \frac{1}{9M}\right) \tag{3.80}$$

Inverting this formula we can find the number of turns around the source to reach some $\bar{r}$

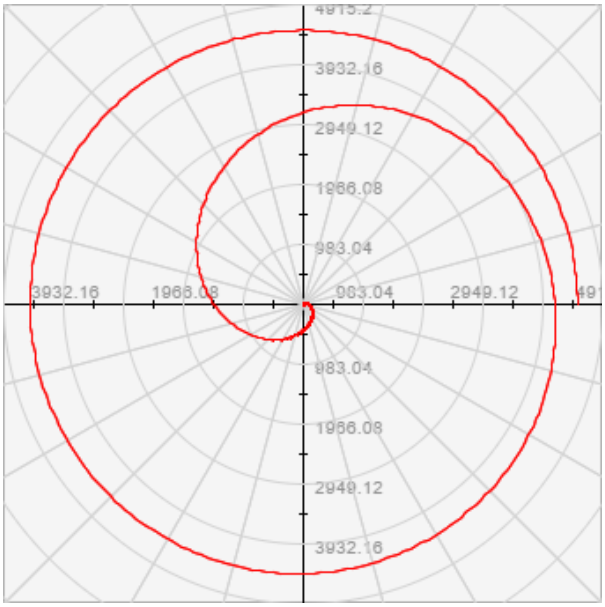


Figure 3.15: Modified orbit with $M \longrightarrow M + \Delta M$ in the case $R_H = 3000m$, $\Delta M = 0.001M$ if we have a massless particle.

starting from $r = 3M$ as a function of mass deviation $\Delta M$:

$$\phi_{\bar{r}}(\Delta M) = \cosh^{-1}\left(\left(\frac{1}{\bar{r}} - \frac{1}{3M}\right)\frac{9M^2}{\Delta M} + 1\right) \tag{3.81}$$

the same considerations of the massive case holds in this case.

# Part II

# Fuzzy Black Hole Space-Times

# Chapter 4

# Horizon Wave Function

In this chapter we introduce the Horizon Wave Function (HWF) that give us a probability distribution for the gravitational radius.

## 4.1 Quantized gravitational radius

In quantum mechanics, the states of a system are codified in terms of some wave function $\psi_s \in L^2\left(\mathbb{R}^3\right)$. Wave functions have to be in the space of all possible states the system can have and we can decompose the matter state on the basis of energy eigenstates of the system:

$$|\psi_s\rangle = \sum_{E_\alpha} C\left(E_\alpha\right)|E_\alpha\rangle \tag{4.1}$$

If our system has an Hamiltonian $H$, in quantum mechanics this quantity becomes an operator acting on the system's states space, $\widehat{H}\,|E_\alpha\rangle = E_\alpha\,|E_\alpha\rangle$ ($|E_\alpha\rangle$ are the energy eigenstates with eigenvalue $E_\alpha$) so one obtains the energy spectrum.

This can be applied on the study of the event horizon. Consider a system in which one has two sets of variables which correspond to the matter ($E$) and gravitational ($R_H$) degrees of freedom, the state of this system can be described by means of:

$$|\Psi\rangle = \sum_{\alpha,\beta} c_{\alpha,\beta}\,|E_\alpha, R_{H\beta}\rangle \tag{4.2}$$

Now one can identify the ADM mass function to the mean value for the Hamiltonian on the matter state:

$$\lim_{r\to\infty} m(r) = m \to \langle\psi_s|\,\widehat{H}\,|\psi_s\rangle = \sum_{\alpha} \left|c_s\left(E_\alpha\right)\right|^2 E_\alpha \tag{4.3}$$

As we have seen, in General Relativity when we are faced with the Schwarzschild solution, we can introduce the gravitational radius defined by the relation:

$$r_H\left(r\right) = 2\frac{l_P}{m_P} m\left(r\right) \tag{4.4}$$

in which $m\left(r\right)$ is the Misner-Sharp mass function defining in that way a local gravitational radius. Instead, when we use the asymptotic value of $m\left(r\right)$ given by the ADM mass $m$, we define a global gravitational radius. In the last case we are not interested in the interior structure of the source but only on its asymptotic mass.

The Schwarzschild radius is defined in terms of total energy (or as we have seen to the ADM mass)[1]:

$$r_H = 2\frac{l_P E}{m_P} = 2M \tag{4.6}$$

So, similar to energy, we do not have a precise value for $r_H$ in quantum mechanics, but the Schwarzschild radius becomes an observable and, in the space of the states of the system, acts as an adjoint operator $\widehat{r}_H = \widehat{r}_H^{\dagger}$. In this way we can define the gravitational radius eigenstates as:

$$\widehat{R}_H \left|R_{H_\beta}\right\rangle = R_{H_\beta} \left|R_{H_\beta}\right\rangle \tag{4.7}$$

From here the condition for the Schwarzschild radius reads as:

$$\left(\widehat{H} - \frac{m_P}{2l_P}\widehat{R}_H\right)|\Psi\rangle = 0 \tag{4.8}$$

which can be satisfied by the wave function:

$$|\Psi\rangle = \sum_\alpha c\left(E_\alpha, \frac{2l_P}{m_P}E_\alpha\right)|E_\alpha\rangle\,|R_{H\alpha}\rangle \tag{4.9}$$

From this function we can extract both matter state and gravitational state:

$$\begin{cases} |\psi_S\rangle = \sum_\alpha c_S\left(E_\alpha\right)|E_\alpha\rangle \\ |\psi_H\rangle = \sum_\alpha c_S\left(\frac{m_P}{2l_P}R_{H\alpha}\right)|R_{H\alpha}\rangle \end{cases} \tag{4.10}$$

In doing so we can introduce another wave function $\psi_H\left(r_H\right)$: the **Horizon Wave Function** (HWF) [5]. This object is defined by the relation:

$$\psi_H\left(R_H\right) = \langle R_H|\psi_H\rangle = C\left(\frac{m_P R_H}{2l_P}\right) \tag{4.11}$$

We have to normalize $|\psi_H\rangle$, as usual, with the Schrödinger scalar product:

$$\begin{aligned} \langle\psi_H|\phi_H\rangle &= \int_0^\infty dr_H \int_0^\pi d\theta \int_0^{2\pi} d\varphi r_H^2 \sin\theta \psi_H^*\left(r_H\right)\phi_H\left(r_H\right) \\ &= 4\pi\int_0^\infty dr_H r_H^2 \psi_H^*\left(r_H\right)\phi\left(r_H\right) \end{aligned} \tag{4.12}$$

Normalization requires:

$$\langle\psi_H|\psi_H\rangle = 1 \tag{4.13}$$

In this way, HWF describes the states for the Schwarzschild radius of a certain source, so it can be used in calculating the probabilities to have some values for $r_H$ and the probability to

[1] Considering quantum effect we have to take into account that the Schwarzschild radius should not be covered by the corresponding Compton lenght:

$$r_H = 2M \gtrsim \lambda_M = \frac{l_P^2}{M} \tag{4.5}$$

which means that $m > m_P$ and $M > l_P$.

have a Black Hole instead of a simple particle. In fact, if a source can be represented by the wave function $\psi_S(r)$, the probability that the source has $r < r_H$ is given by:

$$P(r < r_H) = 4\pi \int_0^{r_H} dr r^2 |\psi_S(r)|^2 \tag{4.14}$$

At the same time, the corresponding HWF defines the probability density that the particle has a Schwarzschild radius which is equal to $r_H$:

$$p_H(r_H) = 4\pi r_H^2 |\psi_H(r_H)|^2 \tag{4.15}$$

From here, one obtain the probability density that the particle is a Black Hole in the following way:

$$p_{BH}(r_H) = P(r < r_H)\, p_H(r_H) \tag{4.16}$$

since there are no restrictions on the possible values of $r_H$, the final probability is:

$$P_{BH} = \int_0^{\infty} p_{BH}(r_H)\, dr_H \tag{4.17}$$

At this point it is possible to study the fluctuations of $r$ and $r_H$ and to obtain a more general form of the uncertainty principle (GUP). The uncertainty in $r$ is given by:

$$\Delta r^2 = \langle \psi_S(r)^2 \rangle - \langle \psi_S(r) \rangle^2 \tag{4.18}$$

For $r_H$:

$$\Delta r_H^2 = \langle \psi_H(r_H)^2 \rangle - \langle \psi_H(r_H) \rangle^2 \tag{4.19}$$

Finally, to obtain the GUP we need to calculate the uncertainty in $p$:

$$\Delta p^2 = \langle \psi_S(p)^2 \rangle - \langle \psi_S(p) \rangle^2 \tag{4.20}$$

In such a way that the total uncertainty in measuring the radius is a linear combination of the square root of (4.18) and (4.19) which are related with (4.20) to give us the generalized uncertainty principle.

Another way to study Black Holes formation is in terms of collisions of two (or more) particles. The states of a system of N particles are codified in a wave function of the form:

$$\psi_S(x_1, x_2, ...x_N) = \prod_{i=1}^{N} \psi_{Si}(x_i) \tag{4.21}$$

Like in the previous case, one can decompose the WF on the complete and orthonormal basis of energy eigenstates, and from (4.6) one obtains the HWF. In this case, $\psi_H(r_H)$ describes the states of the whole system of colliding particles of the system.

If we have two particles one of the parameters of scattering phenomena is the impact parameter $b$, at the end of the scattering we face with a Black Hole if:

$$b < r_H \tag{4.22}$$

in which $r_H$ came from (4.6) and $E$ represents the total energy of the whole system. This condition is known as the **Hoop conjecture**. As in the case of a single particle we can define the probability of having a Black Hole in the case of N particles too.

## 4.2 Gaussian sources

What we have said about the HWF can be applied, for an example, at the case in which the source can be described by a Gaussian Wave Function centred at the origin of the coordinate system (this is an important example because any other localized wave function can be expressed as a sum of Gaussian functions).

$$\psi_S(r) = \frac{e^{-\frac{r^2}{2l^2}}}{(l\sqrt{\pi})^{\frac{3}{2}}} \tag{4.23}$$

$l$ is a length scale that define the width of the gaussian and now we consider the case in which $l$ is the Compton length of the particle $l \sim l_P \frac{m_P}{m}$. The correspondent wave function in the momentum space (Fourier transform) is given by:

$$\tilde{\psi}_S(p) \sim \frac{e^{-\frac{p^2}{2\Delta^2}}}{(\Delta\sqrt{\pi})^{\frac{3}{2}}} \tag{4.24}$$

From the Minkowskian mass-shell condition $m^2 = E^2 - p^2$ [2] ($m$ is the rest mass of the particle which is not equal to the total energy $m \leqslant E$) we can write:

$$\tilde{\psi}_S(E) \sim \frac{e^{-\frac{E^2-m^2}{2\Delta^2}}}{(\Delta\sqrt{\pi})^{\frac{3}{2}}} \tag{4.25}$$

and then from the Schwarzschild radius relation $R_H = \frac{2ml_P}{m_P} = 2M$, $r_H = \frac{2El_P}{m_P}$:

$$\tilde{\psi}_S(r_H) \sim \frac{e^{-\frac{\left(\frac{m_P r_H}{2l_P}\right)^2 - \left(\frac{m_P R_H}{2l_P}\right)^2}{2\Delta^2}}}{(\Delta\sqrt{\pi})^{\frac{3}{2}}} \tag{4.26}$$

Normalizing with the scalar product:

$$\psi_H(r_H) = \frac{1}{4l_P^3}\sqrt{\frac{l^3}{\pi\Gamma\left(\frac{3}{2}, \frac{m^2}{\Delta^2}\right)}}\theta(r_H - R_H)\, e^{-\frac{l^2 r_H^2}{8l_P^4}} \tag{4.27}$$

this latter can be used for calculate the probability that the particle is a Black Hole. (4.27) represents a Gaussian function of the gravitational radius $r_H$ centered in $r_H = R_H$ ($R_H = 2m\frac{l_P}{m_P}$) cut for $r_H < R_H$.

Let us calculate the deviation $\Delta r_H$ and how the GUP works here.

$$\begin{aligned} \Delta r_H^2 &= \langle r_H \rangle^2 - \langle {r_H}^2 \rangle = \left( \int |\psi_H(\vec{r}_H)|^2 \vec{r}_H d\vec{r}_H \right)^2 - \int |\psi_H(\vec{r}_H)|^2 \vec{r}_H^2 d\vec{r}_H \\ &= \left( 4\pi \int_0^\infty dr_H r_H^3 |\psi_H(r_H)|^2 \right)^2 - 4\pi \int_0^\infty dr_H r_H^4 |\psi_H(r_H)|^2 \end{aligned} \tag{4.28}$$

[2] We use that relation because in the definition of Misner-Sharp mass we calculate the total energy as if the space were flat.

substituting (4.27) in the latter equation:

$$\Delta r_H = 2\frac{l_P^2}{l}\sqrt{\left(\frac{E_{-\frac{3}{2}}(1)}{E_{-\frac{1}{2}}(1)} - \frac{E_{-1}(1)}{E_{-\frac{1}{2}}(1)}\right)} \tag{4.29}$$

where we have defined the function:

$$E_n(x) = \int_1^\infty \frac{e^{-xt}}{t^n} dt \tag{4.30}$$

So we see that in the case of a Gaussian source wave function $\Delta r_H \sim l^{-1} \sim m \sim R_H$ which means that the fluctuations in $r_H$ are of the same magnitude of the $R_H$ itself. For this reason the HWF derived from the Gaussian source cannot be used in the case of an astronomical Black Hole ($m >> m_P$) because they should behave semi-classically, so we cannot model them as a tiny mass source which deforms the space-time metric around it. We should find another kind of WF to describe macroscopic BHs, such like extended state (in fact any localized state can be expressed in terms of Gaussian states) or talking about BHs as a Bose-Einstein condensate (BEC) of gravitons.

Now we see as the GUP works in this example of Gaussian source. Let us calculate the uncertainty in $r$ given by (4.18) and in the present case become:

$$\Delta r = l^2 \frac{3\pi - 8}{2\pi} = l^2 \Delta_{QM} \tag{4.31}$$

The uncertainty in $p$ is given by (4.20):

$$\Delta p^2 = \Delta_{QM} \frac{l_P^2 m_P^2}{l^2} \tag{4.32}$$

So, the total uncertainty in radius is given by:

$$\Delta R = \Delta r + \epsilon \Delta r_H \tag{4.33}$$

with some constant $\epsilon$ and expressing $\Delta r_H$ in term of $\Delta p$ the equation (4.33) represent the GUP.

In the previous paragraph we wrote about the probability to have a Black Hole from a given WF. Inserting $\psi_S(r)$ and $\psi_H(r_H)$ of the present example we can calculate effectively this probability. Results that the particle is more probably a Black Hole if $m \gtrsim m_P$ while the probability density goes rapidly to zero for $m < m_P$ Fig. 4.1.

After that, we can apply these results in the case of the radially infalling particle, and calculate the time difference for a particle that starts its motion from the initial conditions $r(\tau_0) = r_0$ and $\dot{r}(\tau_0) = 0$ but with $M_1 = M$ and $M_2 = M + \frac{\Delta r_H}{2}$, so the time difference from

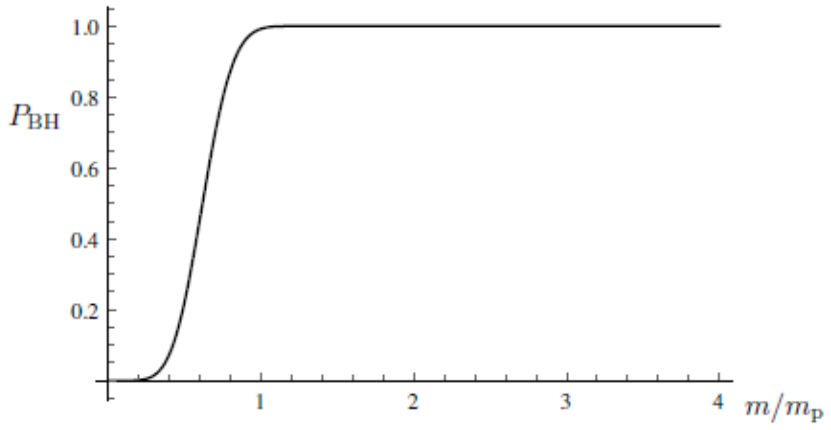


Figure 4.1: Probability that a particle with $m \sim l^{-1}$ is a Black Hole [5].

(3.52) is:

$$\begin{aligned}\Delta\tau_1 &= \tau_1 - \tau_2 = \frac{\pi}{2\sqrt{\frac{8M}{r_0^3}}} + \frac{r}{\sqrt{\frac{2M}{r_0}}}\sqrt{\frac{r_0}{r}-1} + \frac{1}{\sqrt{\frac{8M}{r_0^3}}}\arctan\left(\frac{r_0-2r}{2r\sqrt{\frac{r_0}{r}-1}}\right) \\ &- \frac{\pi}{2\sqrt{\frac{8\left(M+\frac{l_P^2}{l}\sqrt{\left(\frac{E_{-\frac{3}{2}}(1)}{E_{-\frac{1}{2}}(1)}-\frac{E_{-1}(1)}{E_{-\frac{1}{2}}(1)}\right)}\right)}{r_0^3}}} - \frac{r}{\sqrt{\frac{2\left(M+\frac{l_P^2}{l}\sqrt{\left(\frac{E_{-\frac{3}{2}}(1)}{E_{-\frac{1}{2}}(1)}-\frac{E_{-1}(1)}{E_{-\frac{1}{2}}(1)}\right)}\right)}{r_0}}}\sqrt{\frac{r_0}{r}-1} \\ &- \frac{\arctan\left(\frac{r_0-2r}{2r\sqrt{\frac{r_0}{r}-1}}\right)}{\sqrt{\frac{8\left(M+\frac{l_P^2}{l}\sqrt{\left(\frac{E_{-\frac{3}{2}}(1)}{E_{-\frac{1}{2}}(1)}-\frac{E_{-1}(1)}{E_{-\frac{1}{2}}(1)}\right)}\right)}{r_0^3}}}\end{aligned} \tag{4.34}$$

while in the more general case, if $M_2 = M + n\frac{\Delta r_H}{2}$:

$$\begin{aligned}\Delta\tau_n &= \tau_1 - \tau_2 = \frac{\pi}{2\sqrt{\frac{8M}{r_0^3}}} + \frac{r}{\sqrt{\frac{2M}{r_0}}}\sqrt{\frac{r_0}{r} - 1} + \frac{1}{\sqrt{\frac{8M}{r_0^3}}}\arctan\left(\frac{r_0 - 2r}{2r\sqrt{\frac{r_0}{r} - 1}}\right) \\ &- \frac{\pi}{2\sqrt{\frac{8\left(M + n\frac{l_P^2}{l}\sqrt{\left(\frac{E_{-\frac{3}{2}}(1)}{E_{-\frac{1}{2}}(1)} - \frac{E_{-1}(1)}{E_{-\frac{1}{2}}(1)}\right)}\right)}{r_0^3}}} - \frac{r}{\sqrt{\frac{2\left(M + n\frac{l_P^2}{l}\sqrt{\left(\frac{E_{-\frac{3}{2}}(1)}{E_{-\frac{1}{2}}(1)} - \frac{E_{-1}(1)}{E_{-\frac{1}{2}}(1)}\right)}\right)}{r_0}}}\sqrt{\frac{r_0}{r} - 1} \\ &- \frac{\arctan\left(\frac{r_0 - 2r}{2r\sqrt{\frac{r_0}{r} - 1}}\right)}{\sqrt{\frac{8\left(M + n\frac{l_P^2}{l}\sqrt{\left(\frac{E_{-\frac{3}{2}}(1)}{E_{-\frac{1}{2}}(1)} - \frac{E_{-1}(1)}{E_{-\frac{1}{2}}(1)}\right)}\right)}{r_0^3}}}\end{aligned} \tag{4.35}$$

So, as we have seen, if we have a probability distribution for $E \sim M$, there is also a probability distribution for the fall time associated with the HWF.

# Chapter 5

# Modified unstable circular orbits

Now we can study the particular case in which Black Hole's mass $M$ is not a simple single value but it is represented by some probability distribution. Let's study how this situation reflects itself on the particles motion.

We have calculated in the previous chapter how corrections in $M$ modify orbits (starting from unstable circular orbit). So if we have a probability distribution for $\Delta M$ (and $r_H$), a test particle with given initial conditions does not follow a fixed trajectory but there is a probability distribution for all the possible trajectories of the particle. At this point, we can study two situations:

- Starting from the unperturbed orbits equation we consider initial conditions for the unstable circular orbit and then study how deviations from these initial conditions affect the starting circular trajectory. To do that, suppose that to have a discrete distribution for the initial conditions, so if we have the modified initial conditions:

$$r_i(0) = r_{0-} + dr_i \tag{5.1}$$

$$\dot{r_i}(0) = 0 \tag{5.2}$$

  every correction $dr_i$ has a corresponding probability $P_i$ to occur (with $i$ discrete collection of indexes). Consequently the particle trajectory generated from the i-th initial conditions has a probability $P_i$ to occur, so if we have a probability distribution for initial conditions there is a correspondent trajectories probability distribution;

- Starting from the fixed initial conditions for the unstable circular orbit:

$$r(0) = r_{0-} \tag{5.3}$$

$$\dot{r}(0) = 0 \tag{5.4}$$

  consider deviation from $M$ and study how they affect the particle motion, so in this situation consider a discrete collection of corrections $\Delta M_i$ for $M$ with the correspondent probability $P_i$ to occur:

$$M_i = M + \Delta M_i \tag{5.5}$$

  with $i$ discrete collection of indexes. In this case we have a probability distribution of modified orbits equations and consequently of particle trajectories.

The latter case is the same that we have studied in the previous chapter and the resulting orbits have the form:

$$u_i(\phi) = u_{0+} - 3\Delta M_i \frac{u_{0+}^2 + \frac{1}{3L^2}}{\sqrt{1 - 12\frac{M^2}{L^2}}} + 3\Delta M_i \frac{u_{0+}^2 + \frac{1}{3L^2}}{\sqrt{1 - 12\frac{M^2}{L^2}}} \cosh\left(\sqrt[4]{1 - 12\frac{M^2}{L^2}}\phi\right) \tag{5.6}$$

until $\left|\frac{\Delta M_i}{M}\right| << 1$. Some examples are represented in Fig. 5.1 (in the following figures $u(\phi)$ is in $m^{-1}$ and $\phi$ in $rad$).

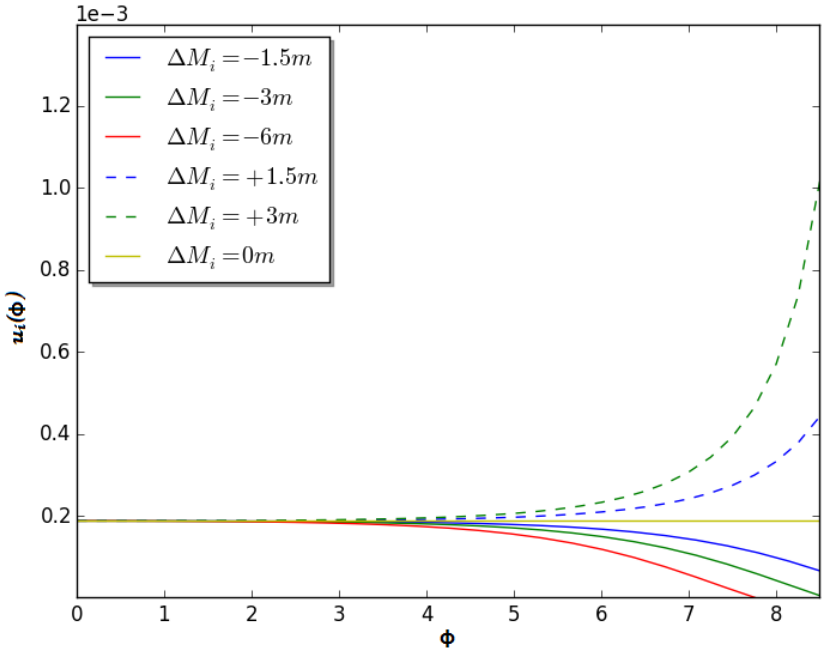


Figure 5.1: Orbits (obtained with the numerical method) generated from different corrections on $M$ starting from the unstable circular orbit (solid yellow) for $M = 1500m$ and $L = 7250m$.

For a certain distribution $P_i$ of $M_i$ we have a distribution of capture or escape orbits due to positive or negative corrections respectively. As we have seen this distribution could come from the Horizon Wave Function of the source. In this way, starting from this wave function, it will be possible to calculate the probability that a particle is in $r = \bar{r}$ after a certain number of turns $\bar{N} = \frac{\bar{\phi}}{2\pi}$ (or equivalently for a certain value $\bar{\tau}$), which is the probability of the correction $\Delta M_{\bar{i}}$ which generates the trajectory such that:

$$u_{\bar{i}}\left(\bar{\phi}\right) = \frac{1}{\bar{r}} \tag{5.7}$$

This could be compared with observational data.

Instead, in the first case, we have a fixed $M$ and corrected initial conditions:

$$u_i\left(0\right) = u_{o+} + \delta_{i0} \tag{5.8}$$

$$\dot{u}_i(0) = 0 \tag{5.9}$$

so we started from energy levels which are lower than that of the unstable circular orbit ($L$ is fixed at the same value) so we have capture or escape at $r = \infty$ for negative or positive corrections respectively. The orbit has the form:

$$u_i(\phi) = u_{0+} + \delta_i(\phi) \tag{5.10}$$

with

$$\delta_i(0) = \Delta u_{i0} = \delta_{i0} u_{0+} \tag{5.11}$$

$$\dot{\delta}_i(0) = 0 \tag{5.12}$$

and finally we have the equation at first order in $\delta_{i0}$ is:

$$\frac{d^2\delta_i}{d\phi^2} = \sqrt{1 - 12\frac{M^2}{L^2}}\delta_i + 3M\delta_i^2 \tag{5.13}$$

$$y_i = \frac{d\delta_i}{d\phi} \tag{5.14}$$

$$\frac{dy_i}{d\phi} = \frac{dy_i}{d\delta_i}\frac{d\delta_i}{d\phi} = y_i\frac{dy_i}{d\delta_i} = \sqrt{1 - 12\frac{M^2}{L^2}}\delta_i + 3M\delta_i^2 \tag{5.15}$$

$$\frac{d\delta_i}{d\phi} = \left(\sqrt{1 - 12\frac{M^2}{L^2}}\delta_i^2 + 2M\delta_i^3 + C\right)^{1/2} \tag{5.16}$$

This equation can be solved by means of elliptical integrals.

However if we have small corrections $\left|\frac{\delta_i(\phi)}{u_{0+}}\right| << 1$, $|\delta_{i0}| << 1$, it is possible to solve the problem with a perturbation method.

$$\delta_i(\phi) = \delta_{i0}\delta_i'(\phi) + o\left(\delta_{i0}^2\right) \tag{5.17}$$

at the first order in $\delta_{i0}$ we have the equation:

$$\frac{d^2\delta_i'(\phi)}{d\phi^2} = \sqrt{1 - 12\frac{M^2}{L^2}}\delta_i'(\phi) \tag{5.18}$$

from here we can solve this equation and taking into account the previous initial conditions we have:

$$u_i(\phi) = u_{0+} + \delta_{i0}u_{0+}\cosh\left(\left(1 - 12\frac{M^2}{L^2}\right)^{\frac{1}{4}}\phi\right) \tag{5.19}$$

In the massless case we have the first order equation for $\delta_i(\phi)$ which reads:

$$\frac{d^2\delta_i(\phi)}{d\phi^2} = \delta_i(\phi) \tag{5.20}$$

from the initial conditions the solution is:

$$u(\phi) = \frac{1}{3M} + \Delta u_0\cosh(\phi) \tag{5.21}$$

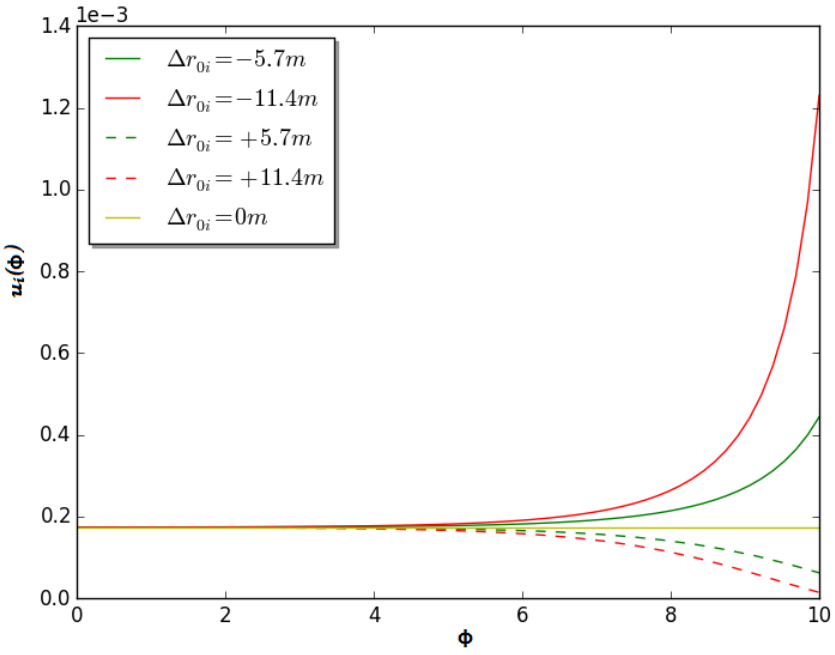


Figure 5.2: Orbits (obtained with numerical method) generated from correction on the initial conditions of the unstable circular orbit for $M = 1500m$ and $L = 6300m$

We see from (5.19) and (5.21) that even small perturbations in initial conditions of the unstable circular orbit generate divergent corrections at the orbit Fig. 5.2.

The equation (5.13) for $\delta_i(\phi)$ is different from that of $u_{1i}(\phi)$ so the two kind of corrections modify the orbits in different way Fig. 5.3.

We can see from Fig. 5.1 that if we have corrections to $M$ of different magnitude they affect the motion in such a way that the different modified orbits tend to become more and more distant as $\phi$ increases; in Fig. 5.4 it is shown how small differences in $M_i$ are amplified after one turn around the source, it should be an amplification of the small mass deviations.

However an observed orbit could come both from errors in measurements of initial conditions or from an error in measurement of $M$ but with different relative errors (Fig. 5.3).

Let's see when the two cases generate superposed orbits. From fixed $\frac{\Delta M}{M}$ we can adjust $\frac{\Delta r_0}{r_0}$ in such a way that the behavior of the orbits results effectively the same and then we compare each other. Here we show some of these situations using the numerical approach, e.g. we see in Fig. 5.5 and Fig. 5.6 that for $\frac{\Delta r_0}{r_0} \sim 0.1\%$ and $\frac{\Delta M}{M} \sim 0.06\%$ the two kind of orbits that these correction generate are very similar and for $\frac{\Delta r_0}{r_0} \sim 0.1\%$ and $\frac{\Delta M}{M} \sim 0.0567\%$ two orbits are superposed. In this way we see that in this case the relative deviation from $r_{0-}$ has to be bigger than the relative deviation from $M$ to obtain the same trajectory.

The same analysis can be done for a lot of other situations and in doing so, every trajectory should have two probabilities to occur: one due to the distribution of the deviations in the initial conditions and the other due to the distributions of the deviation from the mass of the source $M$.

We can also perform this study of the orbits with an analytic method using the perturbation

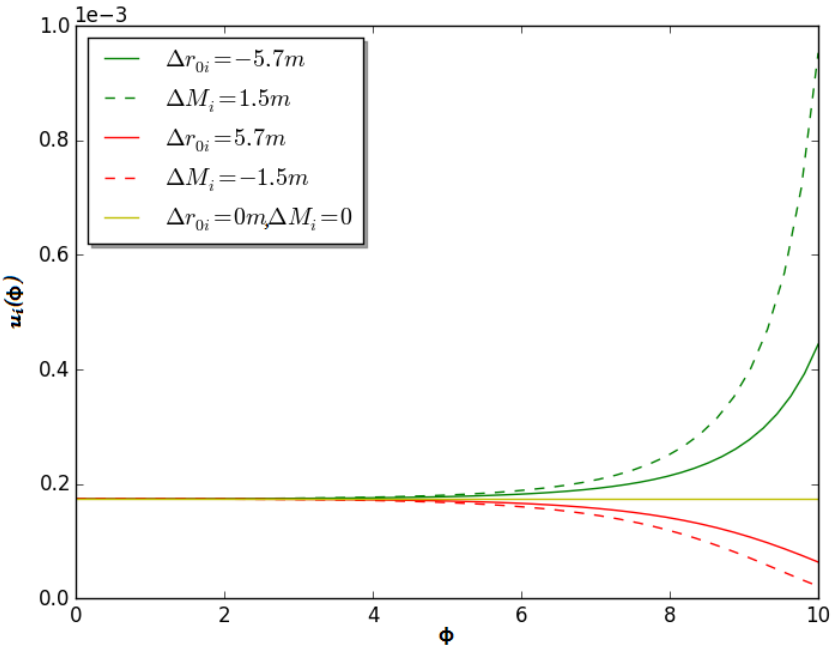


Figure 5.3: Different corrected orbits, in the same color we have the same relative correction (%), solid line for corrections in initial condition and dashed line for corrections in $M$. ($M = 1500m$, $L = 6300m$)

formula, some examples are in Tab. 5.1 in which we see some values of the two kind of corrections needed to have the same $\Delta r$ after a certain number of turns around the source. Here we consider $\phi = 2\pi$ for $L = 4.2$; $L = 4.5$; $L = 5$ and $\phi = \frac{3\pi}{2}$ for $L = 18$;$L = 25$.[1]

| $L$ | $\delta_{\%}M$ | $\delta_{\%}r_0$ | $\frac{\delta_{\%}r_0}{\delta_{\%}M}$ | $\Delta r$ |
|---|---|---|---|---|
| 4.2 | 0.0565 | -0.1 | -1.77 | -0.20088 |
| 4.2 | -0.0565 | 0.1 | -1.77 | 0.224401 |
| 4.2 | 0.1154 | -0.2 | -1.744 | -0.38904 |
| 4.2 | -0.1147 | 0.2 | -1.733 | 0.484792 |
| 4.2 | 0.173 | -0.3 | -1.734 | -0.55509 |
| 4.2 | -0.1724 | 0.3 | -1.74 | 0.778182 |
| 4.2 | 0.2312 | -0.4 | -1.73 | -0.70737 |
| 4.2 | -0.2273 | 0.4 | -1.76 | 1.096912 |
| 4.2 | 0.28925 | -0.5 | -1.729 | -0.84579 |
| 4.2 | -0.2863 | 0.5 | -1.746 | 1.492509 |
| 4.2 | 0.34747 | -0.6 | -1.727 | -0.97282 |
| 4.2 | -0.3435 | 0.6 | -1.747 | 1.941768 |
| 4.2 | 0.4058 | -0.7 | -1.725 | -1.08969 |
| 4.2 | -0.40015 | 0.7 | -1.749 | 2.468229 |
| 4.2 | 0.46425 | -0.8 | -1.723 | -1.1976 |

[1] $L$ and $\Delta r$ are expressed in $M$ units.

| | | | | |
|---|---|---|---|---|
| 4.2 | -0.457 | 0.8 | -1.751 | 3.102772 |
| 4.2 | 0.5228 | -0.9 | -1.721 | -1.29751 |
| 4.2 | -0.5134 | 0.9 | -1.753 | 3.872598 |
| 4.2 | 0.58145 | -1 | -1.72 | -1.39027 |
| 4.2 | -0.5701 | 1 | -1.754 | 4.84042 |
| 4.5 | 0.06844 | -0.1 | -1.461 | -0.28853 |
| 4.5 | -0.0683 | 0.1 | -1.464 | 0.343197 |
| 4.5 | 0.13701 | -0.2 | -1.46 | -0.53445 |
| 4.5 | -0.1365 | 0.2 | -1.465 | 0.758492 |
| 4.5 | 0.20572 | -0.3 | -1.458 | -0.74659 |
| 4.5 | -0.2044 | 0.3 | -1.468 | 0 |
| 4.5 | 0.27455 | -0.4 | -1.457 | -0.9314 |
| 4.5 | -0.2723 | 0.4 | -1.469 | 1.917168 |
| 4.5 | 0.3435 | -0.5 | -1.456 | -1.09384 |
| 4.5 | -0.34025 | 0.5 | -1.47 | 2.765058 |
| 4.5 | 0.41267 | -0.6 | -1.454 | -1.23795 |
| 4.5 | -0.4064 | 0.6 | -1.476 | 3.886122 |
| 4.5 | 0.48193 | -0.7 | -1.452 | -1.36642 |
| 4.5 | -0.4755 | 0.7 | -1.472 | 5.575939 |
| 4.5 | 0.55134 | -0.8 | -1.451 | -1.48177 |
| 4.5 | -0.54265 | 0.8 | -1.474 | 8.157501 |
| 5 | 0.0728 | -0.1 | -1.374 | -0.32777 |
| 5 | -0.07265 | 0.1 | -1.376 | 0.402756 |
| 5 | 0.14592 | -0.2 | -1.371 | -0.6003 |
| 5 | -0.1453 | 0.2 | -1.376 | 0.91073 |
| 5 | 0.21909 | -0.3 | -1.369 | -0.82967 |
| 5 | -0.2179 | 0.3 | -1.377 | 1.570824 |
| 5 | 0.29243 | -0.4 | -1.368 | -1.02569 |
| 5 | -0.2901 | 0.4 | -1.379 | 2.458344 |
| 5 | 0.3659 | -0.5 | -1.366 | -1.19504 |
| 5 | -0.3622 | 0.5 | -1.38 | 3.721579 |
| 5 | 0.43953 | -0.6 | -1.365 | -1.34289 |
| 5 | -0.4344 | 0.6 | -1.381 | 5.670013 |
| 5 | 0.51328 | -0.7 | -1.364 | -1.47301 |
| 5 | -0.5065 | 0.7 | -1.382 | 9.055708 |
| 18 | 0.100109 | -0.1 | -0.999 | -0.15326 |
| 18 | -0.09992 | 0.1 | -1.001 | 0.170173 |
| 18 | 0.200418 | -0.2 | -0.998 | -0.29202 |
| 18 | -0.19962 | 0.2 | -1.002 | 0.360182 |
| 18 | 0.300929 | -0.3 | -0.997 | -0.41824 |
| 18 | -0.29913 | 0.3 | -1.003 | 0.573745 |
| 18 | 0.401641 | -0.4 | -0.996 | -0.53356 |
| 18 | -0.39844 | 0.4 | -1.004 | 0.815542 |
| 18 | 0.502556 | -0.5 | -0.995 | -0.63932 |
| 18 | -0.49755 | 0.5 | -1.005 | 1.091521 |
| 25 | 0.100991 | -0.1 | -0.99 | -0.1557 |

| | | | | |
|---|---|---|---|---|
| 25 | -0.10079 | 0.1 | -0.992 | 0.173275 |
| 25 | 0.202184 | -0.2 | -0.989 | -0.29638 |
| 25 | -0.20138 | 0.2 | -0.993 | 0.367271 |
| 25 | 0.30358 | -0.3 | -0.988 | -0.42411 |
| 25 | -0.30176 | 0.3 | -0.994 | 0.585946 |
| 25 | 0.405179 | -0.4 | -0.987 | -0.54059 |
| 25 | -0.40195 | 0.4 | -0.995 | 0.834324 |

Table 5.1: Orbits

We note here that for a fixed value of angular momentum, the ratio $\frac{\delta_{\%} r_0}{\delta_{\%} M}$ remains almost a constant value (in the escape cases it is a little higher than in the capture cases). Now if we gradually increase the value of $L$ we see that first $\frac{\delta_{\%} r_0}{\delta_{\%} M} > 1$ and then becomes $\frac{\delta_{\%} r_0}{\delta_{\%} M} < 1$ (in the case $L = 18$ for the escape cases the ratio is $> 1$ and for the falling cases is $< 1$). It means that the importance of one kind of correction in generating a variation in $r$ depends on $L$.

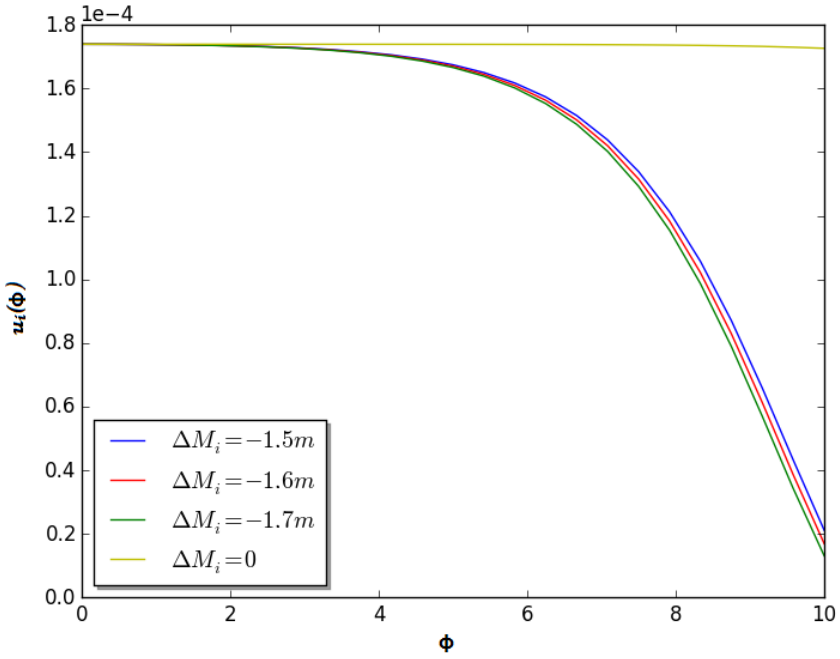


Figure 5.4: Orbits (obtained from numerical method) generate from correction in $M$: blue $\frac{\Delta M}{M} = -0.1\%$, green $\frac{\Delta M}{M} = 0.2\%$, red $\frac{\Delta M}{M} = 0.4\%$. (For $R_H = 3000m$ and $L = 7250$)

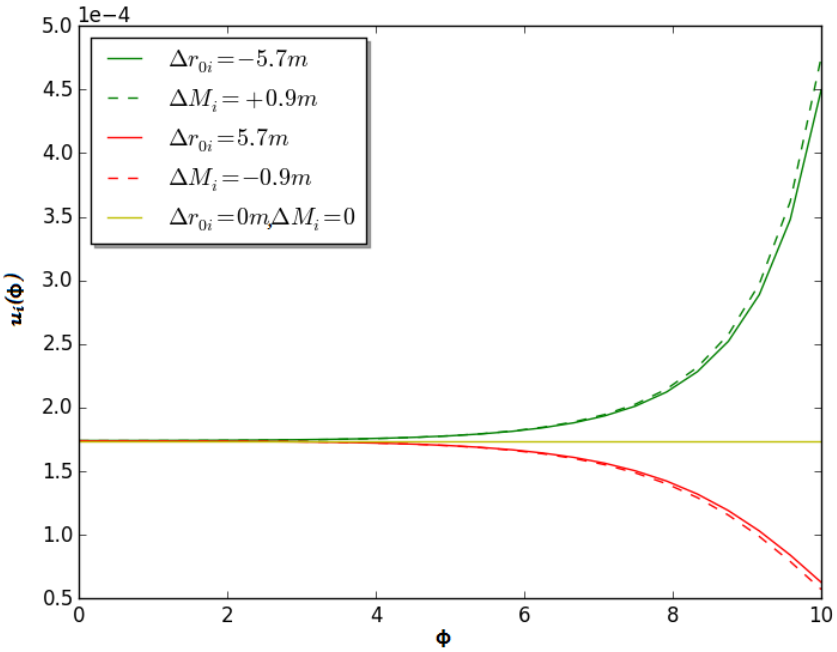


Figure 5.5: Orbits (obtained from numerical method) generate from corrections in initial conditions of the unstable circular orbit $\frac{\Delta r_0}{r_0} \sim \pm 1\%$, and from correction $\frac{\Delta M}{M} \sim \mp 0.6\%$. (For $M = 1500m$ and $L = 6300m$)

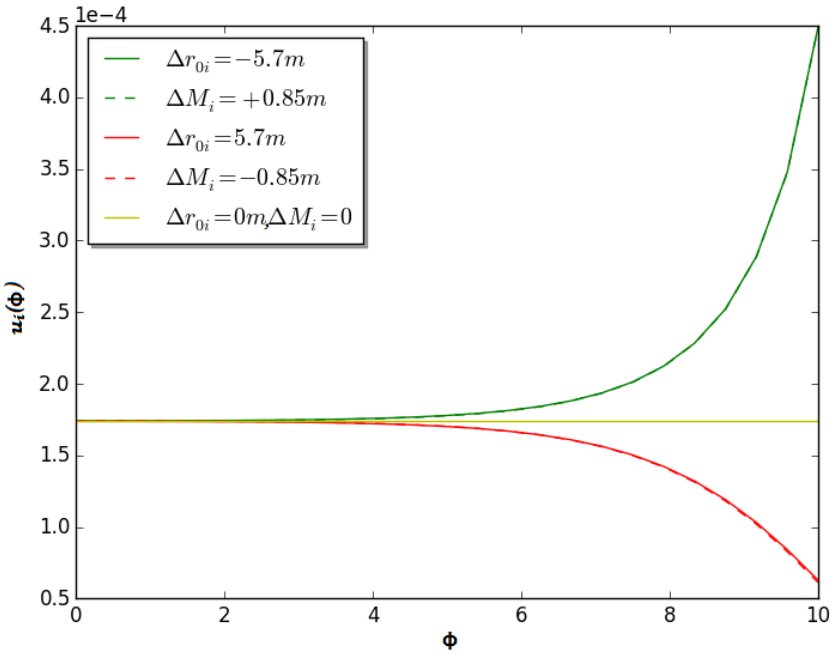


Figure 5.6: Orbits (obtained from numerical method) generate from corrections in initial conditions of the unstable circular orbit $\frac{\Delta r_0}{r_0} \sim \pm 0.1\%$, and from correction $\frac{\Delta M}{M} \sim \mp 0.0567\%$. (For $M = 1500m$ and $L = 6300m$)

# Chapter 6

# Modified radial motion

The same considerations that we have seen in the case of unstable circular orbits can be done in the case of radial motion studying the proper time variations. We will set a fixed final value for $r = r(\tau)$ (in the following examples we set $r = 2M$) and then study the two situations:

- from a given initial condition $\dot{r}(\tau_0) = 0$ and $r(\tau_0) = r_0$ we perform deviation from this value of $r$ coordinate of different magnitude ($\delta r_{0i} = \frac{\Delta r_{0i}}{r_0}$ is the i-th relative deviation). In this way the effective initial conditions are $r_{0eff_i}(\tau_0) = r_0 + \Delta r_{0i}$ and $\dot{r}(\tau_0) = 0$. From here we learn how these deviations influence $\tau$;
- we fix an initial condition $r(\tau_0) = r_0$ and $\dot{r}(\tau_0) = 0$ and starting from a given value of mass $M$ we perform some deviations from it ($\delta M_i = \frac{\Delta M_i}{M}$ is the i-th relative deviation) to have an effective value of mass $M_{eff_i} = M + \Delta M_i$. In doing so we can study how these deviations affect the $\tau$ value.

Setting $d\tau = \tau - \tau_0$ the value obtained from (3.49) when $\delta_{\%} r_0 = 0$ and $\delta_{\%} M = 0$, in the following Tab. 6.1 we show $\Delta d\tau_{r_{0i}}$ which is the i-th deviation from $d\tau$ due to the i-th deviation from $r_0$ while $\Delta d\tau_{M_i}$ represents i-th deviation from $d\tau$ obtaining inserting $M_{eff_i}$ in (3.49). Both i-th kind of deviations have the same relative magnitude (now we have no limit to use the (3.49) analytic formula contrary to the previous case of $L \neq 0$ orbits which is a perturbation formula). We can repeat the same calculus for various $r_0$.

| $r_0$ | $\delta_{\%} r_{0i} = \delta_{\%} M_i$ | $r_{0eff_i}$ | $d\tau_{r_{0i}}$ | $\Delta d\tau_r$ | $M_{eff_i}$ | $d\tau_{M_i}$ | $\Delta d\tau_M$ |
|---|---|---|---|---|---|---|---|
| 4 | 0 | 4 | 7.27131 | 0 | 1 | 7.27131 | 0 |
| 4 | 0.1 | 4.004 | 7.285048 | 0.013738 | 1.001 | 7.26768 | -0.00363 |
| 4 | -0.1 | 3.996 | 7.257577 | -0.01373 | 0.999 | 7.27495 | 0.00364 |
| 4 | 0.2 | 4.008 | 7.298792 | 0.027482 | 1.002 | 7.26405 | -0.00726 |
| 4 | -0.2 | 3.992 | 7.24385 | -0.02746 | 0.998 | 7.27859 | 0.00728 |
| 4 | 0.3 | 4.012 | 7.312541 | 0.041231 | 1.003 | 7.26043 | -0.01088 |
| 4 | -0.3 | 3.988 | 7.230128 | -0.04118 | 0.997 | 7.28224 | 0.01093 |
| 4 | 0.4 | 4.016 | 7.326295 | 0.054985 | 1.004 | 7.25681 | -0.0145 |
| 4 | -0.4 | 3.984 | 7.216412 | -0.0549 | 0.996 | 7.2859 | 0.01459 |
| 4 | 0.5 | 4.02 | 7.340055 | 0.068745 | 1.005 | 7.2532 | -0.01811 |
| 4 | -0.5 | 3.98 | 7.202701 | -0.06861 | 0.995 | 7.28956 | 0.01825 |
| 4 | 0.6 | 4.024 | 7.353821 | 0.082511 | 1.006 | 7.24959 | -0.02172 |
| 4 | -0.6 | 3.976 | 7.188996 | -0.08231 | 0.994 | 7.29322 | 0.02191 |

| | | | | | | | |
|---|---|---|---|---|---|---|---|
| 4 | 0.7 | 4.028 | 7.367592 | 0.096281 | 1.007 | 7.24599 | -0.02532 |
| 4 | -0.7 | 3.972 | 7.175296 | -0.09601 | 0.993 | 7.29689 | 0.02558 |
| 4 | 0.8 | 4.032 | 7.381368 | 0.110058 | 1.008 | 7.2424 | -0.02891 |
| 4 | -0.8 | 3.968 | 7.161601 | -0.10971 | 0.992 | 7.30057 | 0.02926 |
| 4 | 0.9 | 4.036 | 7.39515 | 0.12384 | 1.009 | 7.23881 | -0.0325 |
| 4 | -0.9 | 3.964 | 7.147912 | -0.1234 | 0.991 | 7.30425 | 0.03294 |
| 4 | 1 | 4.04 | 7.408937 | 0.137627 | 1.01 | 7.23522 | -0.03609 |
| 4 | -1 | 3.96 | 7.134228 | -0.13708 | 0.99 | 7.30794 | 0.03663 |
| 5 | 0 | 5 | 10.87804 | 0 | 1 | 10.878 | 0 |
| 5 | 0.1 | 5.005 | 10.89694 | 0.018903 | 1.001 | 10.8726 | -0.00543 |
| 5 | -0.1 | 4.995 | 10.85914 | -0.01889 | 0.999 | 10.8835 | 0.00544 |
| 5 | 0.2 | 5.01 | 10.91585 | 0.037815 | 1.002 | 10.8672 | -0.01086 |
| 5 | -0.2 | 4.99 | 10.84026 | -0.03778 | 0.998 | 10.8889 | 0.01089 |
| 5 | 0.3 | 5.015 | 10.93477 | 0.056736 | 1.003 | 10.8618 | -0.01628 |
| 5 | -0.3 | 4.985 | 10.82138 | -0.05666 | 0.997 | 10.8944 | 0.01635 |
| 5 | 0.4 | 5.02 | 10.9537 | 0.075665 | 1.004 | 10.8563 | -0.02169 |
| 5 | -0.4 | 4.98 | 10.80251 | -0.07553 | 0.996 | 10.8999 | 0.02182 |
| 5 | 0.5 | 5.025 | 10.97264 | 0.094603 | 1.005 | 10.8509 | -0.02709 |
| 5 | -0.5 | 4.975 | 10.78365 | -0.09439 | 0.995 | 10.9053 | 0.0273 |
| 5 | 0.6 | 5.03 | 10.99159 | 0.113549 | 1.006 | 10.8456 | -0.03249 |
| 5 | -0.6 | 4.97 | 10.7648 | -0.11324 | 0.994 | 10.9108 | 0.03278 |
| 5 | 0.7 | 5.035 | 11.01054 | 0.132504 | 1.007 | 10.8402 | -0.03787 |
| 5 | -0.7 | 4.965 | 10.74596 | -0.13208 | 0.993 | 10.9163 | 0.03827 |
| 5 | 0.8 | 5.04 | 11.02951 | 0.151467 | 1.008 | 10.8348 | -0.04325 |
| 5 | -0.8 | 4.96 | 10.72712 | -0.15092 | 0.992 | 10.9218 | 0.04377 |
| 5 | 0.9 | 5.045 | 11.04848 | 0.170439 | 1.009 | 10.8294 | -0.04862 |
| 5 | -0.9 | 4.955 | 10.70829 | -0.16974 | 0.991 | 10.9273 | 0.04928 |
| 5 | 1 | 5.05 | 11.06746 | 0.18942 | 1.01 | 10.8241 | -0.05399 |
| 5 | -1 | 4.95 | 10.68948 | -0.18856 | 0.99 | 10.9328 | 0.0548 |
| 6 | 0 | 6 | 14.82692 | 0 | 1 | 14.8269 | 0 |
| 6 | 0.1 | 6,006 | 14.85162 | 0.024696 | 1.001 | 14.8195 | -0.00741 |
| 6 | -0.1 | 5.994 | 14.80224 | -0.02468 | 0.999 | 14.8343 | 0.00742 |
| 6 | 0.2 | 6,012 | 14.87632 | 0.049403 | 1.002 | 14.8121 | -0.0148 |
| 6 | -0.2 | 5.988 | 14.77756 | -0.04936 | 0.998 | 14.8418 | 0.01485 |
| 6 | 0.3 | 6,018 | 14.90104 | 0.074122 | 1.003 | 14.8047 | -0.02219 |
| 6 | -0.3 | 5.982 | 14.7529 | -0.07402 | 0.997 | 14.8492 | 0.02229 |
| 6 | 0.4 | 6,024 | 14.92577 | 0.098853 | 1.004 | 14.7974 | -0.02957 |
| 6 | -0.4 | 5.976 | 14.72826 | -0.09867 | 0.996 | 14.8567 | 0.02974 |
| 6 | 0.5 | 6,03 | 14.95052 | 0.123596 | 1.005 | 14.79 | -0.03693 |
| 6 | -0.5 | 5.97 | 14.70362 | -0.1233 | 0.995 | 14.8641 | 0.03721 |
| 6 | 0.6 | 6,036 | 14.97527 | 0.14835 | 1.006 | 14.7826 | -0.04428 |
| 6 | -0.6 | 5.964 | 14.67899 | -0.14793 | 0.994 | 14.8716 | 0.04468 |
| 6 | 0.7 | 6,042 | 15.00004 | 0.173116 | 1.007 | 14.7753 | -0.05162 |
| 6 | -0.7 | 5.958 | 14.65438 | -0.17254 | 0.993 | 14.8791 | 0.05217 |
| 6 | 0.8 | 6,048 | 15.02482 | 0.197894 | 1.008 | 14.768 | -0.05895 |
| 6 | -0.8 | 5.952 | 14.62978 | -0.19714 | 0.992 | 14.8866 | 0.05967 |

| | | | | | | | |
|---|---|---|---|---|---|---|---|
| 6 | 0.9 | 6,054 | 15.0496 | 0.222684 | 1.009 | 14.7606 | -0.06627 |
| 6 | -0.9 | 5.946 | 14.60519 | -0.22173 | 0.991 | 14.8941 | 0.06717 |
| 6 | 1 | 6,06 | 15.07441 | 0.247485 | 1.01 | 14.7533 | -0.07358 |
| 6 | -1 | 5.94 | 14.58061 | -0.24631 | 0.99 | 14.9016 | 0.0747 |

Table 6.1: Radial motion

In the examples presented in Tab. 6.1 we have the effects of the two kind of corrections on the proper fall time (from $r_0 = 4M$, $r_0 = 5M$, $r_0 = 6M$ to $r = 2M$), the results are expressed in $M$ units. We can see that a deviation from $r_0$ generates higher deviation from $d\tau$ with respect to those generate by the same relative deviation in $M$. This is true for all our three starting points $r_0 = 4M$, $r_0 = 5M$ and $r_0 = 6M$.

We learn that the i-th deviation $\Delta d\tau_{r_i}$ due to the i-th correction in $r_0$ is higher than the i-th deviation $\Delta d\tau_{M_i}$ generated by the i-th correction in $M$ with the same relative error (we have to compare the i-th positive (negative) correction in $r_0$ with the negative (positive) i-th correction in $M$).

## 6.1 Proper time distribution from mass distribution

As we have seen, for fixed $r_0$ and $r$, different values of mass bring to different values of free fall (escape) proper time. Now we will apply this phenomenon to the situation in which one has a probability distribution for mass values. If one fixes initial conditions $r(\tau_0) = r_0$ and $r(\tau) = r$, a probability distribution for $M$ values means that one has some definite probability $P_i$ to have the mass value $M_i$. For this reason there will be the same probability $P_i$ to have the proper time interval $d\tau_i = \tau_i - \tau_0$ to be able to reach $r$ starting from $r_0$. This proper time interval is obtained inserting $M = M_i$ in (3.49) and the result is that there will be also a probability distribution for the free fall proper time $\tau$.

Now we postulate some reasonable probability distribution for $M$ and study how this distribution reflects itself in the proper time space. We will work with different initial position $r_0$ while we always consider $r = 0$, in this way we can estimate the free fall time needed by the particle to reach the physical singularity (starting from the given initial position).

Now we consider a Gaussian distribution for the mass values. This distribution depends on two important parameters:

- the expectation value for the mass that we label as $M_0$;
- the width of the distribution that we label $\sigma$.

So we study the present situation for different $r_0$ and also for various value for $\sigma$. As first case we fix $M_0 = 300m$ and we assume that $\sigma \sim \lambda_{M_0}$ in which $\lambda_{M_0}$ represents the Compton length associated with the mass $M_0$, so it is defined as $\lambda_{M_0} = \frac{l_P^2}{M_0}$ where $l_P$ is the Planck length. After that we remake the same study but changing $\sigma$ (we take $\sigma = n\lambda_{M_0}$ with $n = 1, 2, 3, 4, 5$) and then changing $r_0$ (e.g. we show the situations for $r_0 = 3M, 7M$). We see some results in Fig.6.1-6.8 ($M$ and $\tau$ are expressed in meters ) where we see also how $\tau$ distribution changes when we modify the Gaussian width.

We see from these graphics that if we consider $\sigma$ not big enough, the probability to have the ratio (at least) $\frac{\Delta\tau_i}{\tau} \sim 1$ considerable deviation from $\tau$ is practically null ($P_i < 10^{-5}$). As

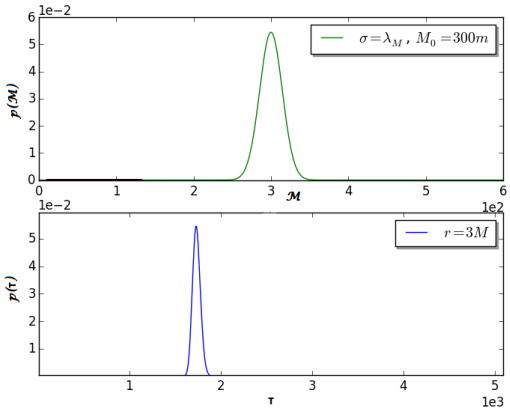


Figure 6.1: Distributions for $M$ and $\tau$ in case $r_0 = 3M$ and $\sigma = \lambda_{M_0}$.

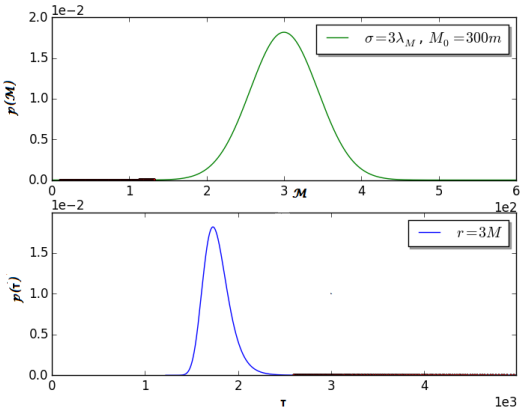


Figure 6.2: Distributions for $M$ and $\tau$ in case $r_0 = 3M$ and $\sigma = 3\lambda_{M_0}$.

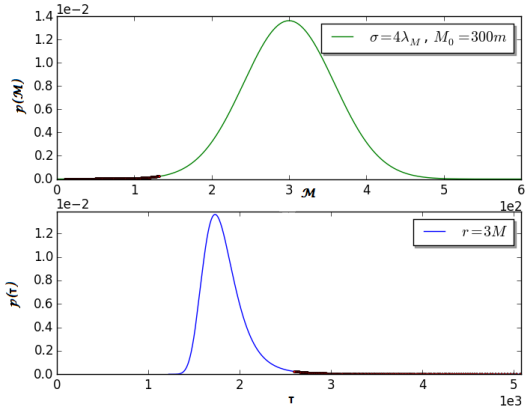


Figure 6.3: Distributions for $M$ and $\tau$ in case $r_0 = 3M$ and $\sigma = 4\lambda_{M_0}$, dark spots imply considerable deviations from $\tau$.

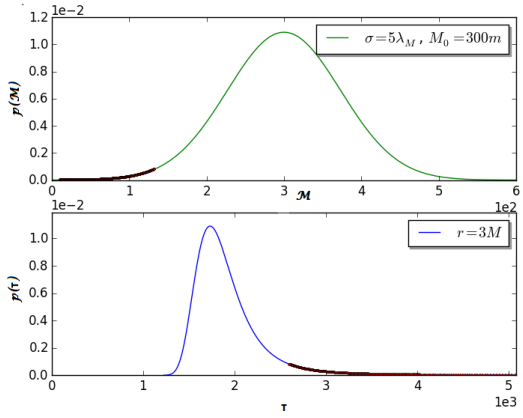


Figure 6.4: Distributions for $M$ and $\tau$ in case $r_0 = 3M$ and $\sigma = 5\lambda_{M_0}$, dark spots imply considerable deviations from $\tau$.

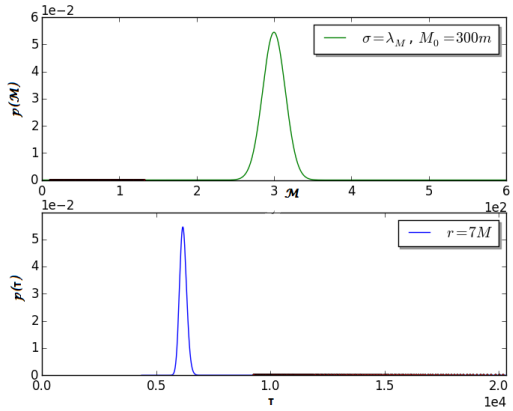


Figure 6.5: Distributions for $M$ and $\tau$ in case $r_0 = 7M$ and $\sigma = \lambda_{M_0}$.

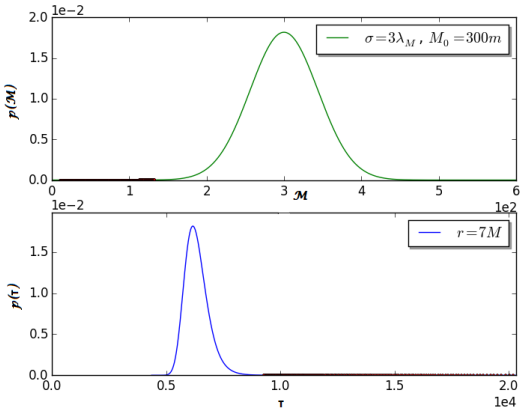


Figure 6.6: Distributions for $M$ and $\tau$ in case $r_0 = 7M$ and $\sigma = 3\lambda_{M_0}$.

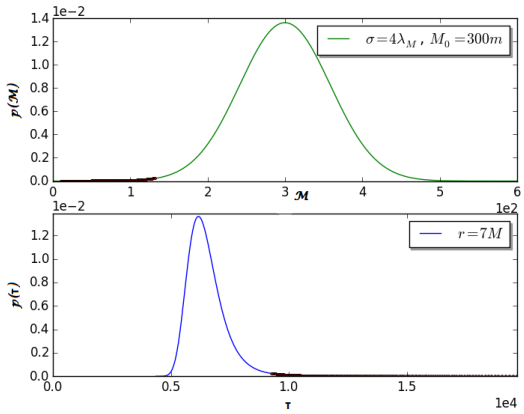


Figure 6.7: Distributions for $M$ and $\tau$ in case $r_0 = 7M$ and $\sigma = 4\lambda_{M_0}$, dark spots imply considerable deviations from $\tau$.

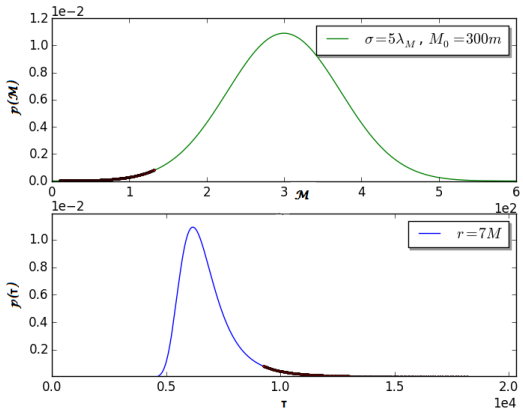


Figure 6.8: Distributions for $M$ and $\tau$ in case $r_0 = 7M$ and $\sigma = 5\lambda_{M_0}$, dark spots imply considerable deviations from $\tau$.

$\sigma$ increases, the probability to have considerable deviations from $\tau$ increases. For example for $\sigma = 5\lambda_{M_0}$ the probability to have the ratio $\delta\tau_i = \frac{\Delta\tau_i}{\tau} \sim 1$ is in the interval $5{\cdot}10^{-5} < P_i < 8{\cdot}10^{-4}$ (we have to take into account that $P_i$ of the maximum is $P_i \sim 0.011$). In this probability interval we have to consider also the relative deviations of mass ($\delta M_i = \frac{\Delta M_i}{M}$) needed to obtain such deviations in $\tau$, in fact we have:

- a region in which relative deviations in $\tau$ are bigger than those in $M$. This occurs when $5 \cdot 10^{-5} < P_i < 4 \cdot 10^{-4}$ and the ratio $\frac{\delta_{Mi}}{\delta_{\tau i}}$ is in the interval $(0.6, 1)$;
- a region in which $\delta_{\tau i}$ and $\delta_{Mi}$ are of similar magnitude ($\delta_{Mi}$ starts to become bigger). This occurs when $5 \cdot 10^{-4} < P_i < 8 \cdot 10^{-4}$ and the ratio $\frac{\delta_{Mi}}{\delta_{\tau i}}$ is in the interval $(1, 1.1)$

So we learn that as $P_i$ increases, both $\delta\tau_i$ and $\delta M_i$ decreases but the former decreases faster. In addition, all these results are the same if we consider different values for $r_0$ as expected considering equation (3.51).

## 6.2 Position distribution from mass distribution

The same considerations of the previous section could be done if we consider $L \neq 0$ and return on the general orbits cases.

Recall the previous situation of modified orbit equations due to fluctuations in $M$. If these corrections are due to some probability distribution for the values of $M$, we can find the corresponding probability distribution of the position of the test particle after a certain number of turns around the source. So we suppose again that the probability distribution for $M$ is a Gaussian centered on $M_0$, with width $\sigma$ and fix the initial conditions. As we have seen, we could start from the unstable circular orbit associated with the mass $M_0$ and the angular momentum $L$:

$$u_{0+} = \frac{1 - \sqrt{1 - 12\frac{M_0^2}{L^2}}}{6M_0} \tag{6.1}$$

then we fix a value for $\phi$ in which we want to study the distribution. Fig. 6.9-6.12 show the results for different Gaussian width and at different values for $\phi$. Distributions have a peak on the value $u = u_{0+}$ and as $\sigma$ increase more value for $u$ will have a non-neglecting probability to occur. As $\phi$ increases, the shape of the distributions changes according to the equation of orbits.

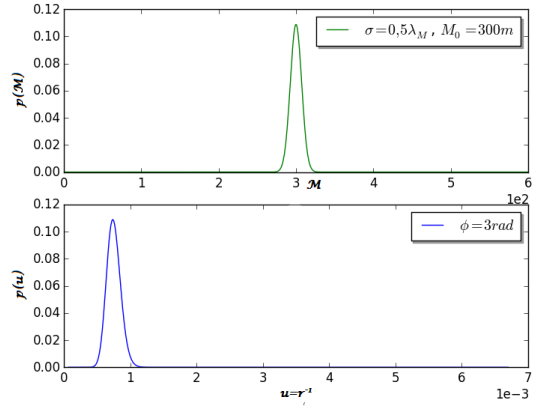


Figure 6.9: Distributions for $M$ and $u = \frac{1}{r}$ in the case $L \sim 4M_0$ and $\sigma = 0.5\lambda_{M_0}$ when $\phi = 3rad$.

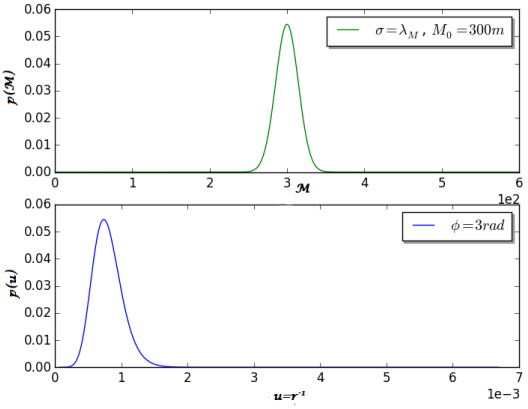


Figure 6.10: Distributions for $M$ and $u = \frac{1}{r}$ in the case $L \sim 4M_0$ and $\sigma = 1\lambda_{M_0}$ when $\phi = 3rad$.

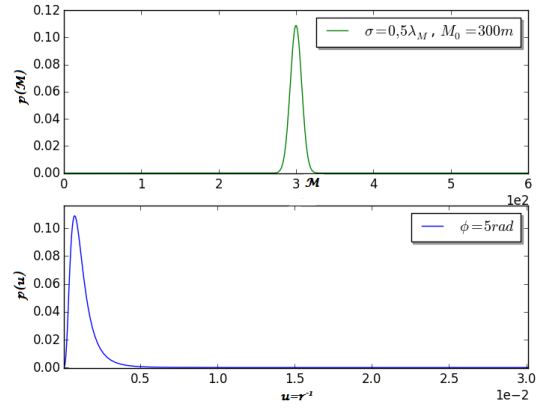


Figure 6.11: Distributions for $M$ and $u = \frac{1}{r}$ in the case $L \sim 4M_0$ and $\sigma = 0.5\lambda_{M_0}$ when $\phi = 5rad$.

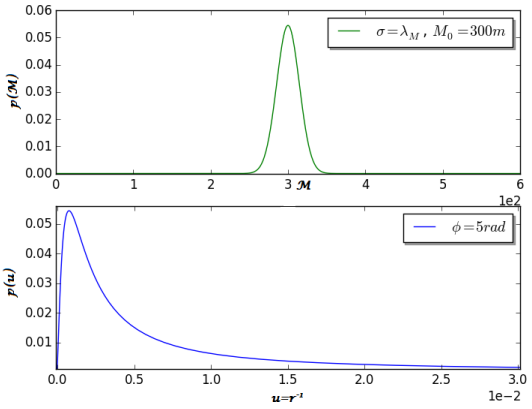


Figure 6.12: Distributions for $M$ and $u = \frac{1}{r}$ in the case $L \sim 4M_0$ and $\sigma = 1\lambda_{M_0}$ when $\phi = 5rad$.

# Chapter 7

# Gravitational Collapses

One of the most important phenomena due to gravity, is the gravitational collapse of stars. To maintain equilibrium, star need to balance gravity attraction (that tends to collapse). In the case of hot stars, this energy come from thermonuclear reactions that take place in the interior regions of the star (and depend on its chemical composition).

During their lives, stars could face with situations in which thermonuclear reactions stop to occur and the internal pressure is not enough to balance the gravitational attraction, so the whole structure collapses. When the thermonuclear reactions stop forever, a collapse occurs until some new pressure source is available. When the contraction goes on, a star's density increases, in this way when it reaches certain values we cannot neglect quantum effects like Pauli exclusion principle. For this reason we find a new source of pressure that could balance the contraction of the star. At this point the source can reach different final high density states depending on the star's collapsing mass. In fact if the mass is not too high, precisely less than the Chandrasekar limit $M \sim 1.4 M_{\odot}$, Pauli pressure of the electrons of the star can balance the gravity attraction, this final state represents a White Dwarf, there is not thermonuclear energy source and the star tend to be cold $T \to 0$.

Another possible final state is the Neutron Star (a cold star too) in which the high density tends to reverse the beta neutron decay and then the neutron Pauli pressure balances the gravity attraction, even in this case we face with a cold star and there is an upper limit to the mass that is known as the Tolman-Oppenheimer-Volkoff limit $M \sim 3 M_{\odot}$. If the source's mass is higher than the TOV limit the complete gravitational collapse occurs. In all of these cases the mass threshold refers to the effective collapsing mass, in fact during the collapse part of the total mass (of the most exterior regions) can be loss, this occur when one faces with a supernova (that can also exhaust all the star mass).

## 7.1 Spherically symmetric case

Restrict us to the study of spherically symmetric static sources, these requirements force the metric to be of the form:

$$ds^2 = e^{2\Phi(r)} dt^2 - e^{2\Psi(r)} dr^2 - r^2 d\Omega^2 \tag{7.1}$$

where $r$ is the usual area-radius as defined in the first chapter.

We can simplify the problem assuming that the interior of the star is made of a perfect fluid. This assumption allows us to use the following stress-energy tensor in the Einstein equations:

$$T_{\mu\nu} = (\rho + p)\, u_\mu u_\nu + p g_{\mu\nu} \tag{7.2}$$

in this expression $u^\mu$ represents the 4-velocity of a fluid comoving observer, $g_{\mu\nu}$ is the metric in this region, $\rho > 0$ and $p > 0$ are energy density and pressure respectively as measured by the comoving observer (for fluid stability reasons we are interested to the case of $\frac{dp}{d\rho} > 0$ only). At this point we define the function $m(r)$ as:

$$e^{2\Psi(r)} = \frac{1}{1 - \frac{2m(r)}{r}} \tag{7.3}$$

This requires $m(r) < \frac{r}{2}$ because of the positivity of the exponential of the left hand side. Thanks to the symmetries of our problem the Einstein equations reduce only to three components and take the form of the Tolman-Oppenheimer-Volkoff (TOV) equations which read:

$$\frac{dm}{dr} = 4\pi r^2 \rho(r) \tag{7.4}$$

$$\frac{d\Phi}{dr} = \frac{m(r) + 4\pi p r^3}{r\,(r - 2m(r))} \tag{7.5}$$

$$\frac{dp}{dr} = -\,(p + \rho)\,\frac{m(r) + 4\pi p r^3}{r\,(r - 2m(r))} \tag{7.6}$$

Now we have to remember that $T$, $p$ and $\rho$ are related by the equation of state of the fluid (in the case of cold stars $T \to 0$ and one obtains the barotropic equation of state in which density depends on pressure $\rho = \rho(p)$ only).

From the TOV equations we have that $\frac{dp}{dr} < 0$, hence one has $\frac{d\rho}{dr} < 0$ and density increases as $r$ decrease. For this reason it could exist some $r_0$ such that in the region $r < r_0$ density is higher than the nuclear densities. This region is defined as the **core** of the star (equation of state is not known for these high density matter), the exterior region $r_0 < r < R$ (where $R$ represents the value for the radius of the star) is known as the **envelope** of the star.

To avoid stress-energy tensor singularity, when $r \to 0$ one has to require that each hypersurfaces at $t = const$ $\Sigma_t$ are smooth manifolds in each point including $r = 0$. This is equivalent to the assumption that $\Sigma_t$ are locally flat everywhere, hence in $r = 0$ too. This implies that $\Psi(r = 0) = 0$ and from (7.3) one obtain $m(0) = 0$. However one can integrate numerically these differential equations using as initial conditions the requirement of continuity at the surface and regularity of the solutions. In this way the problem is solvable and one obtains the solution for the interior of the source. In fact, if we study the exterior of the source the solution is different because for $r \geqslant R$ one have $p(r) = 0$ and $\rho(r) = 0$ and from the TOV equations results:

$$m(r) = m(R) = M = 4\pi \int_0^R r'^2 \rho(r') dr' \tag{7.7}$$

in which $M$ is constant in the whole exterior region $R < r < \infty$ and represents the gravitational mass.

Then for $\Phi(r)$ we have:

$$\Phi(r) = \frac{1}{2} \ln\left(1 - \frac{2M}{r}\right) \tag{7.8}$$

$$e^{2\Phi(r)} = \left(1 - \frac{2M}{r}\right) \tag{7.9}$$

as expected from the Birkhoff theorem we have recovered the Schwarzschild solution in the exterior region. As we have seen, this metric is static but the gravitational collapse is not a static phenomenon, despite this, the metric out of the source remains the Schwarzschild one but its boundary changes during the collapse ($R$ varies during the contraction starting from $R_0$). Now if the mass is less than the TOV limit we have a cold star and from the constrain $m(r) < \frac{r}{2}$ we have a limit on the star's radius $R > 2m(R) = 2M$ but from (7.6) one can obtain an improved limit which reads $R > \frac{9}{4}M$ that is known as the Buchdahl inequality. If $M > 3M_{\odot}$ the complete gravitational collapse force the radius to become smaller than the limit $R = 2M$ where an (event) horizon arises. Once the star's surface crosses the Schwarzschild radius, matter continues to fall and reaches the space-time singularity at $r = 0$ in a finite proper time (see Fig. 7.1). In such a situation, we assist to a Schwarzschild Black Hole formation and as we have already seen in the first chapter, it is useful to change the coordinate system describing this space-time.

For a star with the same mass of our sun $M_{\odot}$ (which will end its life as a withe dwarf) the radius for these three final states would be:

- $R = 7 \cdot 10^3 km$ if it were a Withe Dwarf;
- $R = 10km$ if it were a Neutron Star;
- $R = 3km$ if it were a Schwarzschild Black Hole.

There are no proof that Black Holes are always the final state of a complete gravitational collapse. In fact in more general situations, i.e. if one considers different symmetric properties or different kinds of fluid in the star's body, it might happen that the final state corresponds to a naked singularity, a physical space-time singularity that can interact causally with the exterior region because in this case it is not isolated from the exterior region by means of the event horizon (**Cosmic Censorship Conjecture**). As we have seen, such a situation could cause many problems especially for the predictability of the theory.

## 7.2 Oppenheimer-Snyder model

As we have seen in the previous section, it might happen that during the life of a star, every thermonuclear energy sources ends. If the star mass is big enough, the gravitational collapse occurs. During this process the star could lose energy because matter in the outermost star's shells (envelope) could be expelled during the contraction. Consider now the case in which we can neglect these losses of energy and that we have again a spherically symmetric system. With these conditions we have in the exterior region the Schwarzschild solution as usual. From here we assume that the interior region is spherically symmetric too and composed by an homogeneous density ($\rho_0$) perfect fluid. In this conditions in the Schwarzschild line element the total energy $M = \frac{ml_P}{m_P}$ can be write as $m = \frac{4\pi}{3}\rho_0 R^3$. Studying this situation one finds that relevant physical quantities like $p$ (which is not homogeneous) and $R$ depends only on the parameter $\rho_0$.

If we suppose that the perfect fluid has the equation of state $p = 0$ which is the case of a dust fluid one can write the stress-energy tensor as $T_{\mu\nu} = \rho u_\mu u_\nu$ and the TOV equations can

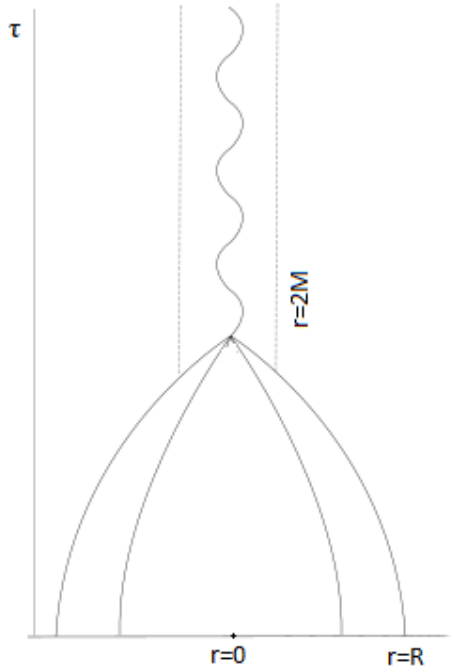


Figure 7.1: Spherically symmetric gravitational collapse: the space-time singularity ($r = 0$) is covered by the event horizon ($r = 2M$) and every shell reach this singularity with the same amount of proper time.

be solved analytically. This is the simplest collapse situation one can faces with and represents the Oppenheimer-Snyder model.

Now if we use a comoving set of coordinates ($T^{\mu\nu} = diag(\rho, 0, 0, 0)$) and considering the Einstein field equations, we are allowed to describe the space-time by means of the Friedmann metric:

$$ds^2 = dt^2 - S(t)\left(\frac{dr^2}{1-\kappa r} + r^2 d\Omega^2\right) \tag{7.10}$$

in which $S(t)$ is the scale factor and $\kappa$ determines the curvature, this quantity can take only three different values $\kappa = +1$ (closed universe), $\kappa = 0$ (flat universe) and $\kappa = -1$(open universe). We are interested to the close solution and we can write:

$$ds^2 = dt^2 - S(t)\left(\frac{dr^2}{1-r} + r^2 d\Omega^2\right) = dt^2 - S(t)\left(d\chi^2 + \chi^2 d\Omega^2\right) \tag{7.11}$$

with $\chi = \sin^{-1} r$.

As we know the exterior solution is different from the interior one, so we have to impose a boundary condition that forces the metric to be continuous at the surface of the star. From here one can use the parametric solutions for these kind of models and we obtain:

$$S(\eta) = \frac{S_m}{2}(1 + \cos\eta) \tag{7.12}$$

$$t(\eta) = \frac{t_m}{2}(\eta + \sin\eta) \tag{7.13}$$

where $\eta$ parametrizes the whole contracting phenomenon, in fact $\eta = 0$ is the beginning of the collapse while the end corresponds to $\eta = \pi$. However in this collapse model one can treat any star's shell as a free radially infalling particle, so its trajectory is governed by the equation (3.51) in which $r_0$ take the value of the starting radius of the shell (where the shell is at rest). We note that if we call $m(r_0)$ the mass inside the shell with starting radius $r = r_0$:

$$\tau \sim \sqrt{\frac{r_0^3}{m(r_0)}} \tag{7.14}$$

and from the homogeneity property $\frac{r_0^3}{m(r_0)} = \frac{3}{4\pi\rho_0}$ is a constant. In this way every shell reach the physical singularity with the same amount of proper time. In this model an event horizon arises when $r$ equal the gravitational radius, this surface covers the singularity and we assist to a Black Hole formation.

## 7.3 Photons emitted from collapsing surface

In this section we want to study the effects generated by the mass $M$ on photons eventually emitted from a radially infalling particle (that could be a particle on the surface of a collapsing star).

We have obtained in the first chapter the equations of motion for a massive particle on the G-P space-time manifold obtaining the 4-velocity along the geodesic:

$$u^\mu = \frac{dx^\mu}{d\tau} = \left(\dot{t}, \dot{r}, 0, 0\right) \tag{7.15}$$

taking into account that for the generic G-P coordinate system:

$$\dot{t} = 1 \tag{7.16}$$

$$\dot{r} = -\sqrt{E^2 - 1 + \frac{2M}{r}} \tag{7.17}$$

Consider now a photon with conserved frequency $\omega_0 = k_\mu \xi^\mu$ (where $\xi^\mu = (1, 0, 0, 0)$ is a Killing 4-vector) and conserved angular momentum $-l = k_\mu \zeta^\mu$ (where $\zeta^\mu = (0, 0, 0, 1)$ is the other Killing 4-vector), so one have:

$$\omega_0 = k^0 g_{00} + k^1 g_{10} = k^0 \frac{1 - \frac{2M}{r}}{E^2} - \frac{v(r)}{E^2} k^1 \tag{7.18}$$

$$k^3 = \frac{l}{r^2} \tag{7.19}$$

So we obtain

$$k^0 = \frac{E^2 \omega_0 + v(r) k^1}{1 - \frac{2M}{r}} \tag{7.20}$$

while $k^1$ is obtained from the condition to have a light-like wave 4-vector:

$$k^\mu k_\mu = k^\mu k^\nu g_{\mu\nu} = k^0 k^0 \frac{1 - \frac{2M}{r}}{E^2} - 2\frac{v(r)}{E^2} k^0 k^1 - \frac{1}{E^2} k^1 k^1 - \frac{l^2}{r^2} = 0 \tag{7.21}$$

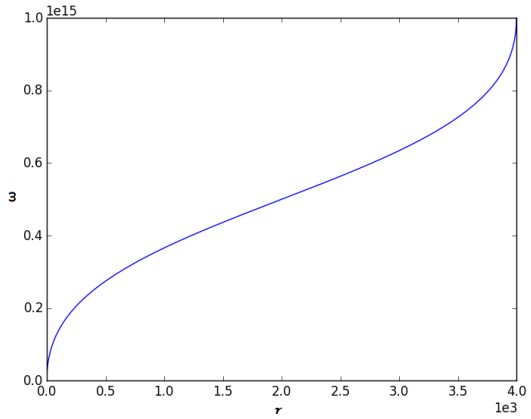


Figure 7.2: $\omega_{-1}(r)$ for $\epsilon = -1$ and fixed $M = 1000m$, $l = 0$, $\omega_0 = 10^{15}Hz$. The observer starts the falling from $r = r_0 = 4000m$ with $\dot{r} = 0$.

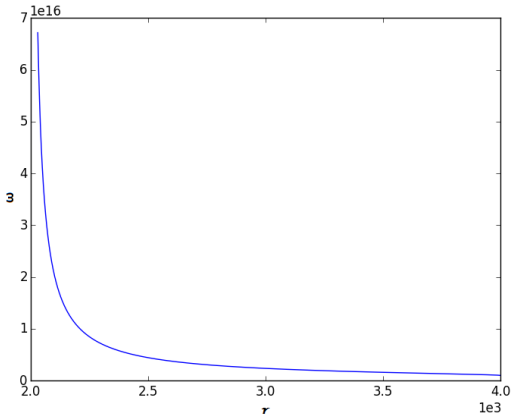


Figure 7.3: $\omega_{+1}(r)$ for $\epsilon = +1$ and fixed $M = 960m$, $E = 1$, $l = 0$, $\omega_0 = 10^{15}Hz$. The observer stars the falling from $r = r_0 = \infty$ with $\dot{r} = 0$.

$$k^1_\epsilon = \epsilon\sqrt{E^2\omega_0^2 - \left(1 - \frac{2M}{r}\right)\frac{l^2}{r^2}} \tag{7.22}$$

so the photon wave 4-vector is:

$$k^\mu = \left(\frac{E^2\omega_0 + \epsilon v(r)\sqrt{E^2\omega_0^2 - \left(1 - \frac{2M}{r}\right)\frac{l^2}{r^2}}}{1 - \frac{2M}{r}}, \epsilon\sqrt{E^2\omega_0^2 - \left(1 - \frac{2M}{r}\right)\frac{l^2}{r^2}}, \frac{l}{r^2}, 0\right) \tag{7.23}$$

In these equations $v(r) = \sqrt{\frac{2M}{r} - \frac{2M}{r_0}}$ for a particle which starts from $r_0$ with $\dot{r} = 0$.

When a radially infalling massive observer meets the photon $k^\mu$ along the geodesic $u^\nu$ (e.g. emission or reception) the frequency measured by the observer is:

$$\omega_\epsilon = k_\mu u^\mu = k^\mu u^\nu g_{\mu\nu} = \frac{\left(1 - \frac{2M}{r_0}\right)\omega_0 + \epsilon\sqrt{E^2\omega_0^2 - \left(1 - \frac{2M}{r}\right)\frac{l^2}{r^2}}\sqrt{E^2 - 1 + \frac{2M}{r}}}{1 - \frac{2M}{r}} \tag{7.24}$$

If a photon were emitted (in $r = r_1$) from a massive falling observer (1) with the conserved value $\omega_0$ its energy $k^0$ depend on $r_1$ and $M$. Then if we have another infalling observer (2) that receives this photon (in $r = r_2$) it sees frequency like $\omega_\epsilon(r_2)$.

For $\epsilon = -1$ we have that the photon direction is the same to the observer's one and $\omega$ decreases as $r$ decreases. For $\epsilon = +1$ the photon direction is the opposite of the observer's one and $\omega$ increases as $r$ decreases.

When the photon is emitted (or observed) near the horizon [13] we can approximate the quantity $\left(1 - \frac{2M}{r}\right) \simeq 0 + \frac{1}{2M}(r - 2M)$ in doing so we can express also $\omega(r)$ in an approximate form which read for $\epsilon = +1$:

$$\omega_{+1}(r) \simeq \frac{4ME^2\omega_0}{(r_{e/o} - 2M)} \tag{7.25}$$

and for $\epsilon = -1$:

$$\omega_{-1}(r) \simeq \frac{\omega_0}{2} + \frac{l^2}{2\omega_0(2M)^2} \tag{7.26}$$

where $r_{e/o}$ is the value of $r$ in which emission/observation takes place. Obviously these measured frequencies depend on the mass of the source so for different values of $M$ we have different behavior for $\omega(r)$ for every set of fixed conserved quantities $\{E, l, \omega_0\}$.

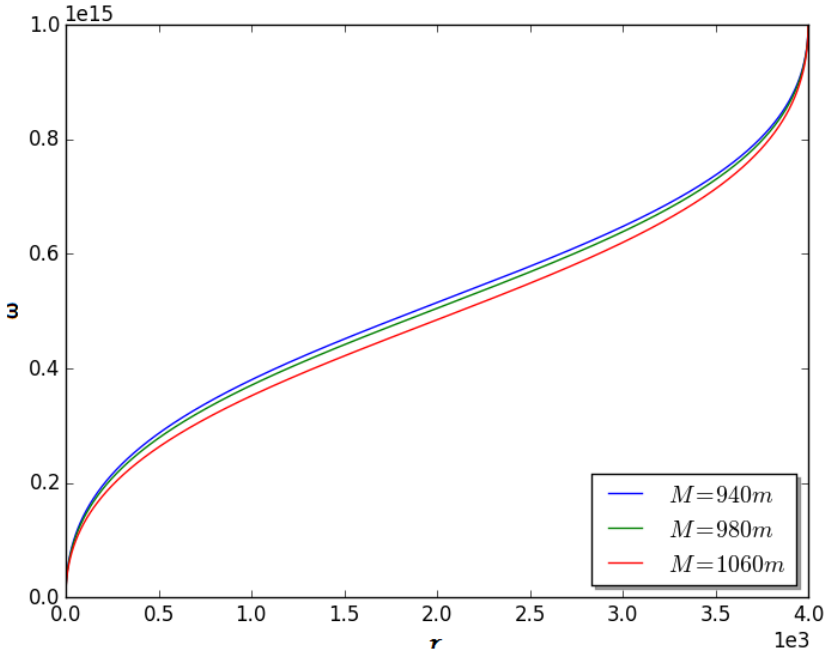


Figure 7.4: $\omega_M(r)$ for $\epsilon = -1$ for fixed $E$, $l = 0$, $\omega_0 = 10^{15} Hz$ starting from $r = r_0 = 4000m$ with $\dot{r} = 0$.

For example, in Figure 7.4, we fix $l$, $\omega_0$ and $E$, we see that as $M$ increases $\omega$ decreases (at some $r$) and there are no problems when we cross the event horizon. In Figure 7.5, we fix $l$,$\omega_0$ and $E$, $\omega$ increases faster for higher values of $M$ and reaches its maximum on the event horizon.

To see how frequency change in time suppose that the observer 1 measures frequency $\omega_1$ for a photon at the horizon, the observer 2 measures frequency $\omega_2$ of the very same photon at the horizon, in [13] there is the calculus of the ratio $\frac{\omega_2}{\omega_1}$ in Kruskal coordinates which reads:

$$\frac{\omega_2}{\omega_1} = \frac{V_1}{V_2} \tag{7.27}$$

where $V = e^{\frac{v}{4M}}$ and $v = t_S + \int_0^r \frac{dr'}{1-\frac{2M}{r'}}$, now from (2.22) we have

$$v = t_P + \int_0^r \left( \frac{dr'}{1 + \sqrt{\frac{2M}{r'}}} \right) \tag{7.28}$$

and

$$\frac{\omega_2}{\omega_1} = e^{\frac{1}{4M}(t_{P1} - t_{P2})} \tag{7.29}$$

so if $t_{P2} > t_{P1}$ then $\omega_2(r_H) < \omega_1(r_H)$, as $t_P$ increases frequency is redshifted.

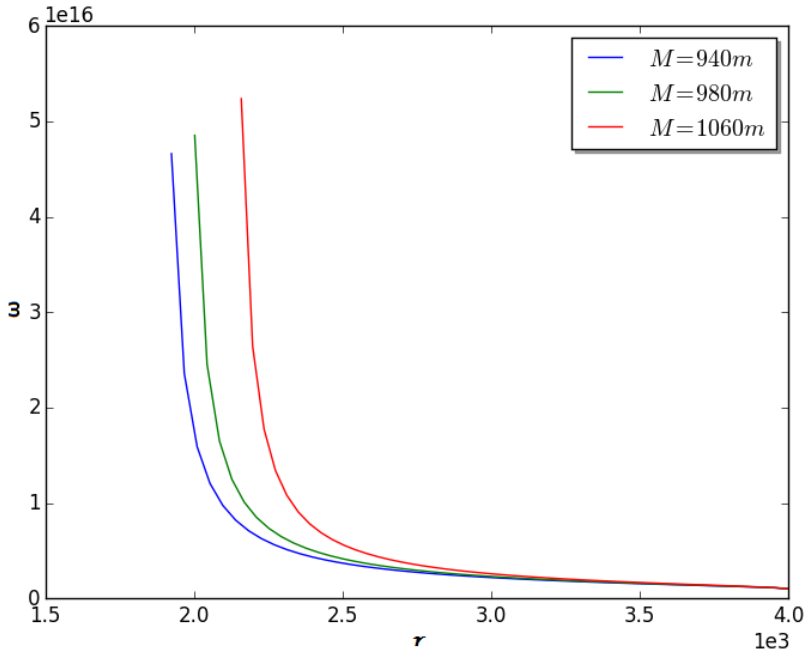


Figure 7.5: $\omega_M(r)$ for $\epsilon = +1$ for fixed $E$, $l = 0$, $\omega_0 = 10^{15} Hz$ starting from $r = r_0 = 4000m$ with $\dot{r} = 0$.

Also in this case we could apply these results at the case in which one have a probability distribution for $M$ that generate a correspondent probability distribution for $\omega(r)$.

Finally $\omega$ depends on $\omega_0$ so if we have a spectrum from the collapsing star and we consider different value of mass for every $\omega_0$ there is a "split" of the curve $\omega(r)$due to $M$ as we see in Figure 7.7

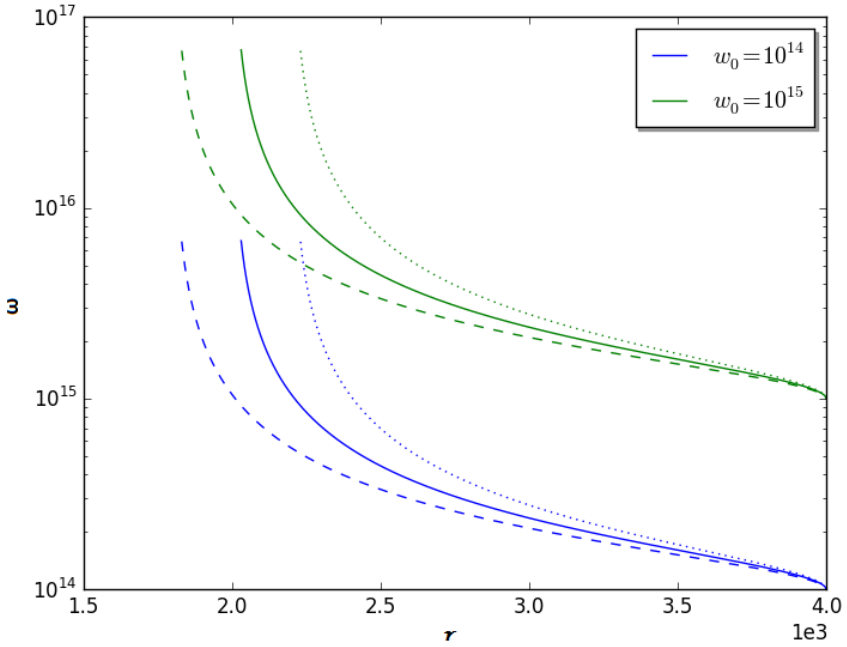


Figure 7.6: $\omega_M(r)$ for $\epsilon = +1$ for fixed $E$, $l = 0$ and various values for $\omega_0$ starting from $r = r_0 = 4000m$ with $\dot{r} = 0$ in semilogarithmic. Dashed lines correspond to $M = 900m$, solid lines $M = 1000m$, dotted lines $M = 1100m$.

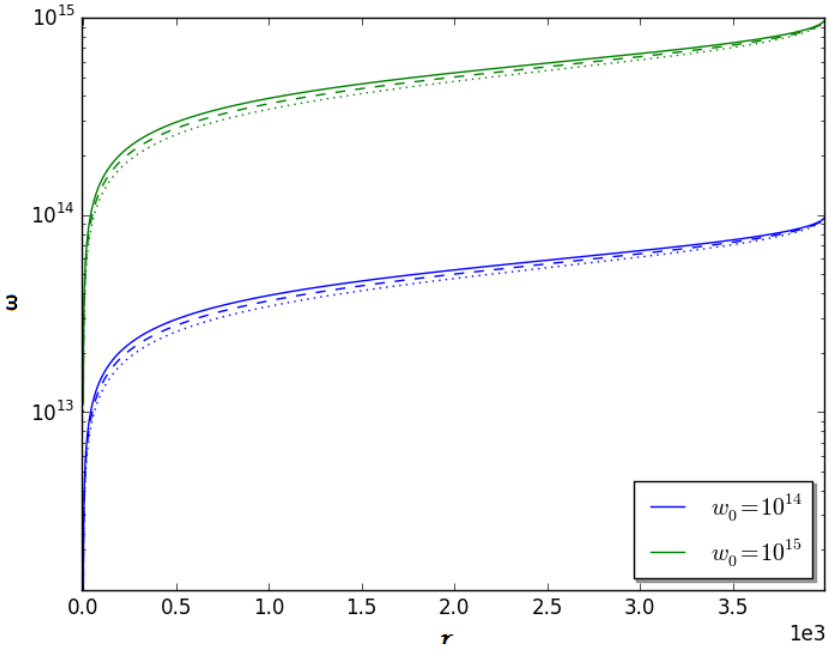


Figure 7.7: $\omega_M(r)$ for $\epsilon = -1$ for fixed $E = 1$, $l = 0$ and various values for $\omega_0$ starting from $r = r_0 = 4000m$ with $\dot{r} = 0$ in semilogarithmic. Dashed lines correspond to $M = 1000m$, solid lines $M = 900m$, dotted lines $M = 1100m$.

# Conclusions

One of the major results arising from the General Theory of Relativity is that a compact astrophysical object, under suitable conditions, could eventually collapse to form a black hole. It is straightforward to infer that such an object could not be directly observed due to the fact that it does not emit any form of detectable radiation (Indeed, the Hawking radiation is predicted to be way weaker with respect to the typical background radiation so it does not appear to be a suitable marker for the detection of astrophysical black holes). Therefore, the only feasible way to experimentally identify the presence of a black hole in a given region is through the study of how its gravitational field deforms the geodesic motion of observable objects in that region.

In this thesis we have presented a study on how quantum gravitational effects could potentially modify some of the main features taken into account for the experimental detection of astrophysical black holes. In particular, in Chapter 1 we have discussed some general properties concerning the geometry of black hole spacetimes focusing on the mathematical formulation of the notions of event horizon and trapping surface and on the conditions that lead to the breakdown of the (classical) relativistic theory of gravity, i.e. the Hawking-Penrose singularity theorem. Then, in Chapter 2 we focussed our attention on a specific type of spacetimes, i.e. the one produced by charge-less static spherically symmetric sources. In this framework we introduced the notions of Misner-Sharp and ADM mass and we discussed their relevance in the context of both the classical and the quantum description of the source and of its gravitational field. In the same chapter we have also introduced the coordinate frame of a free falling observer in a Schwarzschild background. In Chapter 3, that concludes the introductory part of the thesis, we revised the analysis of the geodesic motion of a point particle for a Schwarzschild black hole.

In Chapter 4 and 5, after a brief review of the Horizon Quantum Mechanics, we discussed the effects that the quantum mechanical fluctuation of the mass of a (quantum) source can produce on the geodesic motion of point particle on a perturbed Schwarzschild background. Indeed, if we consider a source described in terms of a static spherically symmetric wave function, according to the Horizon Quantum Mechanics formalism the quantum nature of the source will result in a quantum behaviour of the geometry of the spacetime. In particular, one has that the the radius of the horizon is not sharply defined any longer, but rather follows a certain probability distribution induced by the wave function of the source. These fluctuations of the horizon, or equivalently of the mass of the ADM mass, affect the geodesic motion of a point particle and they can be modelled as small perturbations of the equations of motion. The result of our analysis is that these kind of fluctuations seem to lead to small, but not completely negligible, deviations from the classical trajectories. Therefore we believe that this problem is worth of further studies.

Moreover, in Chapter 6 and 7 we have also discussed how quantum mechanical effects affect properties of the light emitted by a collapsing radially falling source as measure by an in-falling observer.

# Appendix A

# Minkowski's conformal compactification

Here we will perform the conformal compactification on the flat Minkowski space-time to see how this space-time behaves at infinity.

One obtains different kind of infinities. In fact, starting from the physical metric:

$$g_{\mu\nu} = dt^2 - dr^2 - r^2 d\omega^2 \tag{A.1}$$

in which infinities are represented by $t \to \pm\infty$ and $r \to \infty$, one has to apply the following transformations:

$$\begin{cases} w = t - r \\ v = t + r \end{cases} \tag{A.2}$$

and then

$$\begin{cases} w \to q = \arctan w \\ v \to p = \arctan v \end{cases} \tag{A.3}$$

so that the conformal transformed metric ($\Omega = 2\cos p \cos q$) is:

$$\bar{g}_{\mu\nu} = 4dpdq - \sin^2(q-p)\, d\omega^2 \tag{A.4}$$

in which Minkowski's infinities are represented by

- $i^{\pm}$ for $t \to \pm\infty$ and $r$ fixed and finite ($q = p = \frac{\pi}{2}$), a radial timelike geodesic starts in $i^-$ and finishes on $i^+$ so these infinities are called **past** and **future timelike infinity** respectively;

- $\mathcal{I}^{\pm}$, which are null surfaces with $t \mp r$ fixed and finite but $t \to \pm\infty$ and $r = \infty$, radial null geodesics start from $\mathcal{I}^-$ ($q = -\frac{\pi}{2}$, $p \neq \pm\frac{\pi}{2}$) and finish on $\mathcal{I}^+$ ($p = \frac{\pi}{2}$, $q \neq \pm\frac{\pi}{2}$), so these surfaces are called **past** and **future null infinity** respectively;

- $i^0$ for $r \to \infty$ and $t$ fixed and finite ($q = -\frac{\pi}{2}$, $p = \frac{\pi}{2}$), all spacelike geodesics start and finish in $i^0$ which is called the **spacelike infinity**.

Now we can put these results in a diagram which is known as the **Penrose diagram** of the Minkowski space-time Fig.A.1. To do that we perform another coordinate transformation which reads:

$$\begin{cases} R = q - p \\ T = p + q \end{cases} \tag{A.5}$$

to obtain the unphysical metric:

$$\bar{g}_{\mu\nu} = dT^2 - dR^2 - \sin^2 R d\omega^2 \tag{A.6}$$

with $R \in [0, \pi)$ and $T \in (-\pi, \pi)$. If the coordinates were be such that $T \in (-\infty, \infty)$ and

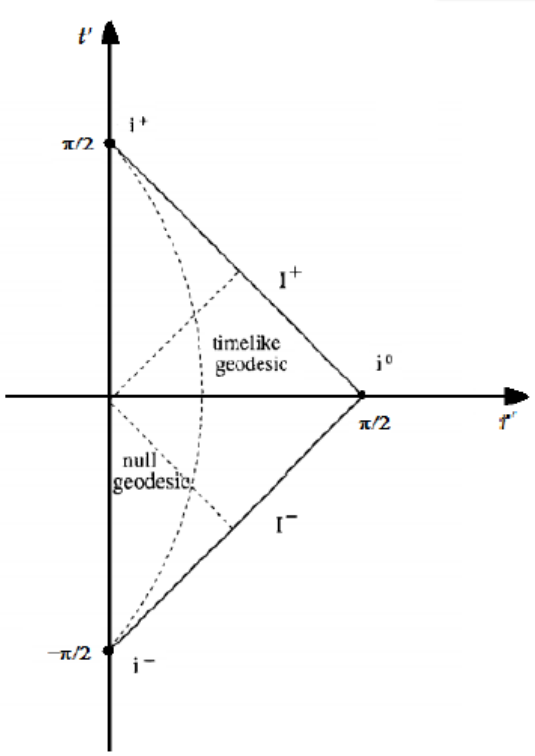


Figure A.1: Penrose diagram of Minkowski space-time

$R \in [0, \pi]$ we face with the (cylindric) Einstein static universe.

# Appendix B

# Christoffel symbols in Gullstrand-Painlevé coordinate system

From the definition of the Christoffel symbols we can see that under a general coordinate transformation they do not behave as tensors. For this reason they depend on the coordinate system or, equivalently, on the observer.

Here we calculate these quantities for the metric in (2.23) and we can check that they do not correspond to those of the Schwarzschid case. From (3.15) the only $\Gamma^{\gamma}_{\mu\nu} \neq 0$ are:

$$\Gamma^t_{tt} = \frac{1}{2}g^{tt}\left(g_{tt,t}\right) + \frac{1}{2}g^{tr}\left(2g_{rt,t} - g_{tt,r}\right) = \sqrt{\frac{M}{2r^3}} \tag{B.1}$$

$$\Gamma^t_{tr} = \Gamma^t_{rt}\frac{1}{2}g^{tt}\left(g_{tt,r}\right) + \frac{1}{2}g^{tr}\left(g_{rr,t} + g_{rt,r} - g_{tt,r}\right) = \frac{M}{r^2\left(1-\frac{2M}{r}\right)} \tag{B.2}$$

$$\Gamma^t_{rr} = \frac{1}{2}g^{tt}\left(2g_{tr,r} - g_{rr,t}\right) + \frac{1}{2}g^{tr}\left(g_{rr,r}\right) = \sqrt{\frac{M}{2r^3}}\frac{1}{1-\frac{2M}{r}} \tag{B.3}$$

$$\Gamma^t_{\theta\theta} = \frac{1}{2}g^{tt}\left(2g_{t\theta,\theta} - g_{\theta\theta,t}\right) + \frac{1}{2}g^{tr}\left(2g_{r\theta,\theta} - g_{\theta\theta,r}\right) = \sqrt{\frac{r^3}{2M}} \tag{B.4}$$

$$\Gamma^t_{\phi\phi} = \frac{1}{2}g^{tt}\left(2g_{t\phi,\phi} - g_{\phi\phi,t}\right) + \frac{1}{2}g^{tr}\left(2g_{r\phi,\phi} - g_{\phi\phi,r}\right) = -\sqrt{\frac{r^3}{2M}}\sin^2\theta \tag{B.5}$$

$$\Gamma^r_{tt} = \frac{1}{2}g^{rr}\left(2g_{rt,t} - g_{tt,r}\right) + \frac{1}{2}g^{rt}\left(g_{tt,t}\right) = \frac{M}{r^2} \tag{B.6}$$

$$\Gamma^r_{tr} = \Gamma^r_{rt} = \frac{1}{2}g^{rr}\left(g_{rt,r} + g_{rr,t} - g_{tr,r}\right) + \frac{1}{2}g^{rt}\left(g_{tt,r} + g_{tr,t} - g_{tr,t}\right) = -\sqrt{\frac{M}{2r^3}} \tag{B.7}$$

$$\Gamma^r_{rr} = \frac{1}{2}g^{rr}\left(g_{rr,r}\right) + \frac{1}{2}g^{rt}\left(2g_{tr,r} - g_{rr,t}\right) = -\frac{1}{2r} \tag{B.8}$$

$$\Gamma^r_{\theta\theta} = \frac{1}{2}g^{rr}\left(-g_{\theta\theta,r}\right) + \frac{1}{2}g^{rt}\left(-g_{\theta\theta,t}\right) = -r \tag{B.9}$$

$$\Gamma^r_{\phi\phi} = \frac{1}{2}g^{rr}\left(-g_{\phi\phi,r}\right) + \frac{1}{2}g^{rt}\left(-g_{\phi\phi,t}\right) = -r\sin^2\theta \tag{B.10}$$

$\Gamma^{\theta}_{\mu\nu}$ and $\Gamma^{\phi}_{\mu\nu}$ are the same of the Schwarzschild case. We note that these are very different from those we have seen in the first chapter so, the geodesic equations will have a different form.

# Appendix C

# Black Hole Shadow

The case of massless particles behavior in the vicinity of a source is very important as in the case of photons. In fact, we detect signals and images from the universe which are electromagnetic signals and are represented by photons.

If we study photons trajectories around a source, we obtain a set of results which could be compared with direct observations of astronomical objects and some simulations. In fact, as we have seen in the first chapter, from the shape of $V_{eff}(r)$ for massless particle (which depends on $L$), we can have:

- circular unstable orbit in $r = 3M$ ($\dot{r} = 0$)with $E = \frac{L^2}{27M^2}$ which defines the photon sphere;
- capture trajectories;
- scattering trajectories.

From these results, we can imagine a Black Hole and a light source of a large angular size (larger than the BH) i.e. a galaxy. Now suppose that the Black Hole is between the large light source and the observer (large light source could be thought at null past infinity). What does the observer see?

Photons come from the light source and when they approach the Black Hole, they behave like the cases previously described for the geodesics motion of massless particles.

Consider the impact parameter of this situation $l$: only the photons with $l > l_{min}$ can reach null future infinity (i.e. the observer), if $l < l_{min}$ photons are captured Fig. C.1. Calculating $l_{min}$ one obtain $l_{min} = \frac{3\sqrt{3}}{2}$ in this way the photon capture cross section is:

$$\sigma_{ph} = l_{min}^2 r_H^2 \pi = 27M^2\pi \tag{C.1}$$

The region $l < l_{min}$ is called Black Hole Shadow and the observer sees a dark spot on a bright background.

For these reasons, a Schwarzschild Black Hole the shape of the shadow is a circle whose size depends on the unique parameter of the Black Hole, the mass $M$.

In most general cases, a Black Hole can rotate around a certain axis and it could be electrically charged. In these cases the shape of the BH shadow becomes more complicated than in the Schwarzschild case (in rotating Black Holes some photons can escape even from region which are nearer to the BH than in the Schwarzschild case and the shape of the shadow

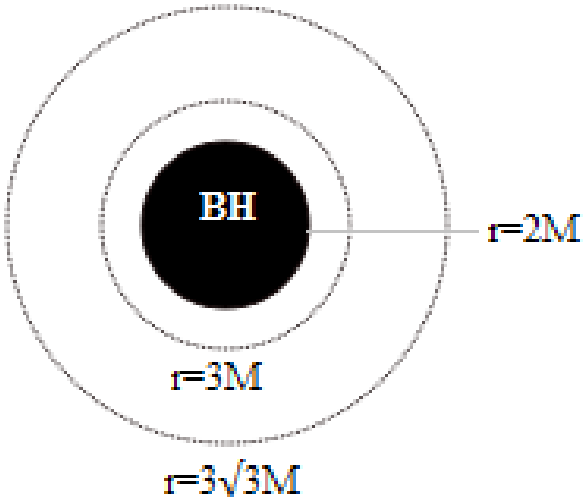


Figure C.1: Possible trajectories for photons when they approach a Schwarzschild Black Hole

is no longer circular, the deformation depends even on the observation point) and depends on the other parameters which describe the BH such as spin and charge.

Thanks to that, we can have a possible way to check some important results of the General Relativity, as the validity of the theoretical metrics obtained from Einstein equations, like the Kerr metric. In fact, with the improvement of the sub-millimeter interferometers, it will allow to investigate these shadows and we could test if there are or not divergences from the theory.

For a rotating source of mass $M$ and with angular momentum $J$, the line element from the Kerr metric is given by:

$$\begin{aligned} ds^2 &= \left(1-\frac{2Mr}{\rho^2}\right)dt^2 - \frac{\rho^2}{\Delta}dr^2 - \rho^2 d\theta^2 - \left(r^2+\alpha^2+\frac{2Mr\alpha^2}{\rho^2}\sin^2\theta\right)\sin^2\theta d\phi^2 \\ &+ \frac{4Mr\alpha\sin^2\theta}{\rho^2}dtd\phi \end{aligned} \tag{C.2}$$

with

$$\alpha = \frac{J}{M} \tag{C.3}$$

$$\rho^2 = r^2 + \alpha^2\cos^2\theta \tag{C.4}$$

$$\Delta = r^2 - 2Mr + \alpha^2 \tag{C.5}$$

To test this metric, one can introduce a new metric, the Cardoso-Pani-Rico parametrization of

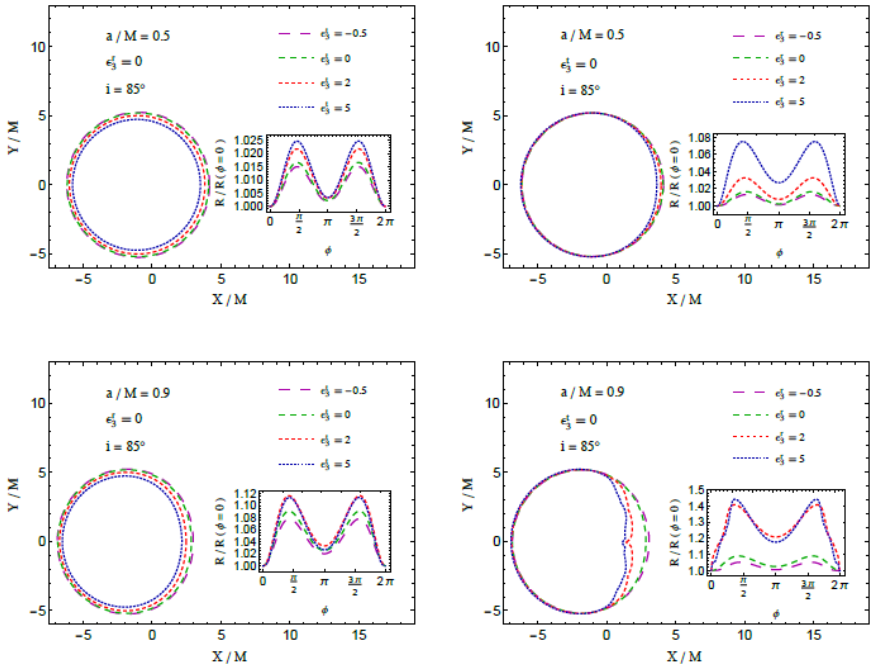


Figure C.2: Divergences from the theoretical Kerr metric affect the shape of the BH shadow [9].

the metric:

$$\begin{aligned} ds^2 &= \left(1-\frac{2Mr}{\Sigma}\right)\left(1+h^t\right)dt^2 - \frac{\Sigma\left(1+h^r\right)}{\Delta + h^r a^2 \sin^2\theta}dr^2 - \Sigma d\theta^2 \\ &- \sin^2\theta\left(\Sigma + a^2\sin^2\theta\left(2\sqrt{\left(1+h^r\right)\left(1+h^t\right)} - \left(1-\frac{2Mr}{\Sigma}\right)\left(1+h^t\right)\right)\right)d\phi^2 \\ &+ 2a\sin^2\theta\left(\sqrt{\left(1+h^r\right)\left(1+h^t\right)} - \left(1-\frac{2Mr}{\Sigma}\right)\left(1+h^t\right)\right)dtd\phi \end{aligned} \tag{C.6}$$

which parametrizes the possible divergence from the Kerr metric through the two set of deformation parameters $(\epsilon_k^t, \epsilon_k^r)$:

$$h^t = \sum_{k=0}^{+\infty}\left(\epsilon_{2k}^t + \epsilon_{2k+1}^t\left(\frac{Mr}{\Sigma}\right)\left(\frac{M^2}{\Sigma}\right)^k\right) \tag{C.7}$$

$$h^r = \sum_{k=0}^{+\infty}\left(\epsilon_{2k}^r + \epsilon_{2k+1}^r\left(\frac{Mr}{\Sigma}\right)\left(\frac{M^2}{\Sigma}\right)^k\right) \tag{C.8}$$

Where $a = \frac{J}{M}$, $\Sigma = r^2 + a^2\cos^2\theta$, $\Delta = r^2 - 2Mr + a^2$. Now if we detect a Black Hole shadow, its shape depends only on the metric and the BH parameters, so from observational data we can define the deformation parameters and test the theoretical Kerr metric Fig. C.2.

# Appendix D

# Quantum treatment of a collapsing source

From the particles equations of motion, one can study what happens during a collapse focusing on the behavior of a particle on the surface of the star. Our results tell us that using the Schwarzschild coordinate system, we cannot see the particle crossing the horizon in fact it needs an infinite amount of Schwarzschild time to reach $r = 2M$. However in the G-P coordinate system, we do not have this problem because the G-P time coordinate represents the particle proper time and it is possible to study the motion also for $r < 2M$ in a finite amount of $t_P$.

Now we want to see what happens if the quantum nature of the particles of the source cannot be neglected. We are looking for a particle on the surface of the star. Let us calculate the classical Action and Hamiltonian from the Lagrangian (we use now the generic G-P metric):

$$\mathcal{L} = -\frac{m}{E}\sqrt{\left(1 - \frac{2M}{r}\right)\dot{t}^2 - \dot{r}^2 - 2v(r)\dot{r}\dot{t}} \tag{D.1}$$

where $m$ is the mass of the particle on the surface (these massive particles are the constituent of the source), dots represent derivative with respect to the parameter $\tau$. From here we can write the Action on a certain path $\gamma$:

$$\mathcal{S}[\gamma] = -\frac{m}{E}\int_{t_i}^{t_f} dt\sqrt{\left(1 - \frac{2M}{r}\right) - \dot{r}^2 - 2v(r)\dot{r}} \tag{D.2}$$

Then we calculate momenta $p$:

$$p = \frac{\partial \mathcal{L}}{\partial \dot{r}} = \frac{m}{E}\frac{\dot{r} + v(r)}{\sqrt{1 - \frac{2M}{r} - \dot{r}^2 - 2\dot{r}v(r)}} \tag{D.3}$$

and, considering classical path ($v(r) = \sqrt{\frac{2M}{r} - \frac{2M}{r_0}}$ and $E^2 = 1 - \frac{2M}{r_0}$), the Hamiltonian $\mathcal{H}$:

$$\mathcal{H} = p\dot{r} - \mathcal{L} = \sqrt{\left(1 - \frac{2M}{r_0}\right)p^2 + m^2} - p\sqrt{\frac{2M}{r} - \frac{2M}{r_0}} \tag{D.4}$$

where $r_0$ is the value for the $r$ coordinate in which $\dot{r} = 0$. $\mathcal{H}$ reduces to the free relativistic Hamiltonian when we are in the limit $M \to 0$.

Now we are ready to study the problem in a quantum point of view and assume that the particle's state is codified in a Gaussian wave function in $(r_i, t_i)$:

$$\psi(r_i, t_i) = Ne^{-\frac{m^2(r-r_c)^2}{\hbar^2}} \tag{D.5}$$

where $N = \sqrt[4]{\frac{\pi}{2}}\sqrt{\frac{\hbar}{m}}$ is the normalization constant and $r_c$ is some value for the initial position of the surface (we assume $r_c >> 2M$). We know from the path integral quantization that one can define the propagator as:

$$G(r_f, t_f; r_i, t_i) = \sum_{\gamma} e^{\frac{i}{\hbar}\mathcal{S}[\gamma]} \tag{D.6}$$

which is the sum of the amplitude due to all possible trajectories $\gamma$, in this sum one has to consider also space-like ($ds^2 < 0$) and light-like ($ds^2 = 0$) trajectories (classically one considers only time-like paths for massive particles), for this reason when $\dot{r}$ appears in the sum we consider the relation $\dot{r}^2 = \left(\frac{dr}{d\tau}\right)^2 = E^2 - \kappa\left(1 - \frac{2M}{r}\right)$ in which $\kappa = 0$ for light-like geodesics, $\kappa = +1$ for time-like geodesics and $\kappa = -1$ for space-like geodesics.

From propagator and the initial Gaussian state one obtains the WF that describes the particle's state at any $(r, t)$ integrating on all the possible initial conditions:

$$\psi(r, t) = \int_0^{\infty} dr_i G(r, t; r_i, t_i)\, \psi(r_i, t_i) \tag{D.7}$$

We can study the problem of finding the quantum WF at some $(r, t)$ supposing that the massive particle wave function $\psi(r, t)$ can be found solving the Schrödinger equation $i\hbar\partial_t\psi = \mathcal{H}\psi$ for our Hamiltonian in (D.4), from here we proceed with a perturbation method in which we set $\epsilon = \sqrt{\frac{2M}{r} - \frac{2M}{r_c}}$ and our equation is:

$$i\hbar\frac{\partial}{\partial t}\psi(r, t) = \left(\sqrt{\left(1 - \frac{2M}{r_c}\right)p^2 + m^2} - p\epsilon\right)\psi(r, t) \tag{D.8}$$

In this way we can write our solution approximated at first order in the form:

$$\psi(r, t) = \psi_0(r, t) + \epsilon\psi_1(r, t) + o\left(\epsilon^2\right) \tag{D.9}$$

where we have:

$$\psi_i(r, t) = \int_{-\infty}^{\infty} dk\psi_i(\tilde{k}, t)e^{ikr} \tag{D.10}$$

$(i = 0, 1)$. So $\psi_0(r, t)$ satisfies the zeroth-order equation:

$$i\hbar\partial_t\psi_0(r, t) = \sqrt{\left(1 - \frac{2M}{r_c}\right)p^2 + m^2}\psi_0(r, t) \tag{D.11}$$

and the solution is:

$$\psi_0(r, t) = \int_{-\infty}^{\infty} dk\tilde{\psi_0}(k, 0)\, e^{-\frac{i}{\hbar}t\sqrt{\left(1-\frac{2M}{r_c}\right)\hbar^2k^2 + m^2}} \tag{D.12}$$

In $t = t_i = 0$ we have the condition that $\psi(r, t)$ is a Gaussian centered in $r = r_c$, this fixes the form for $\tilde{\psi_0}(k, 0)$ and imposes the condition $\psi_1(r, 0) = 0$.

At first order we obtain the equation for $\psi_1(r,t)$ which reads:

$$i\hbar\partial_t\psi_1(r,t) = \sqrt{\left(1-\frac{2M}{r_c}\right)p^2+m^2}\psi_1(r,t) - p\psi_0(r,t) \tag{D.13}$$

From here we obtain:

$$\begin{aligned}
\psi(r,t) &= \frac{\hbar}{m}\frac{N}{\sqrt{2\pi}}\int_{-\infty}^{\infty} dk e^{-\frac{k^2\hbar^2}{4m^2}} e^{-\frac{i}{\hbar}t\sqrt{\left(1-\frac{2M}{r_c}\right)\hbar^2k^2+m^2}} e^{ik(r-r_c)} \\
&+ \sqrt{\frac{2M}{r}-\frac{2M}{r_c}}\frac{\hbar}{m}\frac{N}{\sqrt{2\pi}}\int_{-\infty}^{\infty} dk e^{-\frac{k^2\hbar^2}{4m^2}} e^{ik(r-r_c)} ikt e^{-\frac{i}{\hbar}t\sqrt{\left(1-\frac{2M}{r_c}\right)\hbar^2k^2+m^2}} \\
&+ \sqrt{\frac{2M}{r}-\frac{2M}{r_c}}\int_{-\infty}^{\infty} dk e^{ikr} A e^{-\frac{i}{\hbar}t\sqrt{\left(1-\frac{2M}{r_c}\right)\hbar^2k^2+m^2}}
\end{aligned} \tag{D.14}$$

in which considering the initial conditions $A = 0$. Note that the wave function is not normalized, this is due to the use of the perturbation method that give us a solution which is useful only in the first few instants. From here, knowing that

$$\frac{N}{\sqrt{2\pi}}\int_0^{\infty} dr_i e^{-ikr_i} e^{-\frac{(r_i-r_c)^2m^2}{\hbar^2}} \simeq \frac{N\hbar}{\sqrt{2\pi}m} e^{-\frac{\hbar^2k^2}{4m^2}} e^{-ikr_c} \tag{D.15}$$

and from (D.7) one obtain the propagator:

$$\begin{aligned}
G(r,t,r_i,t_i=0) &= \frac{N}{\sqrt{2\pi}}\int_{-\infty}^{\infty} dk e^{-\frac{(r_i-r_c)^2m^2}{\hbar^2}} e^{ik(r-r_i)} e^{-\frac{i}{\hbar}t\sqrt{\left(1-\frac{2M}{r_c}\right)\hbar^2k^2+m^2}} \\
&+ \sqrt{\frac{2M}{r}-\frac{2M}{r_c}}\frac{N}{\sqrt{2\pi}}\int_{-\infty}^{\infty} dk e^{-\frac{(r_i-r_c)^2m^2}{\hbar^2}} e^{ik(r-r_i)} ikt e^{-\frac{i}{\hbar}t\sqrt{\left(1-\frac{2M}{r_c}\right)\hbar^2k^2+m^2}}
\end{aligned} \tag{D.16}$$

At this point we can integrate (D.14) to study the behavior of the probability of finding the particle at some $r$ in $t > t_i = 0$, in Fig. D.1 we have shown $|\psi(r)|^2$ for different values of $t$ for a fixed $M = \frac{\hbar}{m}$ and $r_c = 30M$.

In this figure, we see that the WF (starting from a Gaussian WF centered in $r_c = 30M$ at $t = 0$) as $t$ increases shows two peaks which represent the radially ingoing (collapse) and outgoing (expanding) possible motions for the particle. As $t$ increases, the peaks become more and more distant from each other. We see that the ingoing peak is higher than the outgoing one at any fixed $t$, so collapse is more probable than expansion of the star. These results are acceptable until $|\epsilon| = \left|\sqrt{\frac{2M}{r}-\frac{2M}{r_c}}\right| << 1$.

Particle's WF is also function of the total energy $M$ as is shown in (D.14) and in Figure D.2.

At fixed time, as the mass $M$ increases, ingoing peaks become higher and higher. Also outgoing peaks become higher and higher as $M$ increases but they are lower than the ingoing ones and are shifted toward smaller values of $r$. However as shown in [7] the Schrödinger approach is not appropriate in this case and one should proceed with a path integral quantization and eventually one can perform some approximation such as the WKB (Wentzel-Kramers-Brillouin) approximation. Also, in this case, we can apply these results in cases in which $M$ does not have a definite value, but there is a probability distribution of masses. In fact if we have a

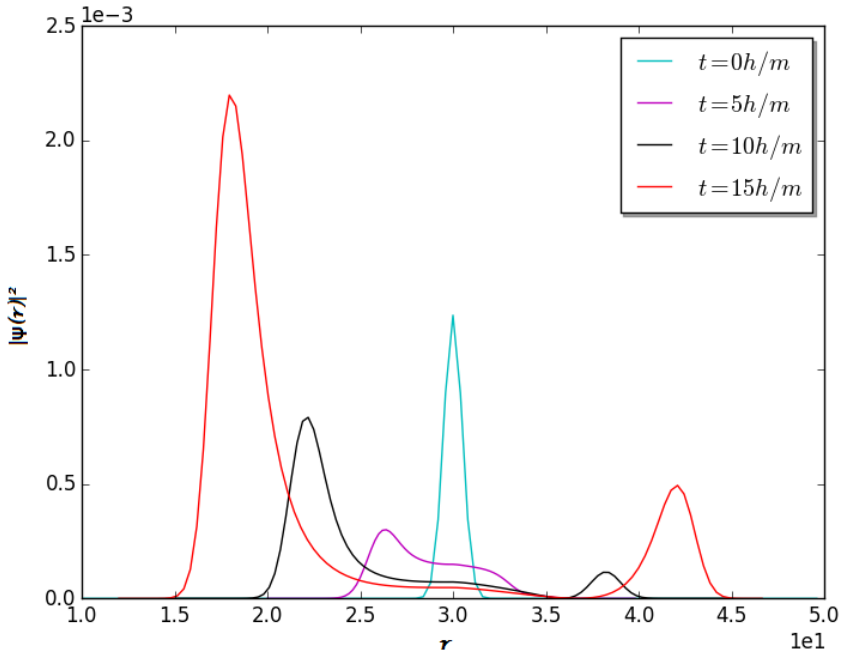


Figure D.1: $|\psi(r)|^2$ for different $t$ with $r_c = 30M$, $m = 10^{-13}eV$, $M = 1\frac{\hbar}{m}$ ($r$ is expressed in $\frac{\hbar}{m} = 1.97328 \cdot 10^{-3}m = M$ units).

probability $P_i$ for the mass $M_i$, $P_i$ also represents the probability to have a certain $\psi_{M_i}(r,t)$ for the particle on the surface of the source. Suppose that $i$ is a set of discrete indexes, for a fixed $t$ the probability distribution to find the particle af some value of $r$ is:

$$\rho(r,t) = \sum_{i=0}^{N} P_i |\psi_{M_i}(r,t)|^2 \tag{D.17}$$

The probability distribution for $r_H$ and hence for $M$ could also be obtained from the HWF of the source so we can study the effects of this latter during the collapse. If this is the case, the probability density to have a gravitational radius $r_H$ is given from:

$$\rho(r_H) = 4\pi r_H^2 |\psi_H(r_H)|^2 \tag{D.18}$$

so if the horizon of the source can be described by means of $\psi_H(r_H)$ and the states of the particle on its surface are (initially) codified in a Gaussian wave function, the probability to find the particle in $r$ at some $t > 0$ (if we exclude the possibility of an angular motion) is:

$$P(r,t) = \int_0^\infty dr_H \rho(r_H) |\psi_{M=\frac{r_H}{2}}(r,t)|^2 \tag{D.19}$$

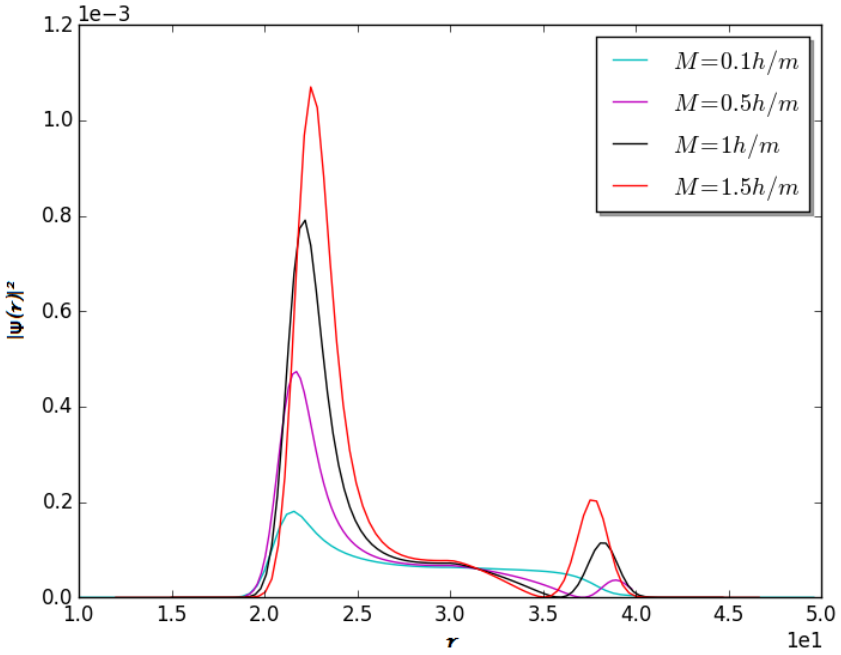


Figure D.2: $|\psi_M(r)|^2$ for different $M$ with $r_c = 30\frac{\hbar}{m}$, $m = 10^{-13}eV$ at $t = 10\frac{\hbar}{m}$ ($r$ is expressed in $\frac{\hbar}{m}$ units).

# Bibliography


[1] Wald, R. (1984). *General Relativity* - Chicago University Press.

[2] Carroll, S. (2003). *Spacetime and Geometry: An Introduction to General Relativity* - Addison-Wesley Pub.

[3] Valeri P. Frolov and Andrei Zelnikov (2011).*Introduction toBlack Hole Physics* - Oxford University Press.

[4] Ray D'Inverno (1992). *Introducing Einstein's Relativity* - Clarendon Press.

[5] R.Casadio, A. Giugno (2016). *"Horizon quantum mechanics: A hitchhiker's guide to quantum black holes"*, International Journal of Modern Physics D Vol. 25, No. 2-World Scientific Publishing Company.

[6] R. Casadio, A. Giugno, A. Giusti (2016). *"Global and Local Horizon Quantum Mechanics"*, arXiv:gr-qc/1605.06617v1

[7] J. Balakrishna, R. Bondarescu (2016). *"Self-graviting stellar collapse:explicit geodesics and path integration"*, arXiv:gr-qc/1501.04250v4

[8] Schulman, L.S. (1981). *Techniques and applications of path integration* - John Wiley & Sons, Inc.

[9] Bambi,C. (2015). *"Testing the Kerr Paradigm with the Black Hole Shadow"*, arXiv:gr-qc/1507.05257v1

[10] Harvey Reall (2016). *Part 3 Black Holes Lectures*

[11] J.R. Oppenheimer and H. Snyder, Phys. Rev. 56 (1939) 455.

[12] S. Weinberg (1972), *Gravitation and Cosmology: Principles and Applications of the General Theory of Relativity* - John Wiley & Sons, Inc.

[13] A. V. Toporensky and O.B. Zaslavskii, *"Redshift of a photon emitted along the black hole horizon,"* arXiv:gr-qc/1611.09807v1